



POLITECNICO
MILANO 1863



POLITECNICO
MILANO 1863

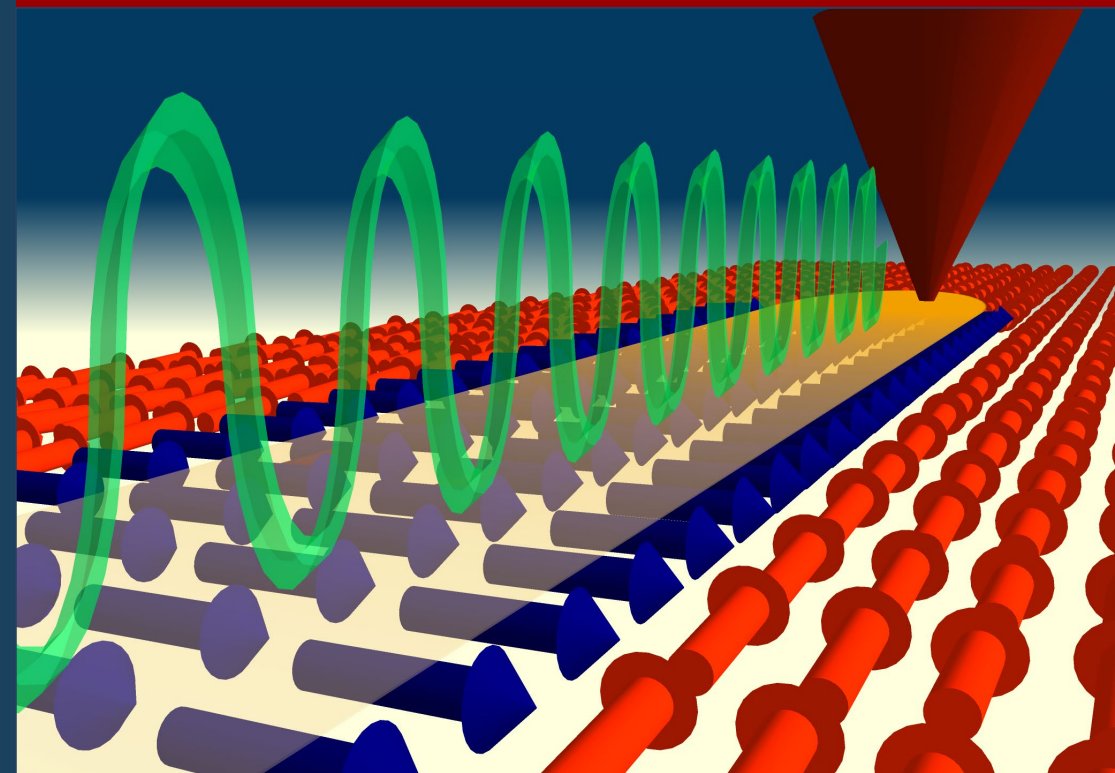
Thermal Scanning Probe Lithography

Edoardo Albisetti

Dipartimento di Fisica - Politecnico di Milano

30/6/21, NanoLito 2021, University of Salamanca

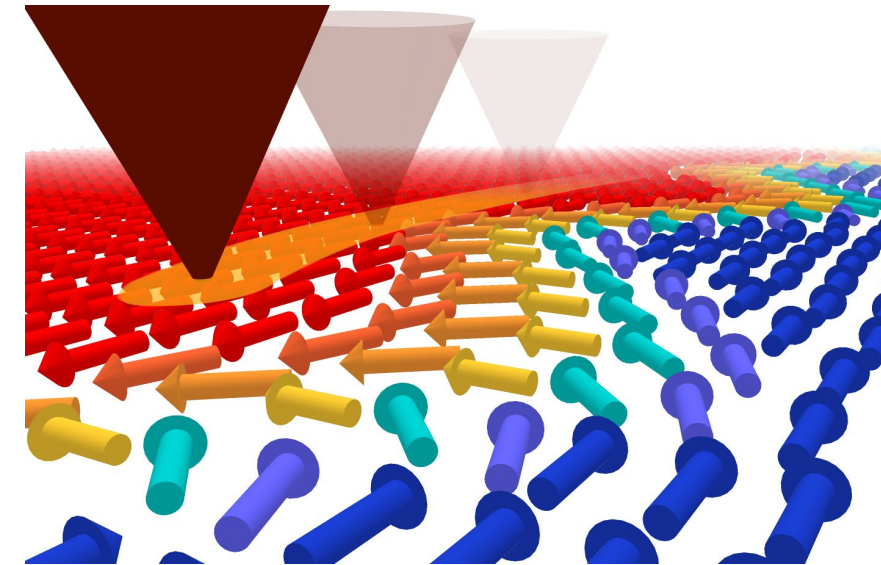
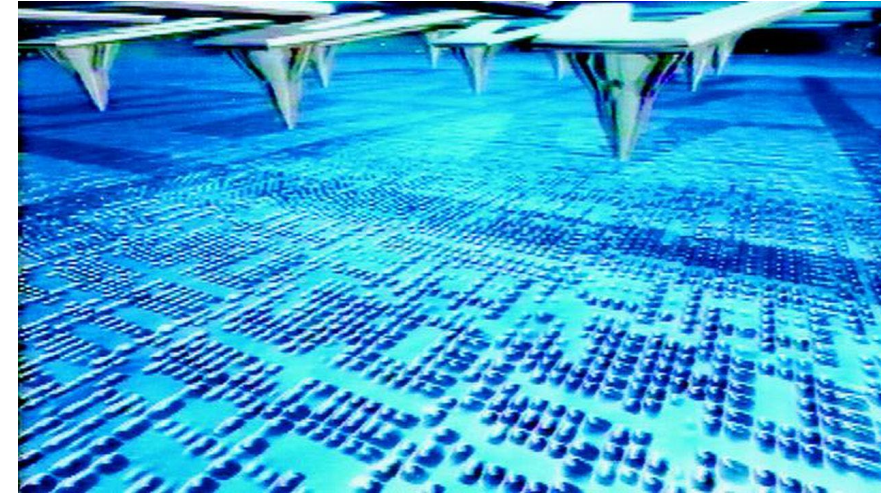
**Nanolito 2021: SUMMER SCHOOL
IN BASICS AND APPLICATIONS OF
NANOLITHOGRAPHY**



Outlook

- ▶ *Scanning Probe Microscopy / Lithography*
- ▶ *Brief history of t-SPL: from milli-pedes to nano-structures*
- ▶ *Experimental: features and limitations of t-SPL*

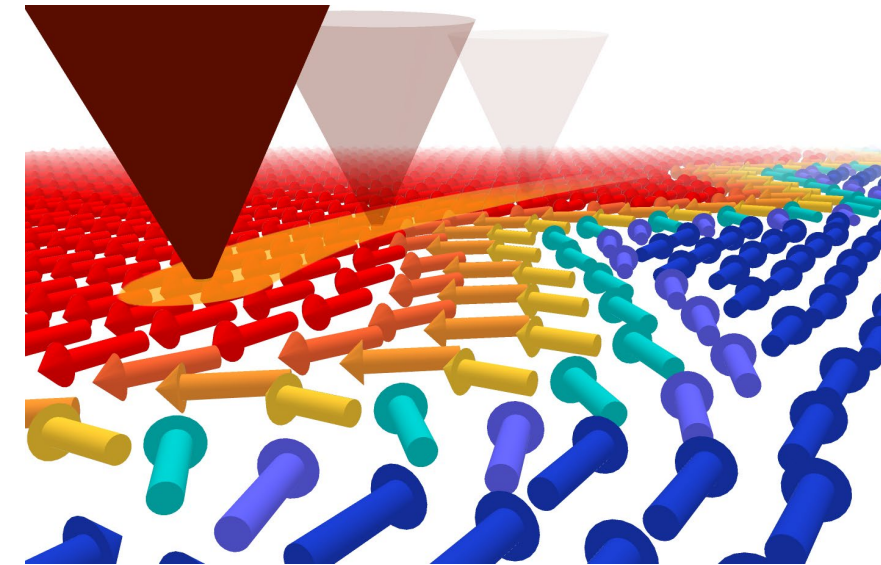
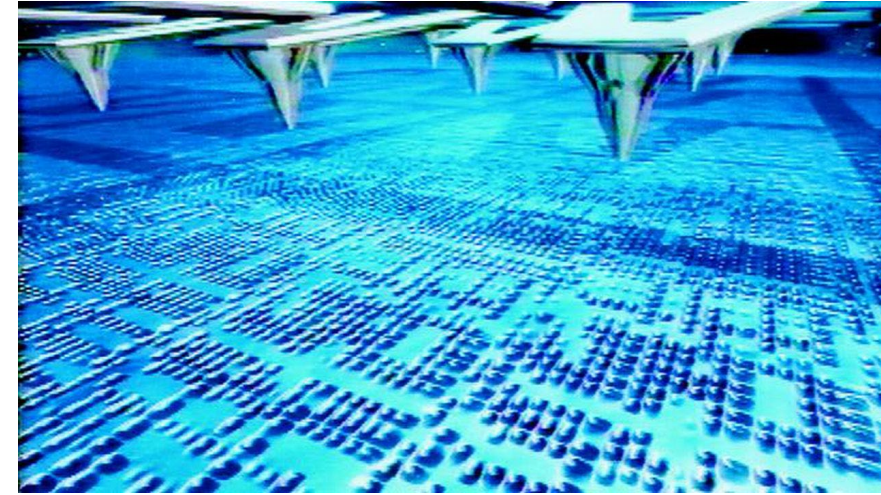
- ▶ *Applications:*
 - 1) *REMOVAL Direct sublimation of organic resists / lithography*
 - 2) *«CHEMICAL conversion» at the nanoscale*
 - 3) *«PHYSICAL conversion»: t-SPL for magnetism*



Outlook

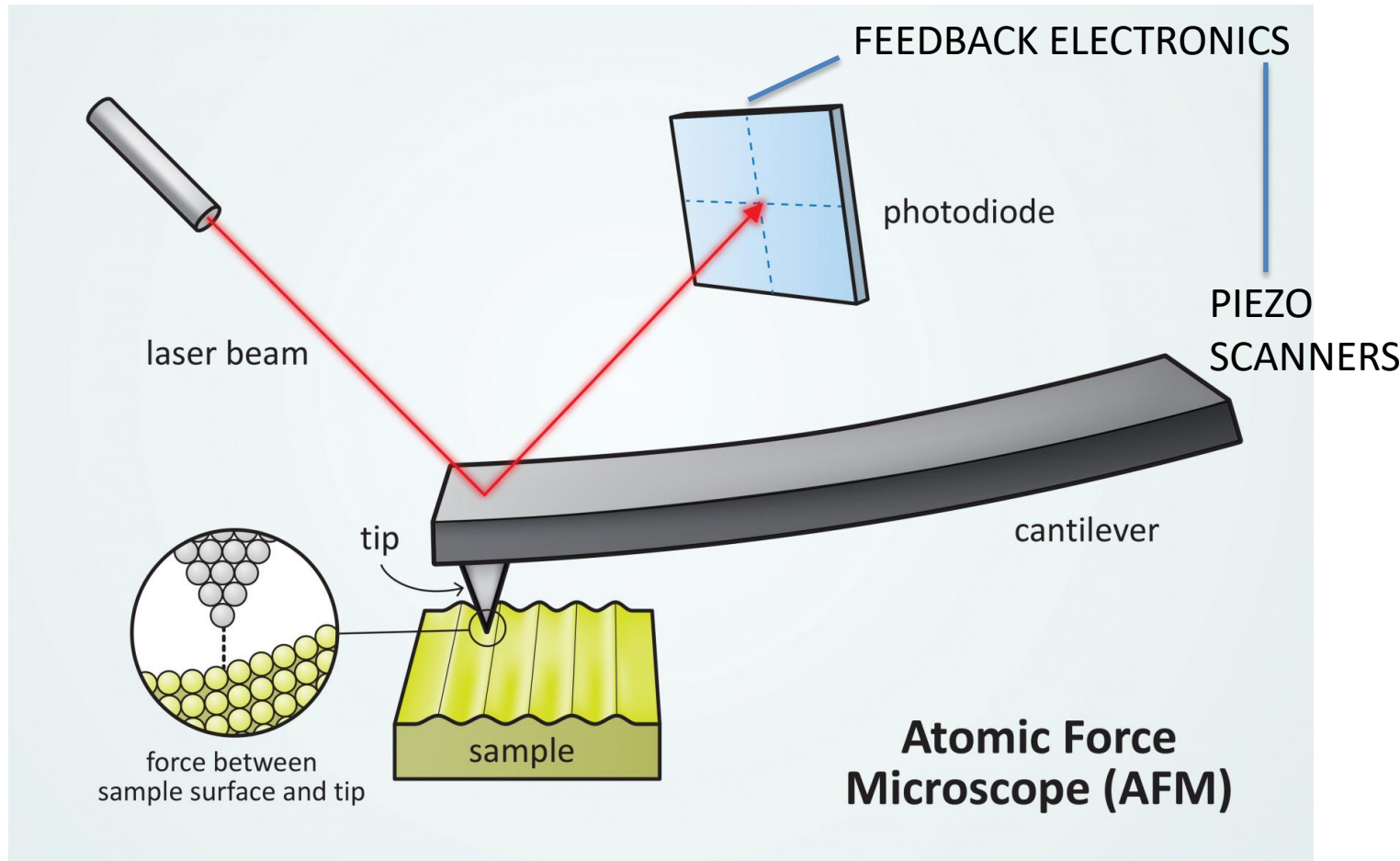
- ▶ **Scanning Probe Microscopy / Lithography**
- ▶ *Brief history of t-SPL: from milli-pedes to nano-structures*
- ▶ *Experimental: features and limitations of t-SPL*

- ▶ *Applications:*
 - 1) *REMOVAL* Direct sublimation of organic resists / lithography
 - 2) «*CHEMICAL conversion*» at the nanoscale
 - 3) «*PHYSICAL conversion*»: t-SPL for magnetism



Scanning Probe Microscopy

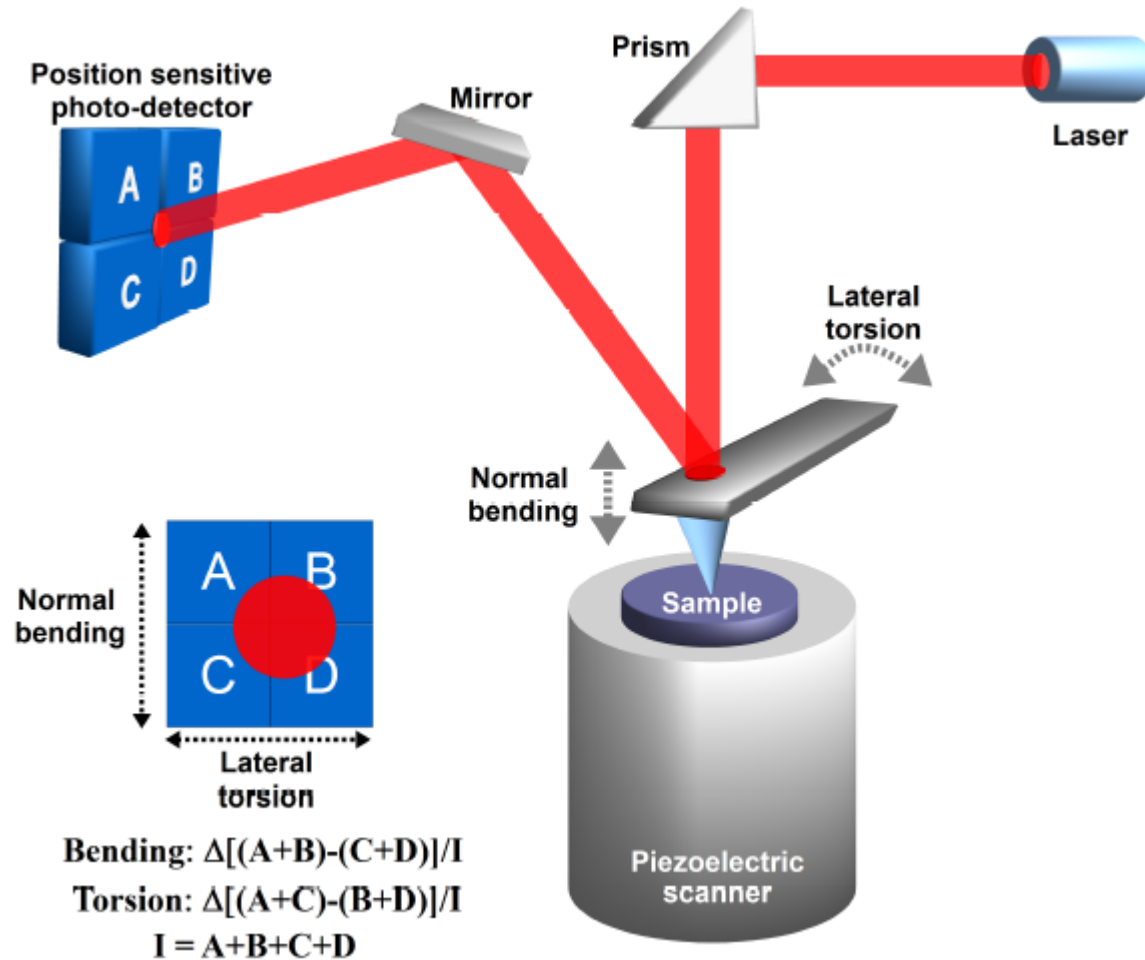
Atomic Force Microscopy



Scanning Probe Microscopy modes:
Magnetic Force Microscopy (MFM)
Lateral Force Microscopy (LFM)
Intermittant and non-contact AFM
Force Modulation Microscopy (FMM)
Electrostatic Force Microscopy (EFM)
...

Depending on the tip-sample interaction

AFM force detection mechanism

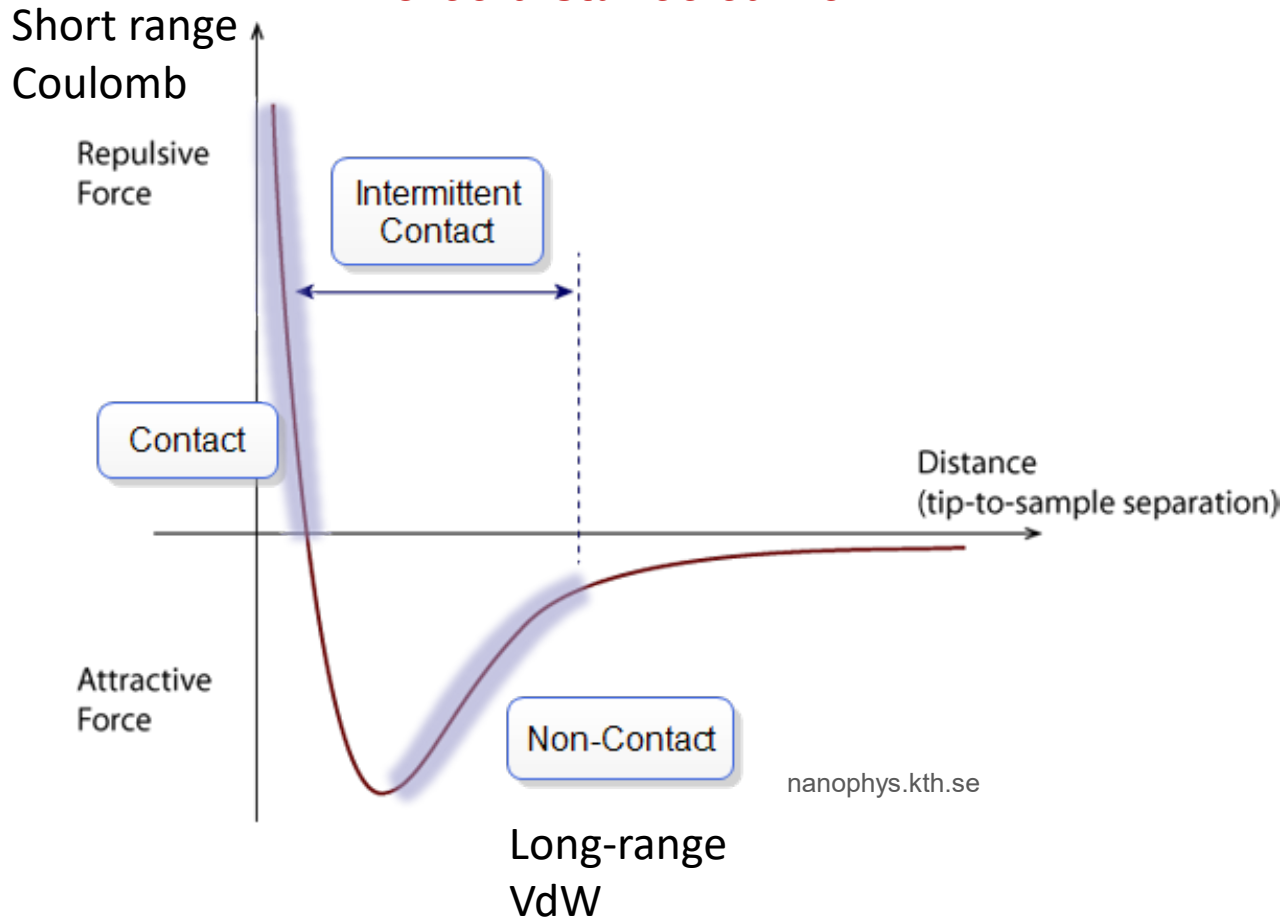


Debin Wang, Ph.D. Thesis GeorgiaTech 2010

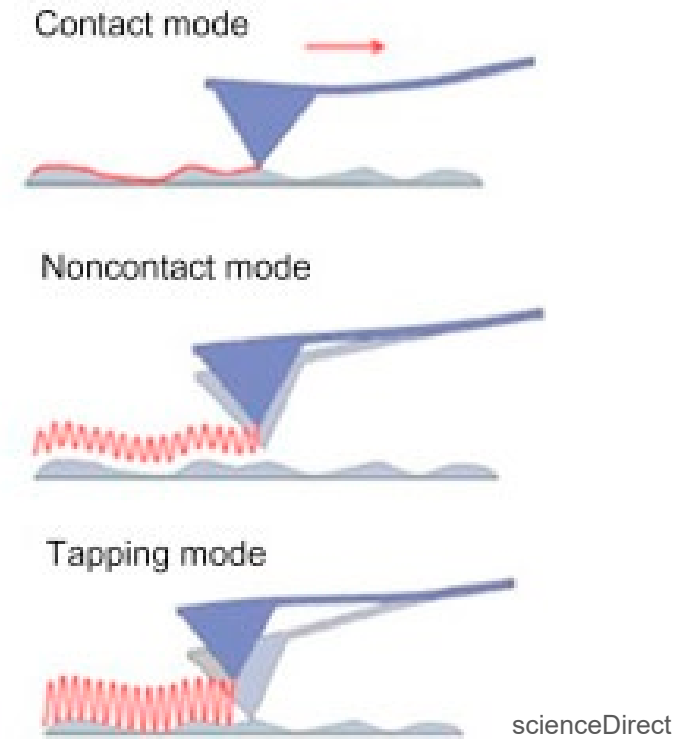
Bending + Torsion force detection
A four-quadrant position sensitive photo-detector is used to detect the vertical bending and torsion of the cantilever to measure the normal and lateral forces.

AFM tip-sample interaction

Force-distance curve

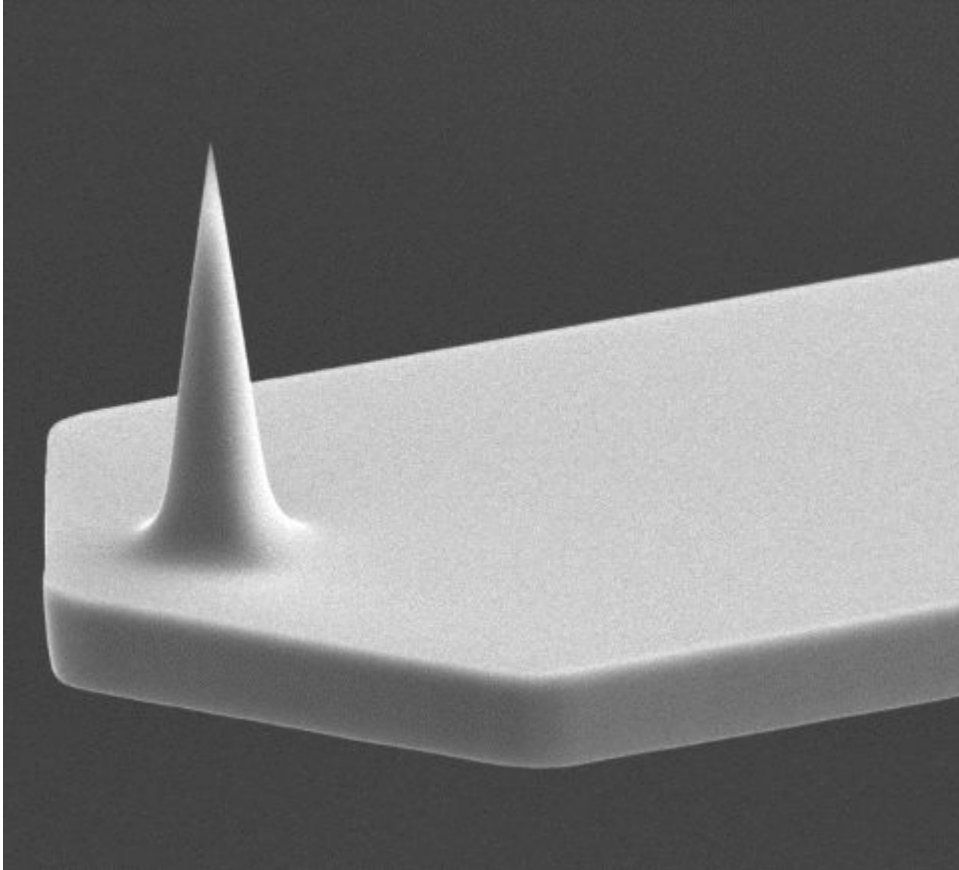


Main AFM modes



AFM Standard Scanning Probes

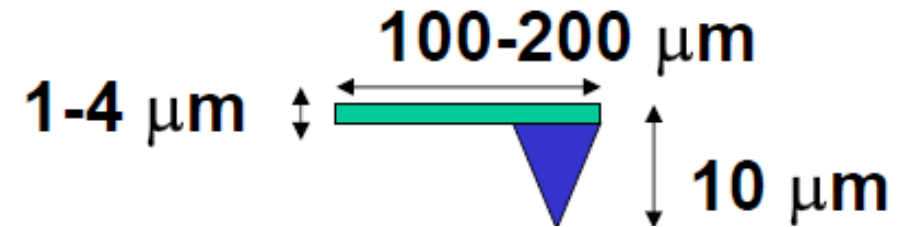
Scanning Probes



Material: Si, Si₃N₄

Shape: pyramidal, conical tip

Typical Dimensions:

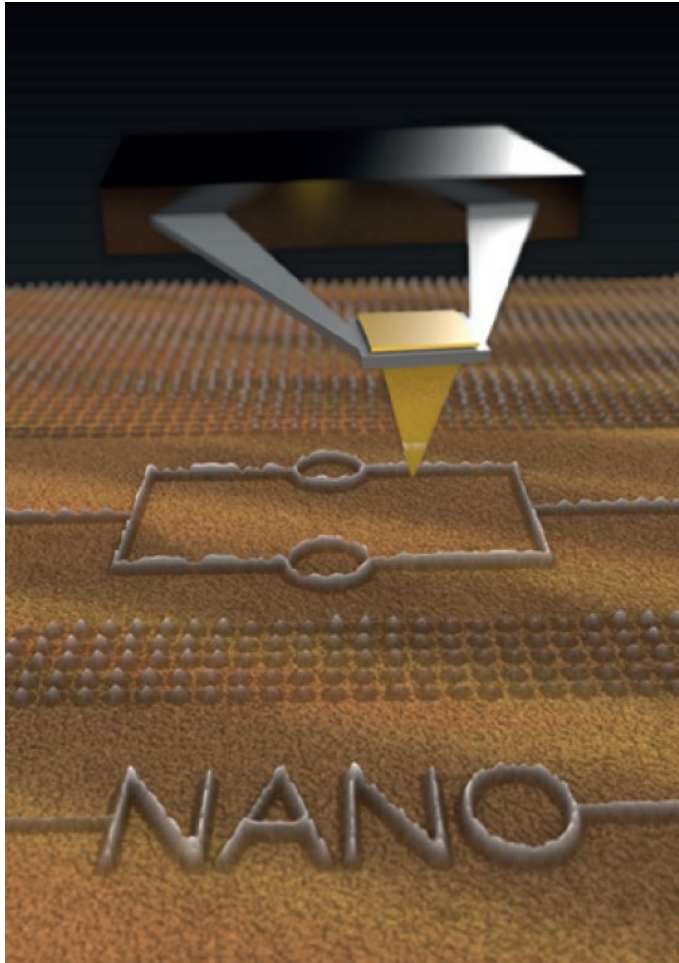


Spring constant (k): 0.1-10N/m

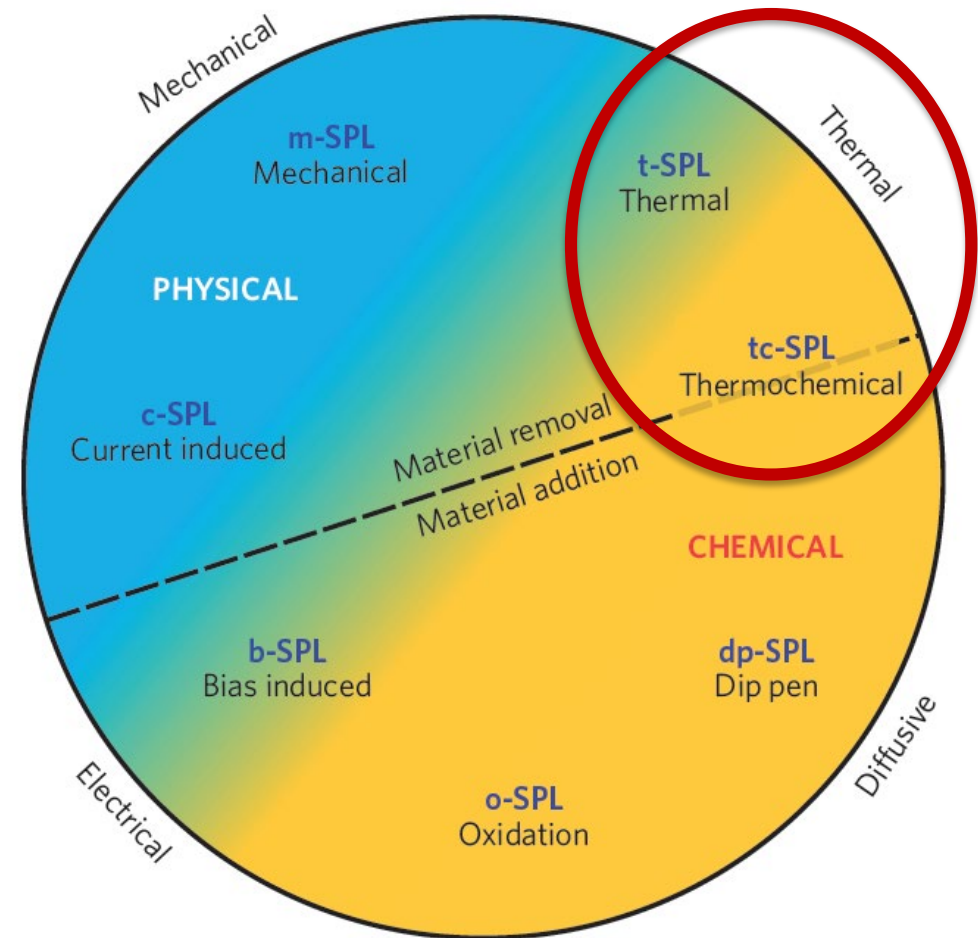
Resonant frequency: 10 kHz-1 MHz

+ different coating depending on the application (magnetic, conductive..)

Scanning Probe Lithography

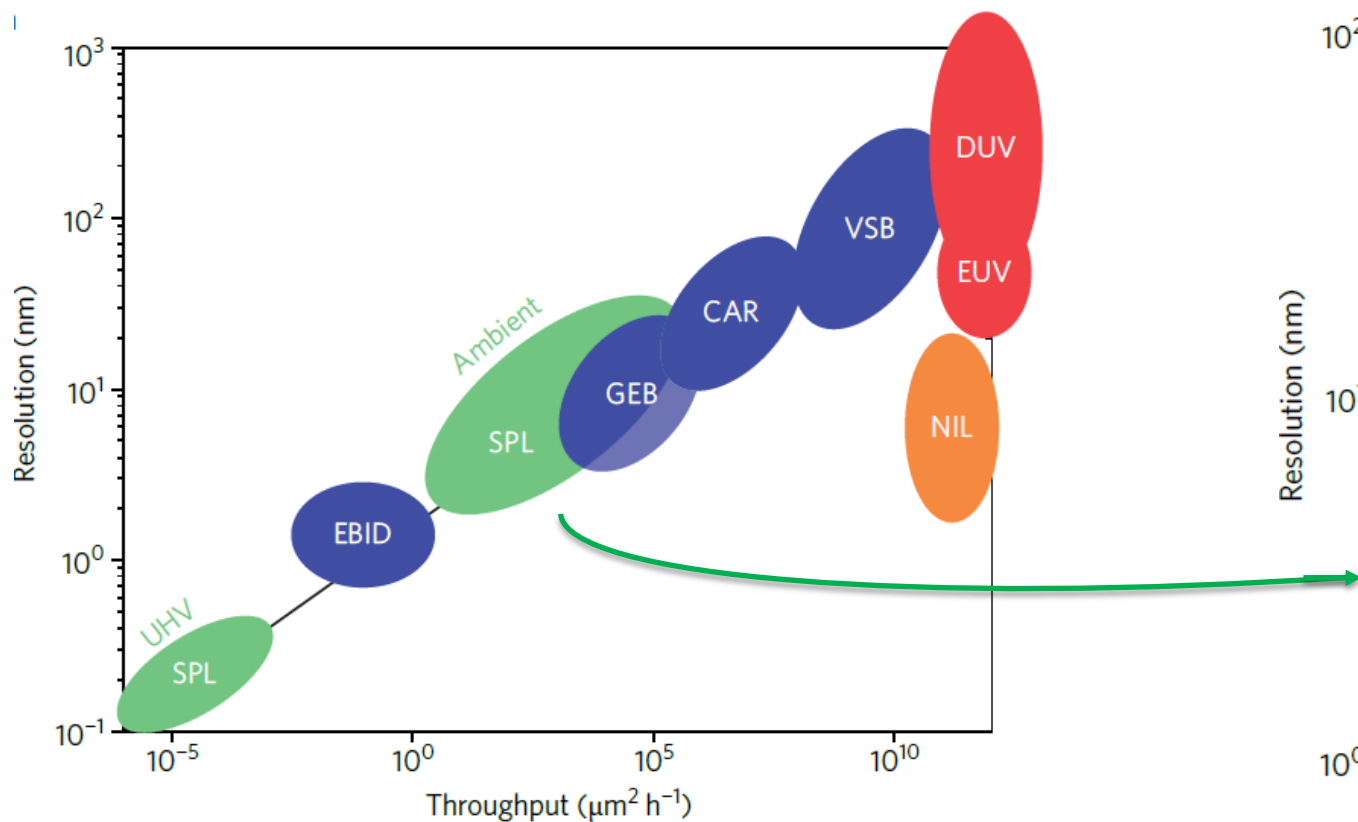


SPL modes

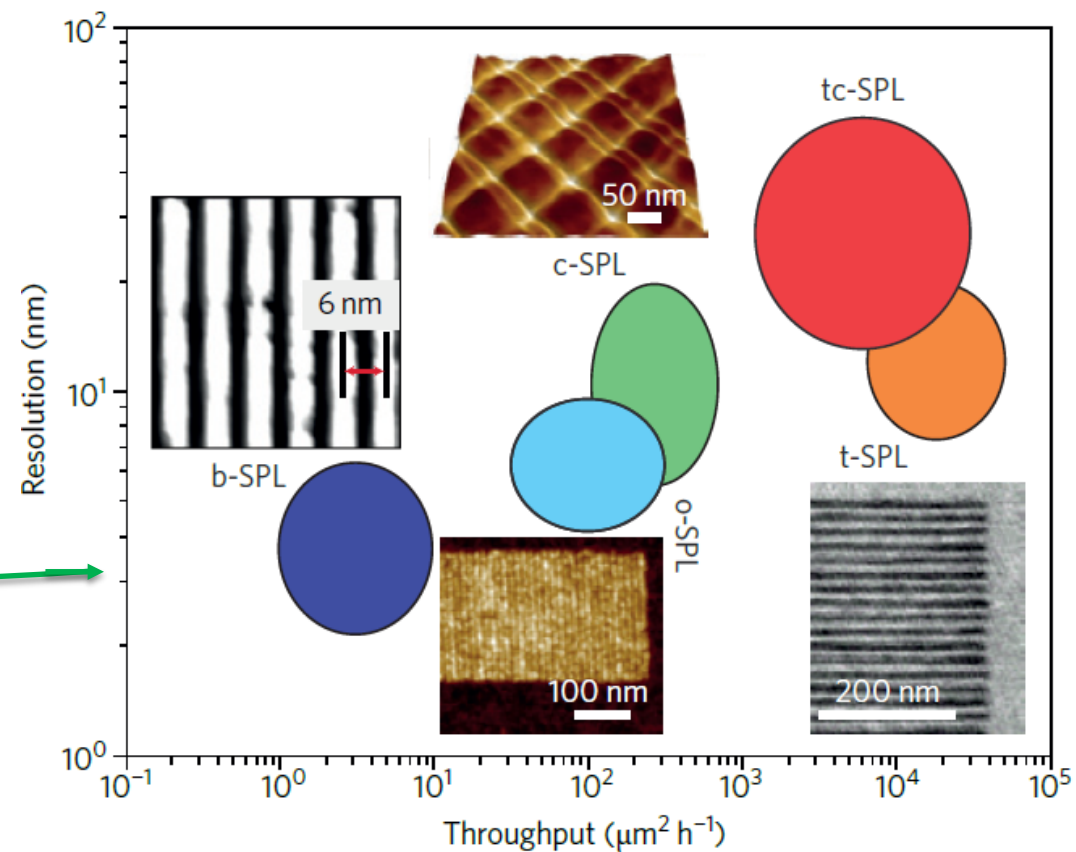


Scanning Probe Lithography: resolution vs throughput

SPL vs others

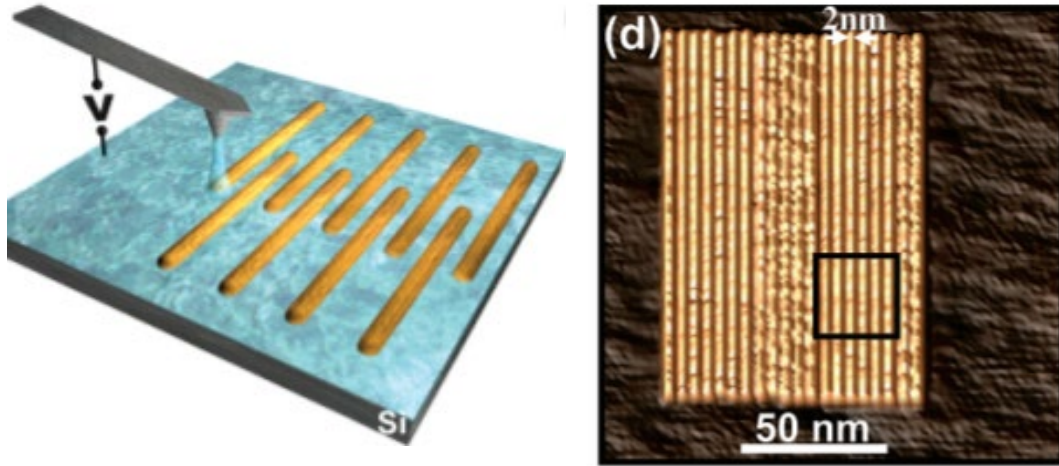


SPL methods



Bias-Scanning Probe Lithography

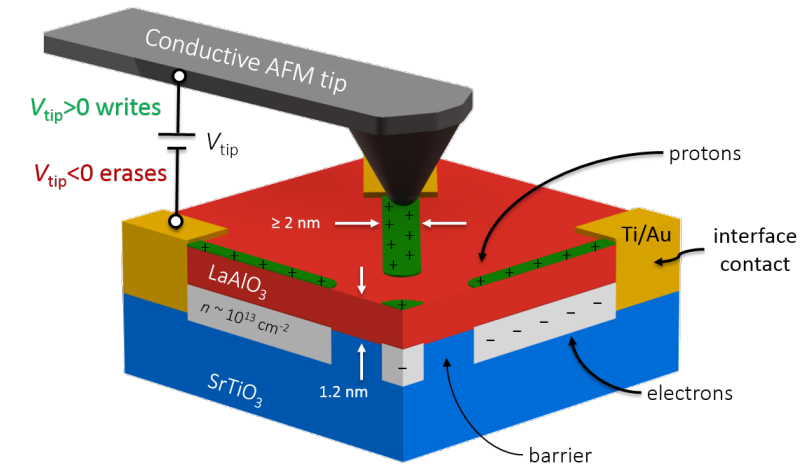
b-SPL induced deposition



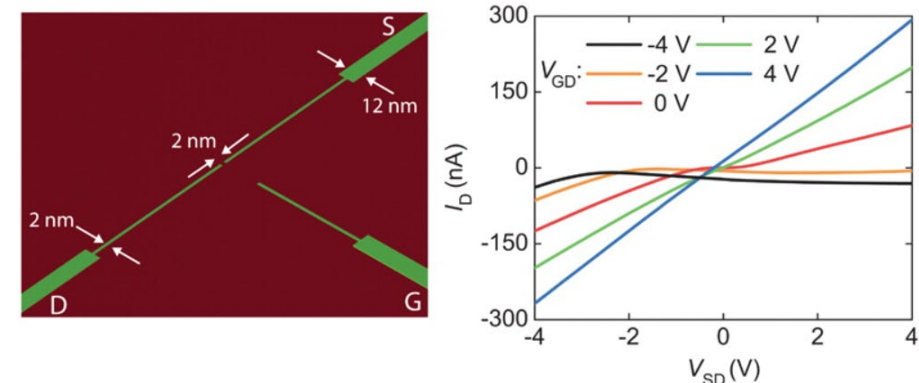
Formation of a nanoscale octane meniscus between a sharp conductive protrusion and a silicon (100) surface. Bias pulse-induced polymerization.

Nano Lett. 2007, 7, 7, 1846–1850

b-SPL conductive nanowires at LAO / STO



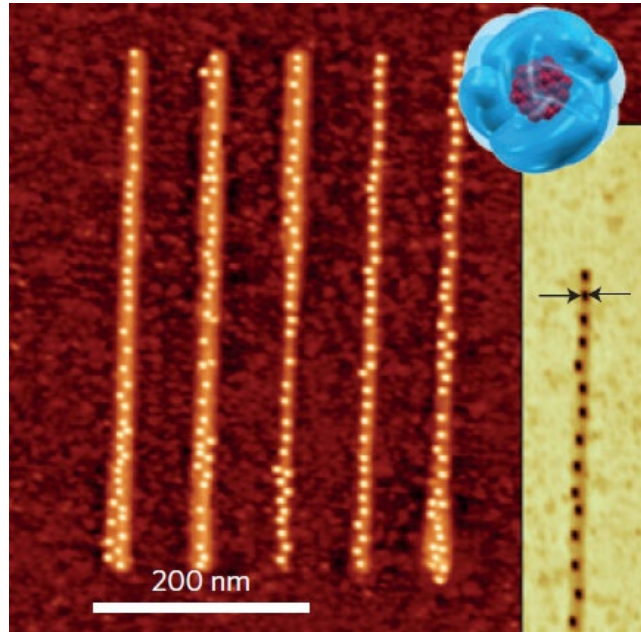
AFM tip moving above LaAlO₃-SrTiO₃ heterostructure, removing oxygen-containing ions and locally changing the charge state of the surface.



10.1126/science.1168294

Oxidation-Scanning Probe Lithography

o-SPL functionalization & molecular architectures

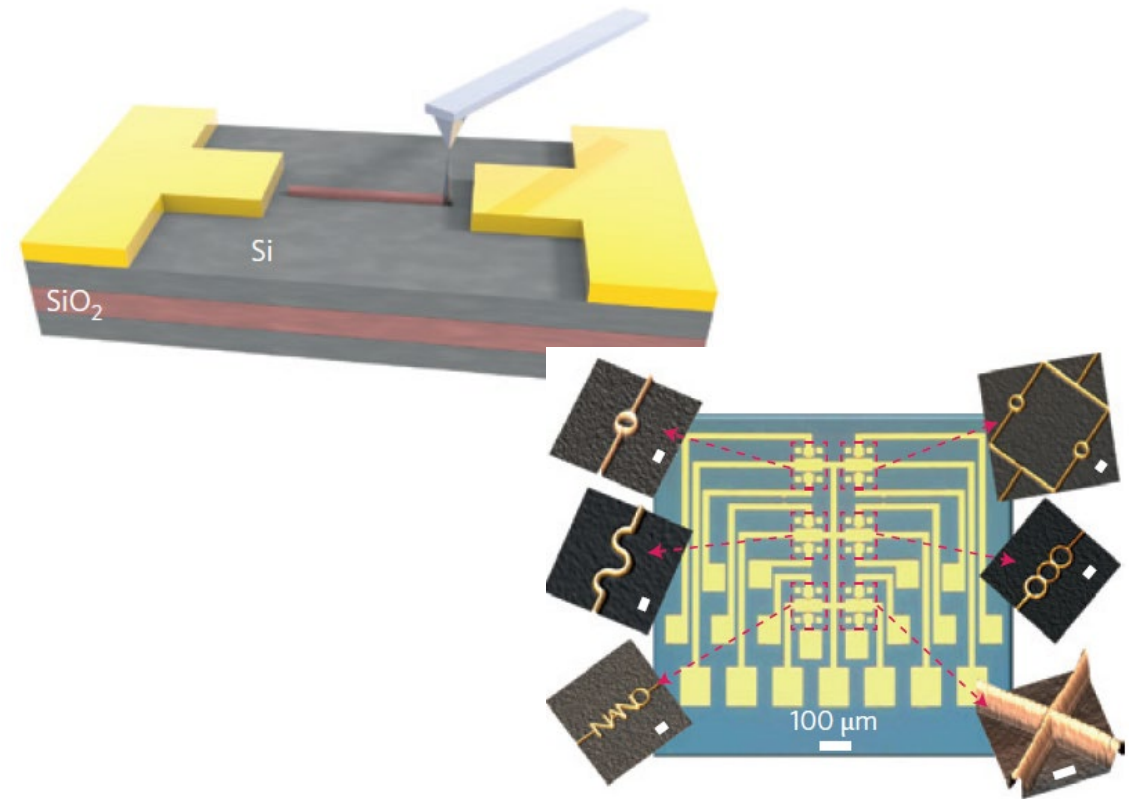


Ferritin
Single-molecule
functionalization

Selective oxidation and/or complete removal of self-assembled monolayers and subsequent surface functionalization of the oxidized region.

Martinez, R. V. et al. Adv. Mater. 22, 588–591 (2010).

o-SPL SiO₂ nanomasks



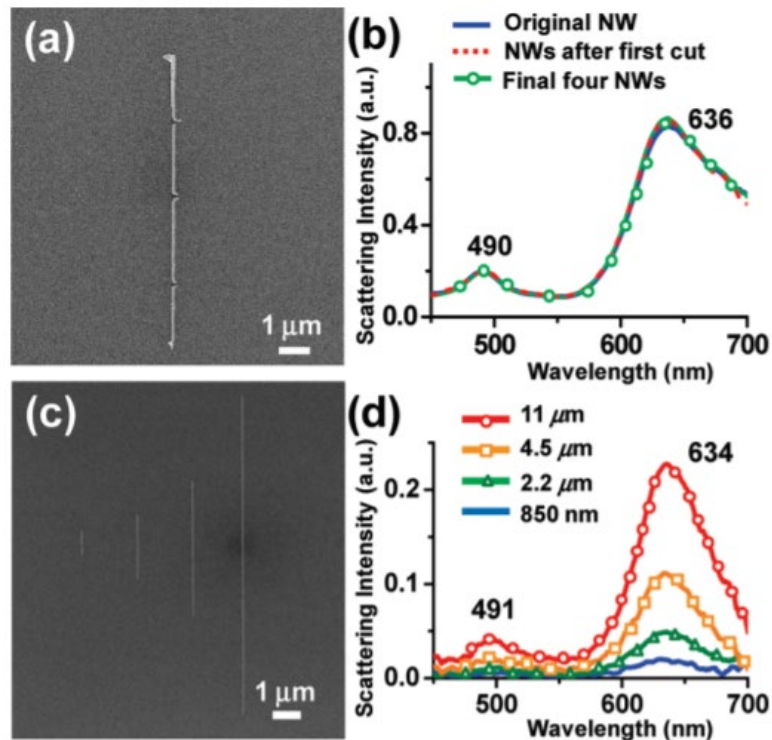
The fabrication of a silicon nanowire transistor involves the patterning of a narrow oxide mask on top of the active layer of a silicon-on-insulator substrate.

Martinez, R. V., Martinez, J. & Garcia, R. Nanotechnology 21, 245301 (2010).

Mechanical-Scanning Probe Lithography

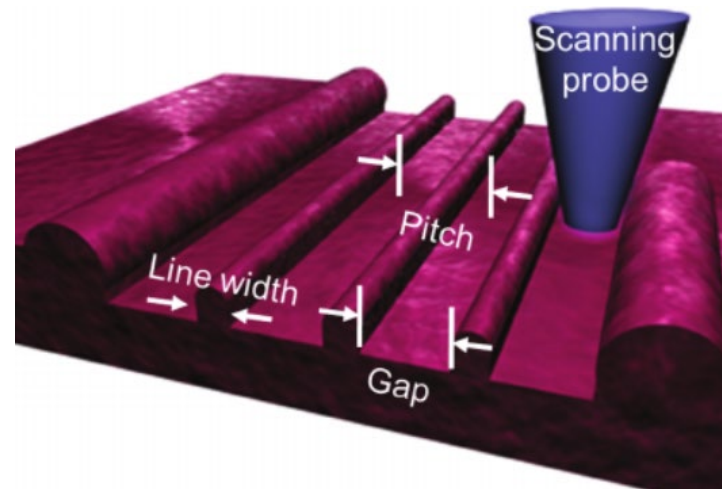
Mechanical SPL (nanomachining) uses the mechanical force exerted by the tip to induce the selective removal of material from a surface.

NW cutting for plasmonics (LSPR)



J. Phys. Chem. C, Vol. 114, No. 23, 2010

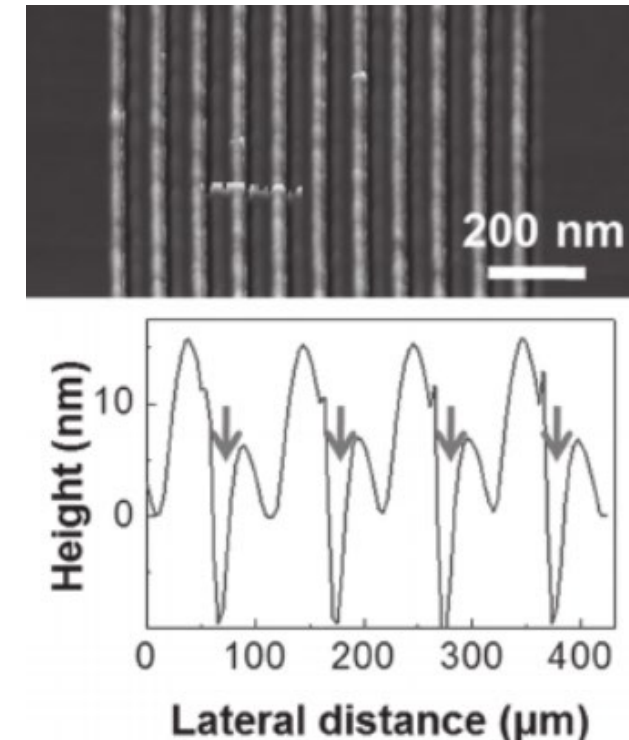
«Plowing» polymers



utilizes a scanning probe as a plow on a polymer-coated surface to generate ridges that can serve as narrow etch masks.

Small 2013, 9, No. 18, 3058–3062

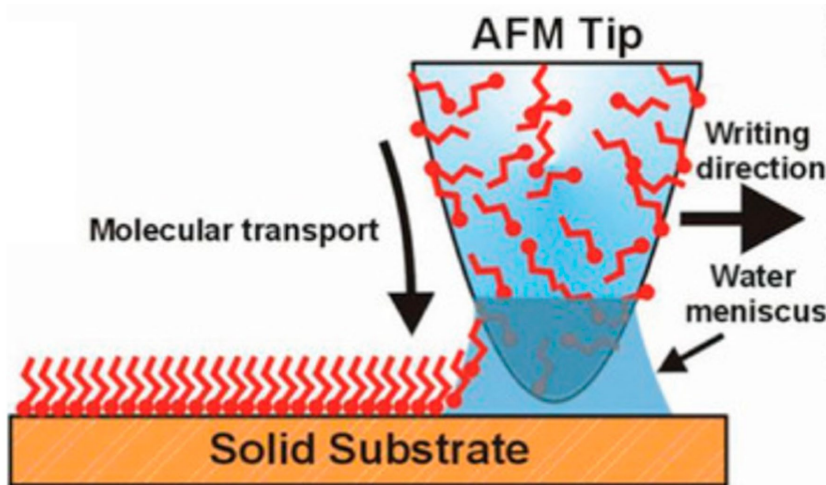
PMMA polymer



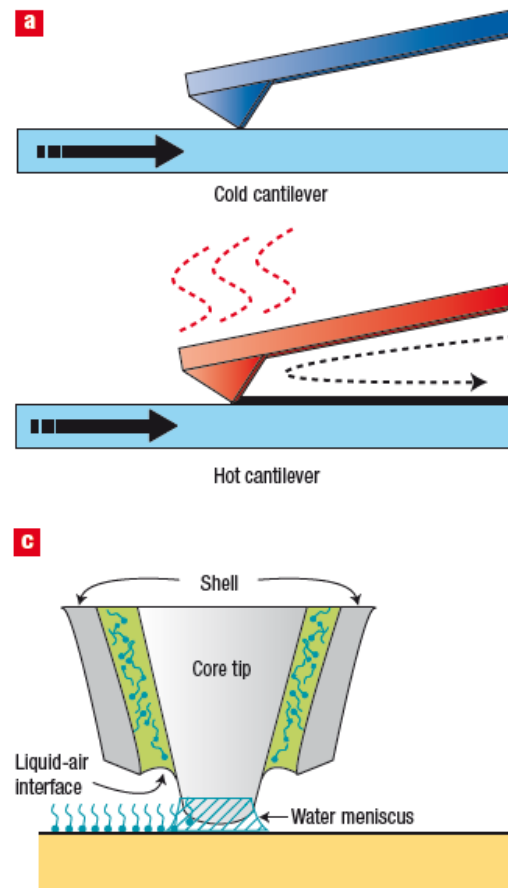
Dip pen-SPL

Direct transport of molecules to surfaces, much like the transfer of ink from a macroscopic dip-pen to paper (sub-100 nm scale)

Dip-pen nanolithography & thermal dip-pen nanolithography



10.1038/nnano.2007.39



Examples of Inks

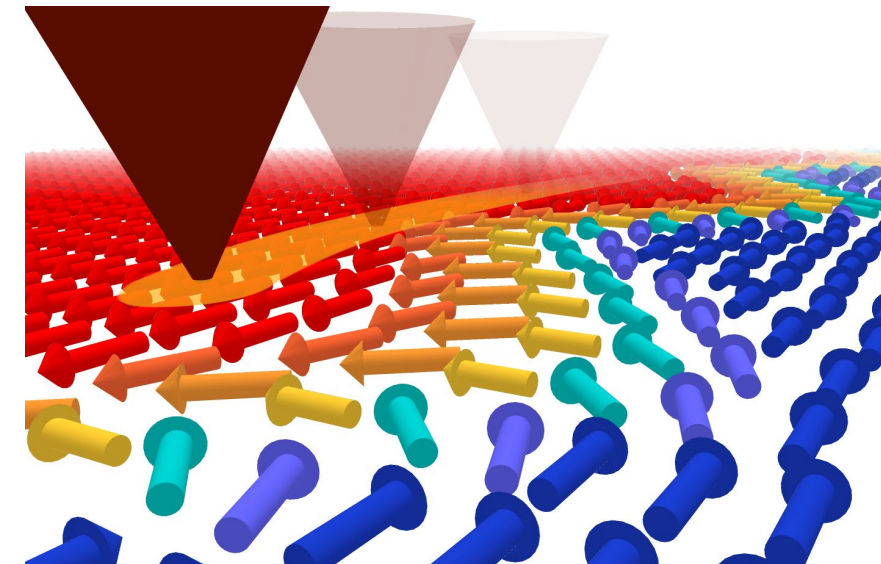
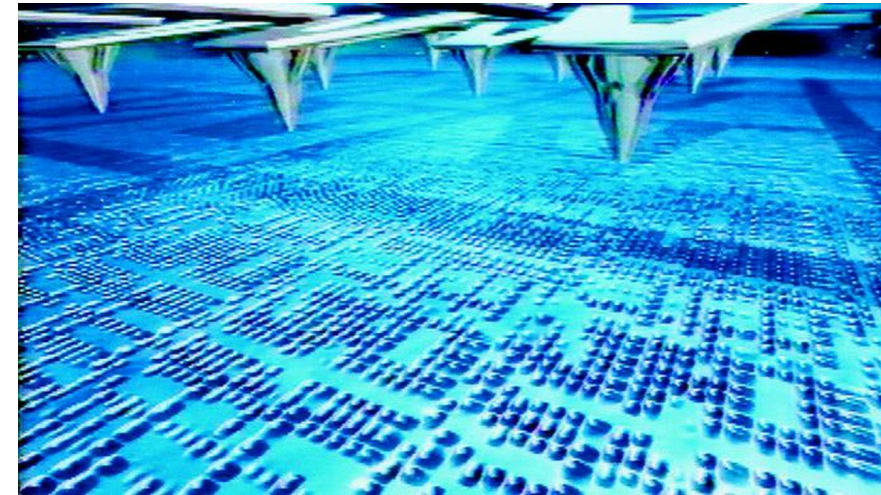
Protein, peptide, DNA, **Hydrogels**, Sol gels, Conductive inks, Lipids, Silanes (liquid phase) written to glass or silicon

Thermal DPN: AFM cantilever whose tip is coated with a solid 'ink'. When the tip is hot enough, the ink melts and flows onto the substrate.

Outlook

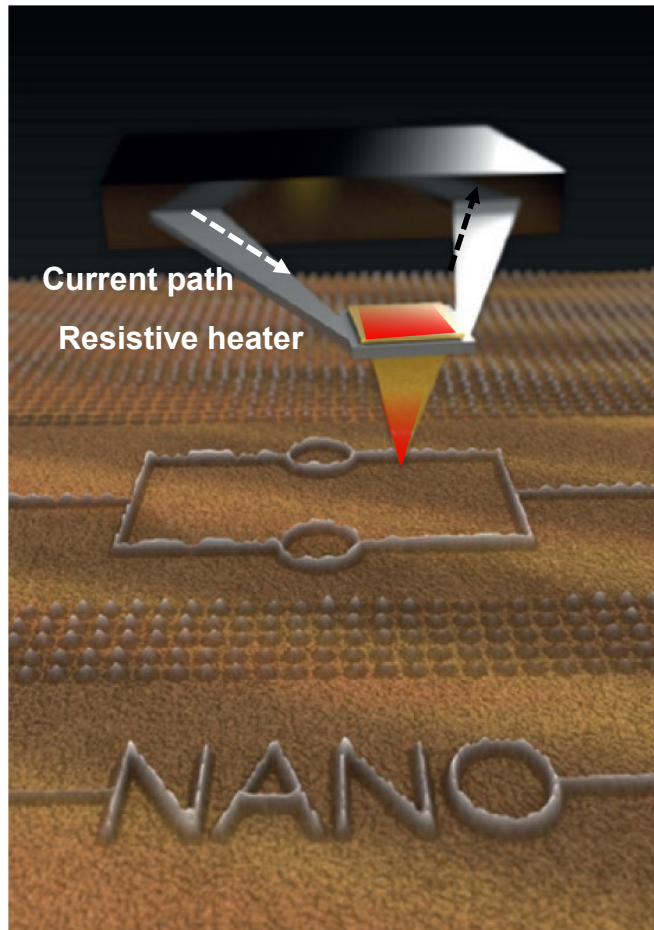
- ▶ *Scanning Probe Microscopy / Lithography*
- ▶ ***Brief history of t-SPL: from milli-pedes to nano-structures***
- ▶ *Experimental: features and limitations of t-SPL*

- ▶ *Applications:*
 - 1) *REMOVAL Direct sublimation of organic resists / lithography*
 - 2) *«CHEMICAL conversion» at the nanoscale*
 - 3) *«PHYSICAL conversion»: t-SPL for magnetism*



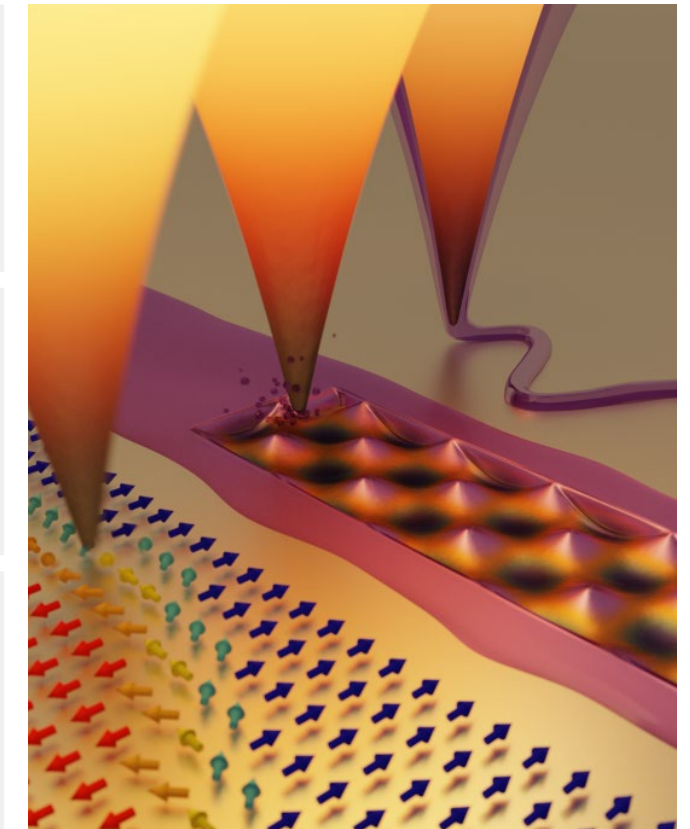
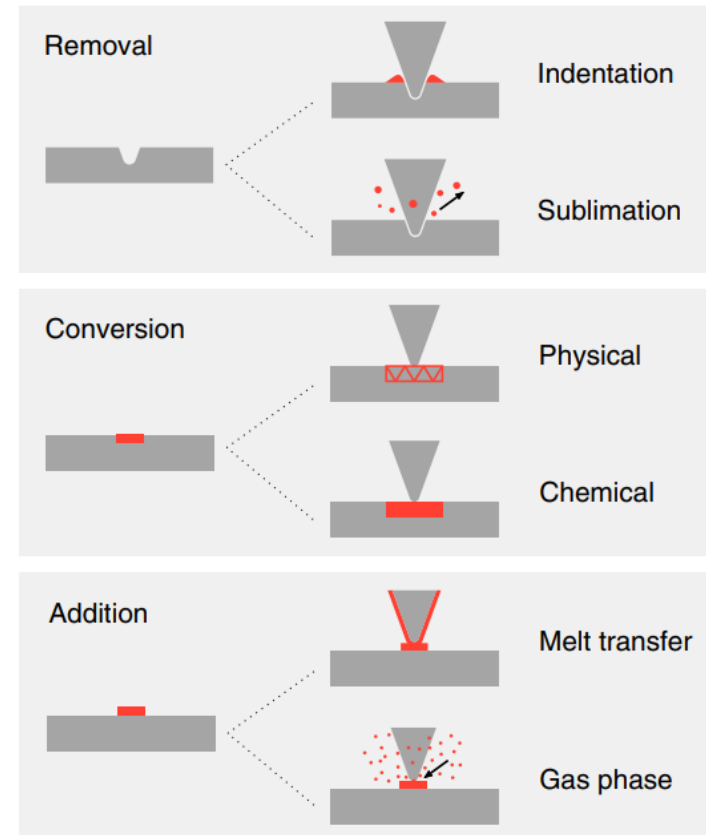
Thermally Assisted Scanning Probe Lithography (t-SPL)

Working principle



Garcia *et al.*, Nat. Nanotech. **9**, 577–587 (2014)

Heat as a localized universal stimulus

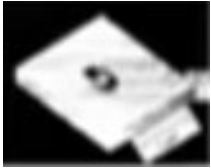


Howell *et al.* Microsystems & Nanoengineering (2020) 6:21

- ▶ Sub-10 nm spatial resolution
- ▶ Microsecond timescale
- ▶ Precise control of temperature (up to 1200°C) / duration (from few us/px)

A brief history of t-SPL

1° patterning with thermal-AFM @IBM



Thermomechanical

Appl. Phys. Lett. 61, 1003–1005 (1992)

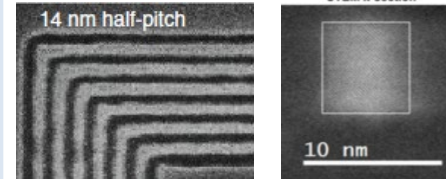
Lithography with t-SPL



Thermochemical
Thermal Dip-pen

Appl. Phys. Lett. 85, 1589 (2004)
Nano Lett. 7, 1064–1069 (2007)

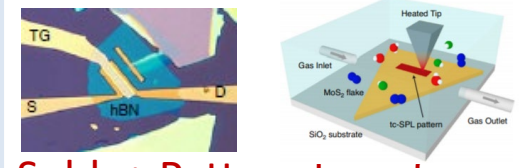
Sub-10 nm Resolution
in Silicon



Subl. + Pattern transfer

ACS Nano 11, 11890–11897 (2017)

FETs, doping
of 2D materials



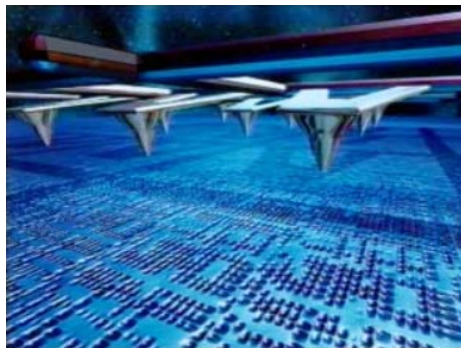
Subl. + Pattern transfer
Defect engineering

Nat. Electron. 2, 17–25 (2019).
Nature Communications 11, 3463 (2020)

1st Commercial
t-SPL Tool

1992 1995 2008 2009 2010 2011 2012 2013 2014 2015 2016 2017 2018 2019

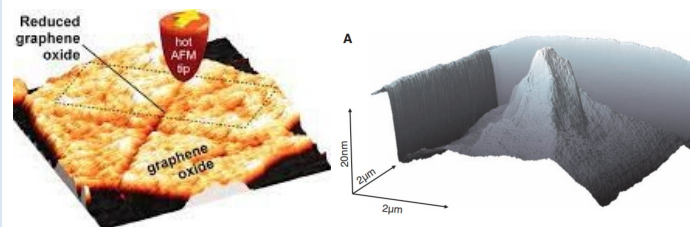
Millipede project by IBM



Thermomechanical for data storage

Microelectron. Eng. 46, 11–17 (1999).

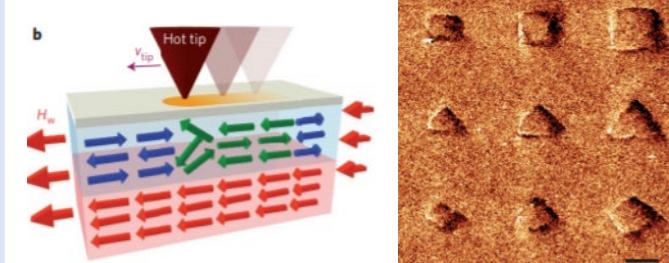
Graphene Oxide, 3D topography



Thermochemical, Sublimation

Science 328, 1373–1376 (2010).
Science 328, 732–735 (2010).

Magnetic domains, spin textures



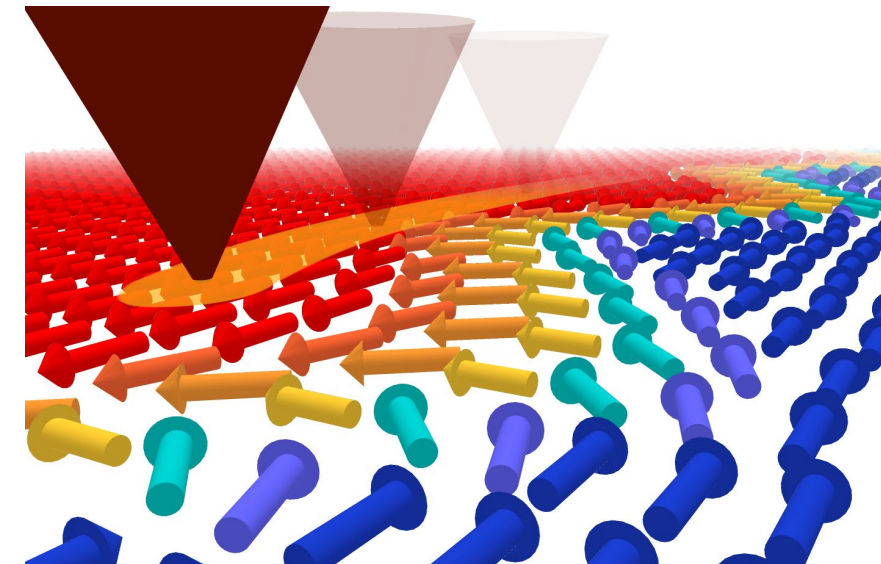
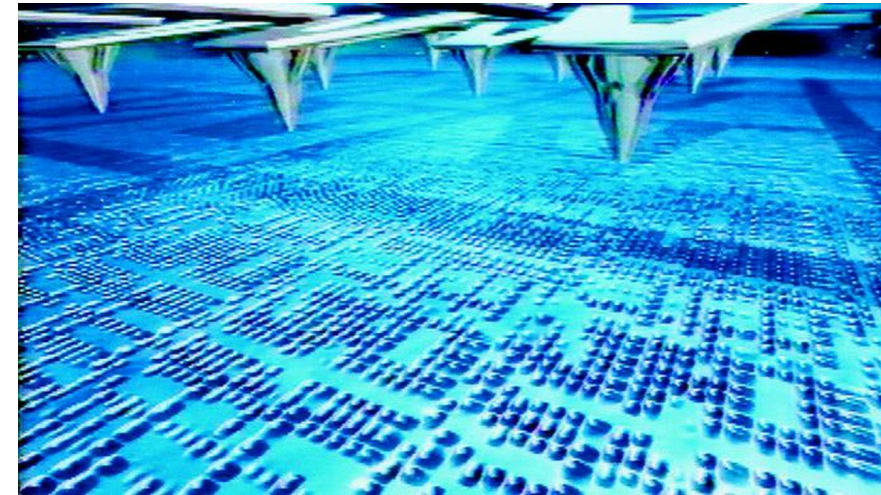
«Physical» magnetic phase transition

Nature Nanotechnology 11, 545–551 (2016)

Outlook

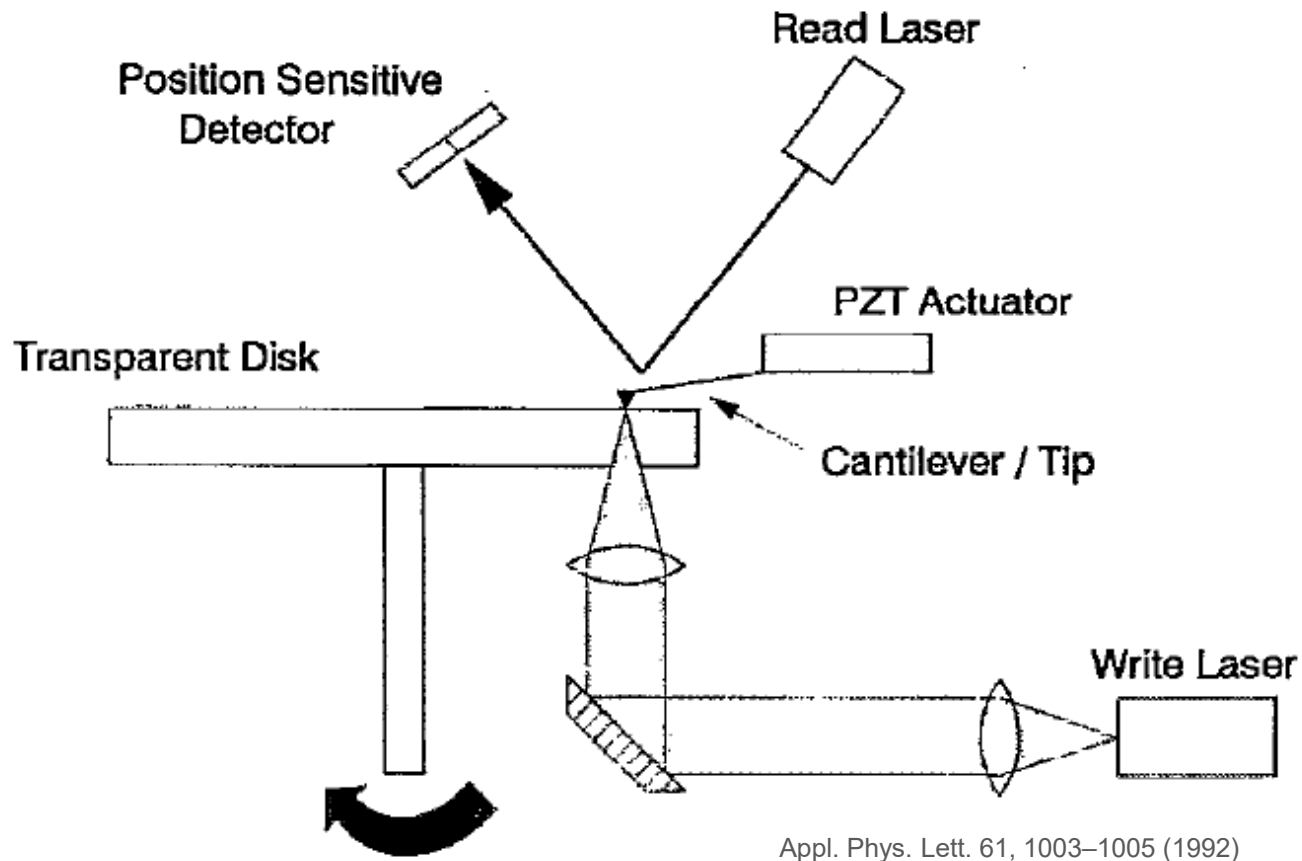
- ▶ *Scanning Probe Microscopy / Lithography*
- ▶ *Brief history of t-SPL: from milli-pedes to nano-structures*
- ▶ ***Experimental: features and limitations of t-SPL***

- ▶ *Applications:*
 - 1) *REMOVAL Direct sublimation of organic resists / lithography*
 - 2) *«CHEMICAL conversion» at the nanoscale*
 - 3) *«PHYSICAL conversion»: t-SPL for magnetism*



Thermal cantilevers #1: laser heating on standard AFM tip

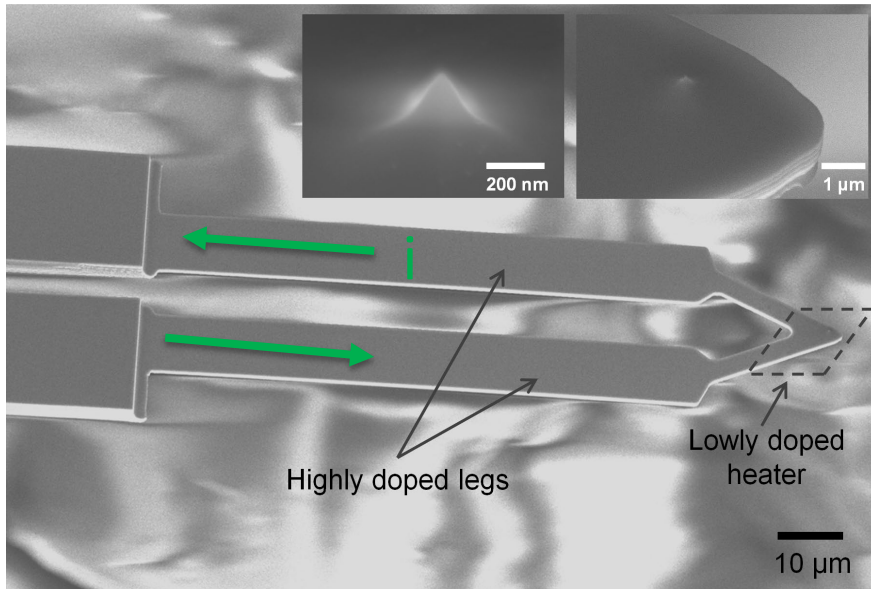
Conventional AFM tip, heated by a laser focused on the cantilever



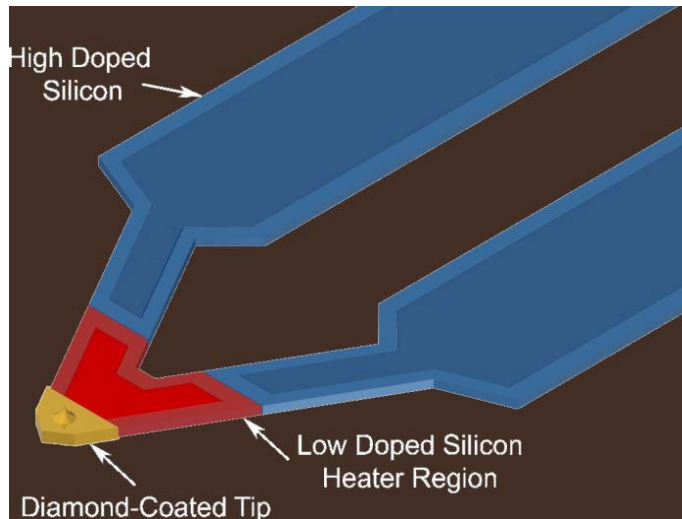
Pros / cons

- + Uses standard AFM tips
- Hard to scale and integrate
- Complex setup (laser, lenses, focusing..)

Thermal cantilevers #2: resistive heating for writing

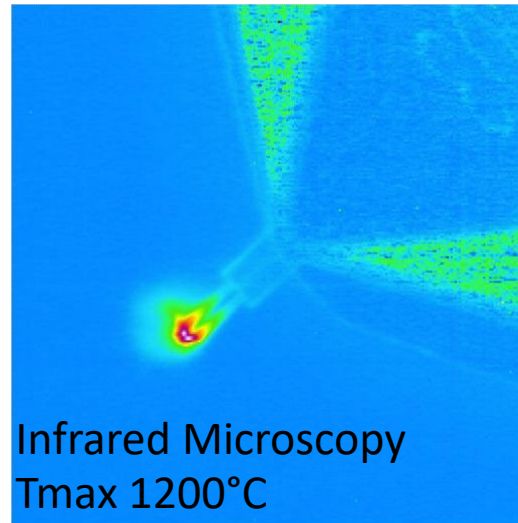


D. Wang Ph.D. Thesis, GeorgiaTech 2010



Fletcher et al., ACS Nano (2010) 4:3338

Microfabricated AFM tip, with a resistive heater located on top of the tip, which can be heated controllably via Joule effect. The sensing is performed via conventional optical lever + photodetector

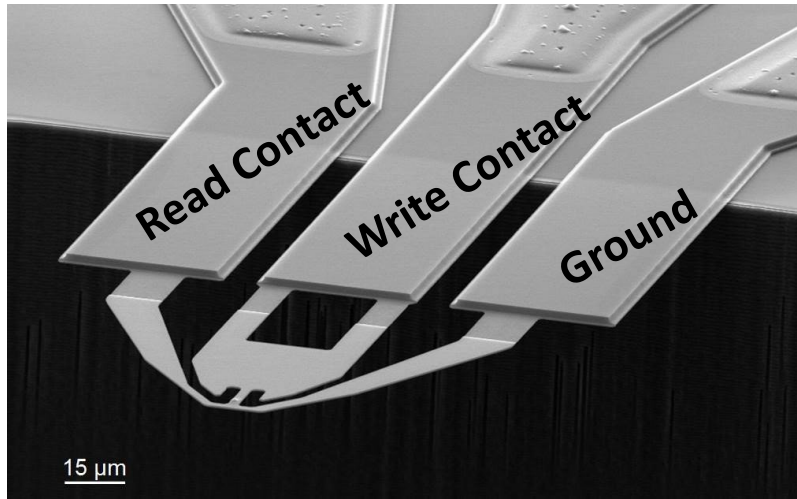


Pros / cons

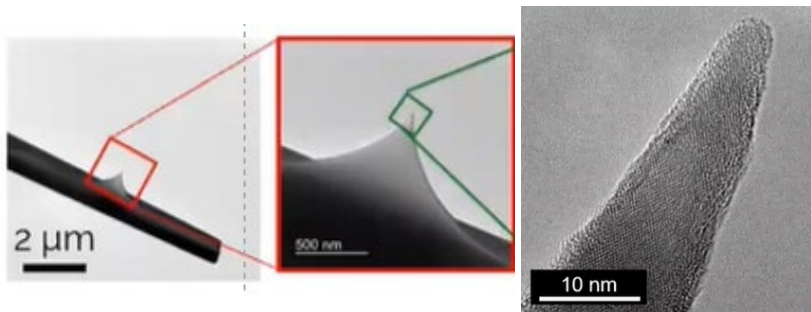
- + Integrated
- + Highly controlled temperature
- Complex fabrication with respect to standard TIP
- Hardly scalable (reading is still via laser)

Thermal cantilevers #3: resistive heating for writing AND reading

“Millipede concept”. Microfabricated AFM tip, with a resistive heater located on top of the tip, which can be heated controllably via Joule effect. The sensing is performed via a second resistive heater which is used as a distance sensor (resistance changes when approaching the surface).

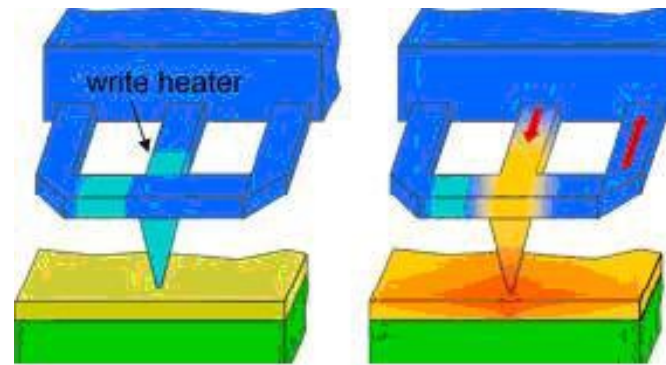


Quantum Design

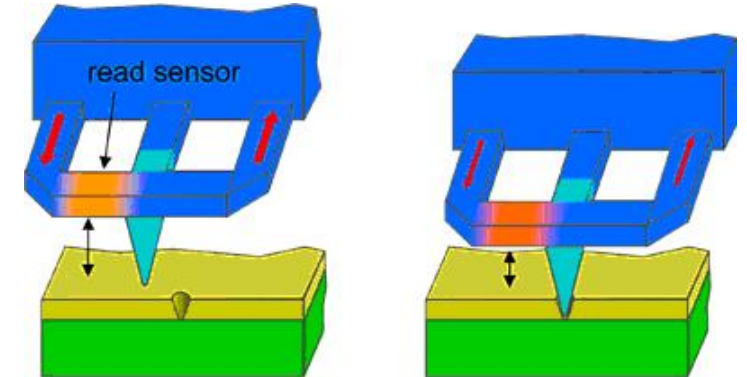


Heidelberg Instruments

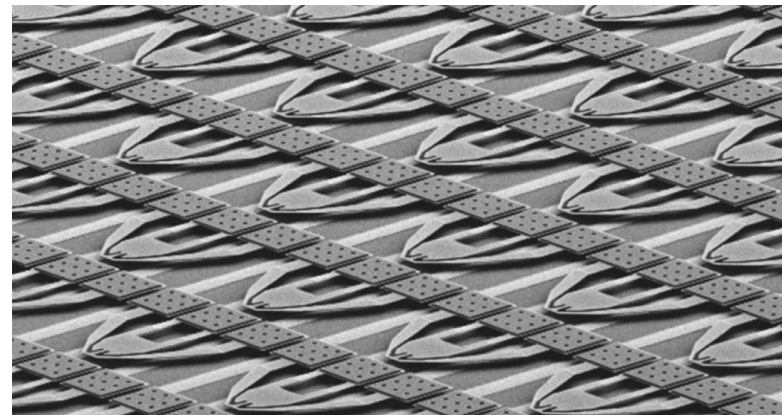
Writing operation



Reading operation



Parallelization



Pros / cons

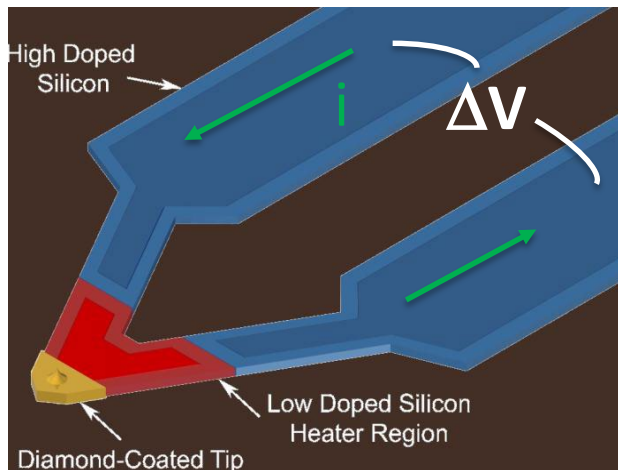
- + Integrated
- + Controlled temperature
- + Multiplexing capability
- Complex fabrication with respect to standard TIP

Thermal cantilevers: thermal characteristics

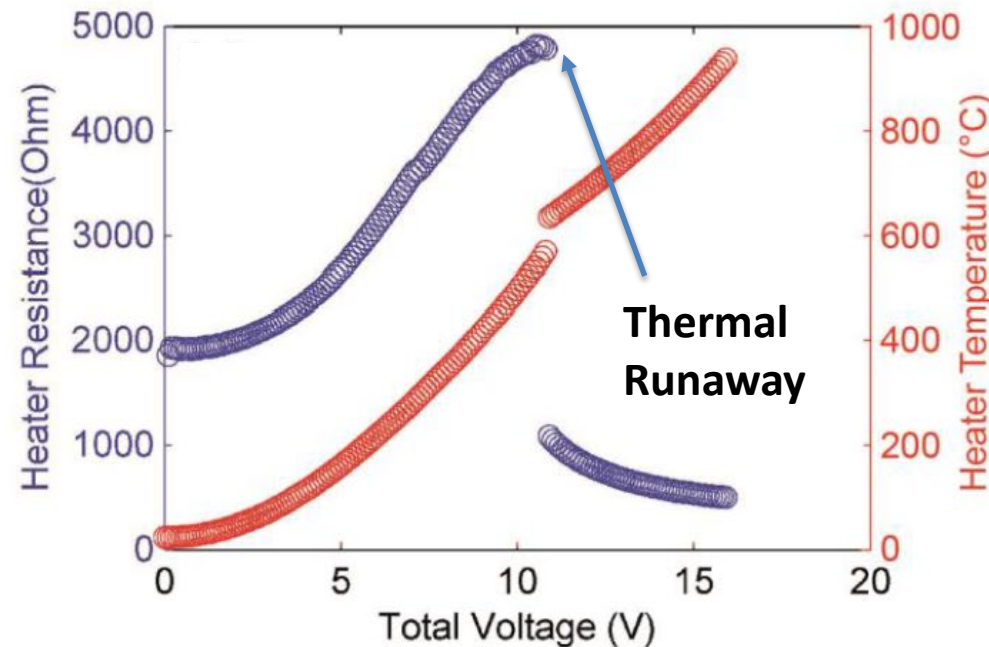
In semiconducting Si, the intrinsic carrier density varies widely with temperature. When the temperature of the heater region reaches a certain level (T_i), the intrinsic carrier density in the silicon exceeds the dopant carrier density. Above T_i , the extra carriers that become available cause the heater region to decrease in resistance, which in turn allows more current to flow, thereby generating more resistive heating ($P = Vi$).

$$T_H = RT + \frac{T_i - RT}{P_i} P_H$$

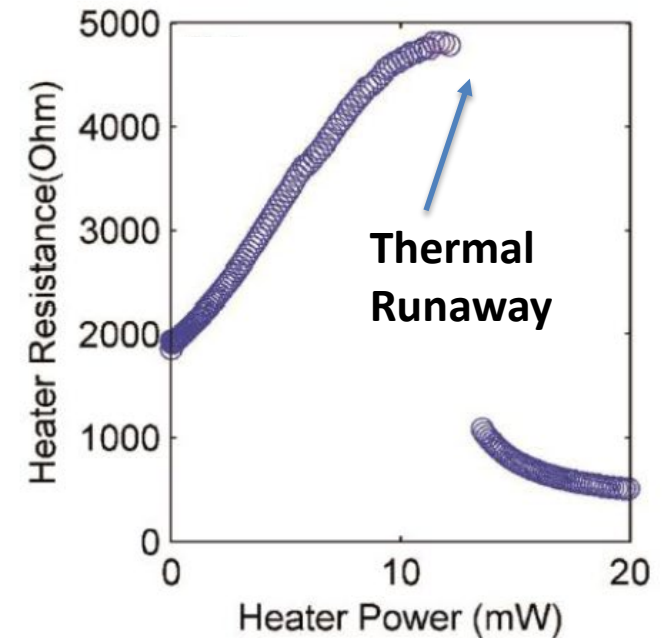
T_i around 550°C



Applied Voltage vs Resistance / Temp

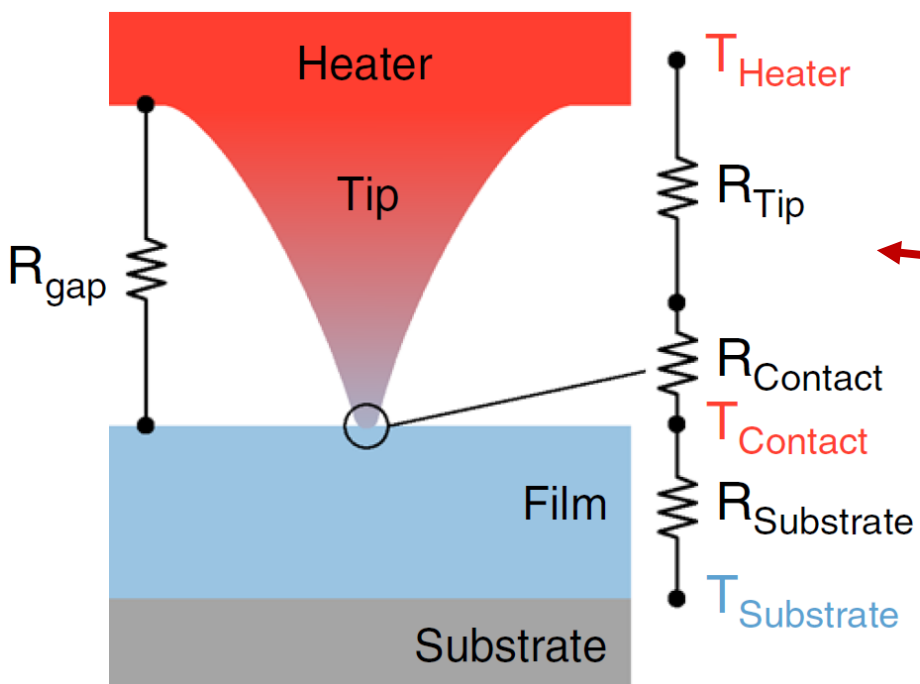


Power vs Resistance



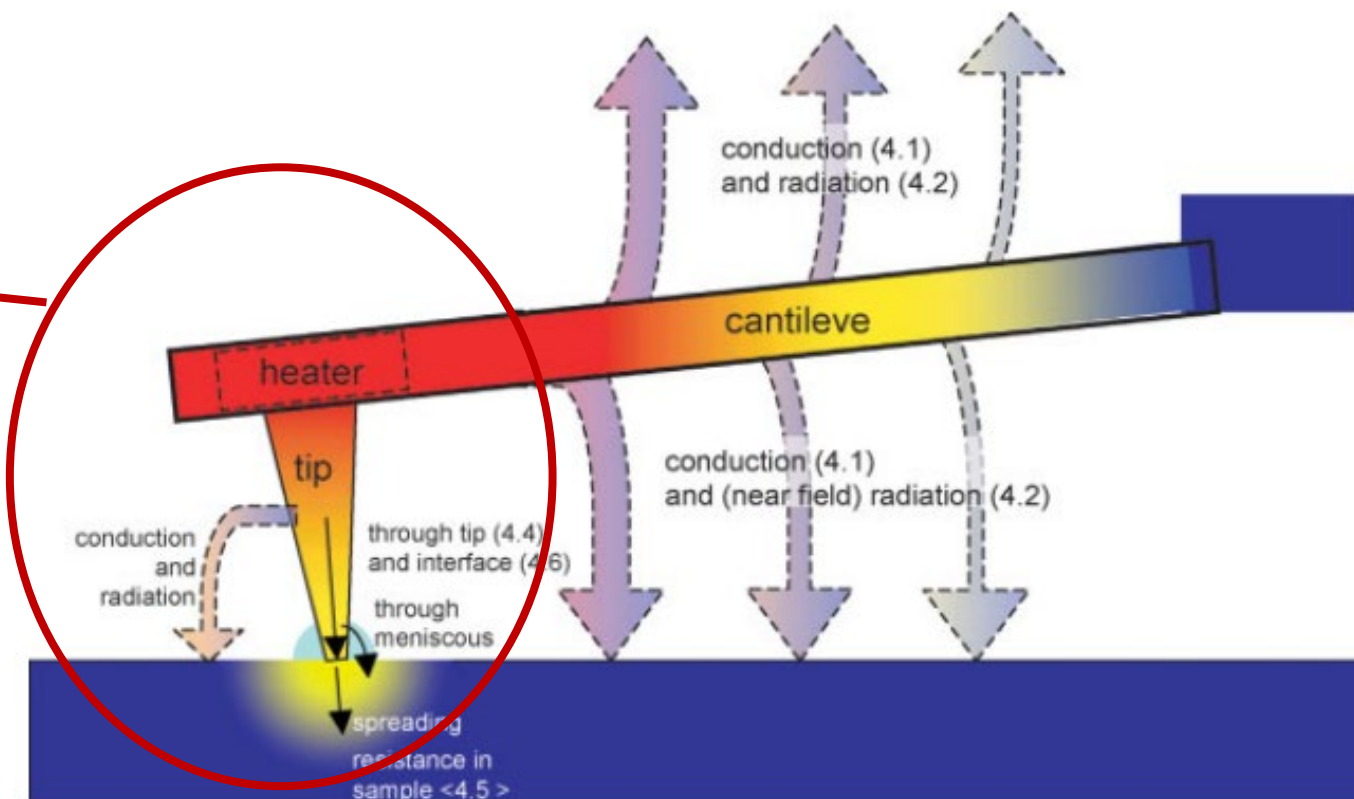
Thermal transport from tip to sample

Tip/Sample Thermal resistance model



Howell et al. Microsystems & Nanoengineering (2020) 6:21

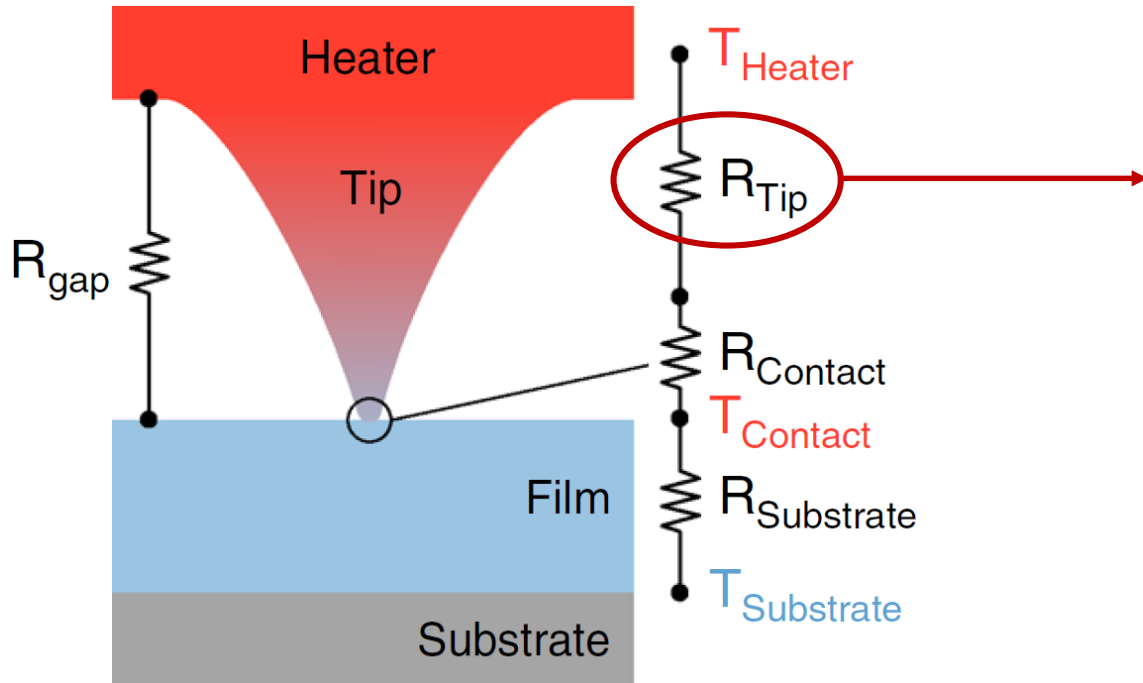
Heat transfer pathes



Nanotechnology 121–169, <https://doi.org/10.1002/9783527628155.nanotech066>

Thermal transport from tip to sample

Tip/Sample Thermal resistance model



Conductance of the phonons within the silicon tip and from the layer of native oxide covering it. $R > R_{\text{bulk}}$

- Enhanced phonon scattering with boundary surfaces.
- Reduction of the cross section area towards the tip apex (T over 90% of R_{tip} occurs at the first 10% of the tip length).

Sharp tips, lower opening angle -> Lower T

$$k = \frac{1}{3} C v (\Lambda_0^{-1} + d^{-1})^{-1}$$

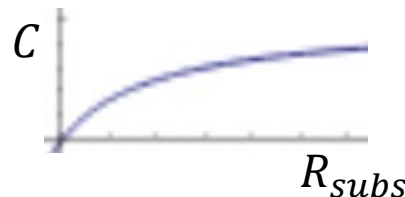
C heat capacity

v phonon speed

Λ_0 phonon mean free path

d diameter

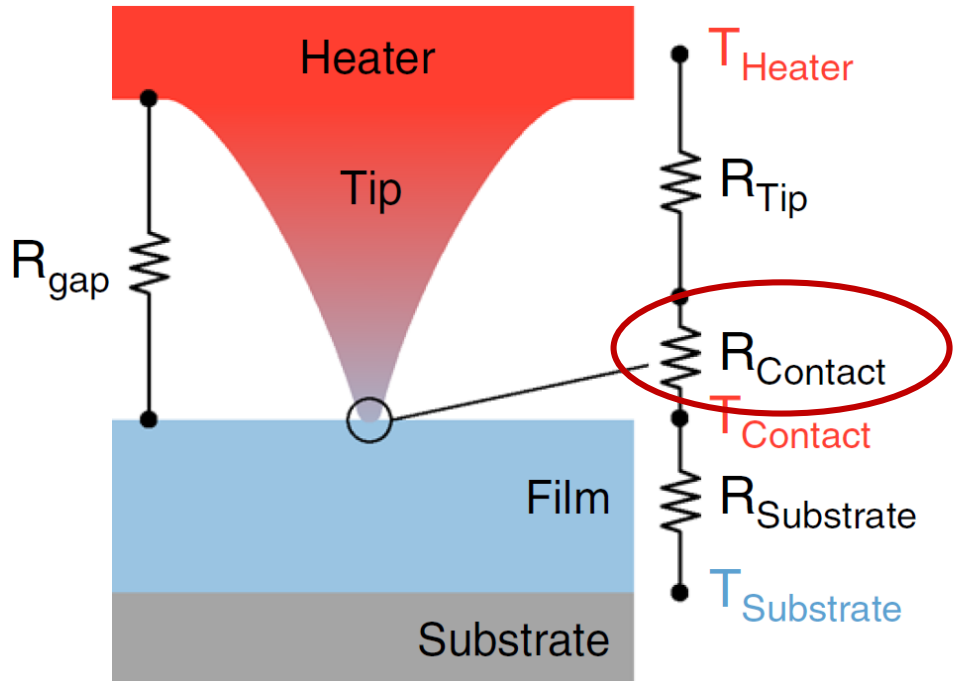
$$C = \frac{T_{\text{cont}}}{T_{\text{heat}}} = \frac{R_{\text{subs}}}{R_{\text{tip}} + R_{\text{cont}} + R_{\text{subs}}}$$



Howell et al. Microsystems & Nanoengineering (2020) 6:21

Thermal transport from tip to sample

Tip/Sample Thermal resistance model



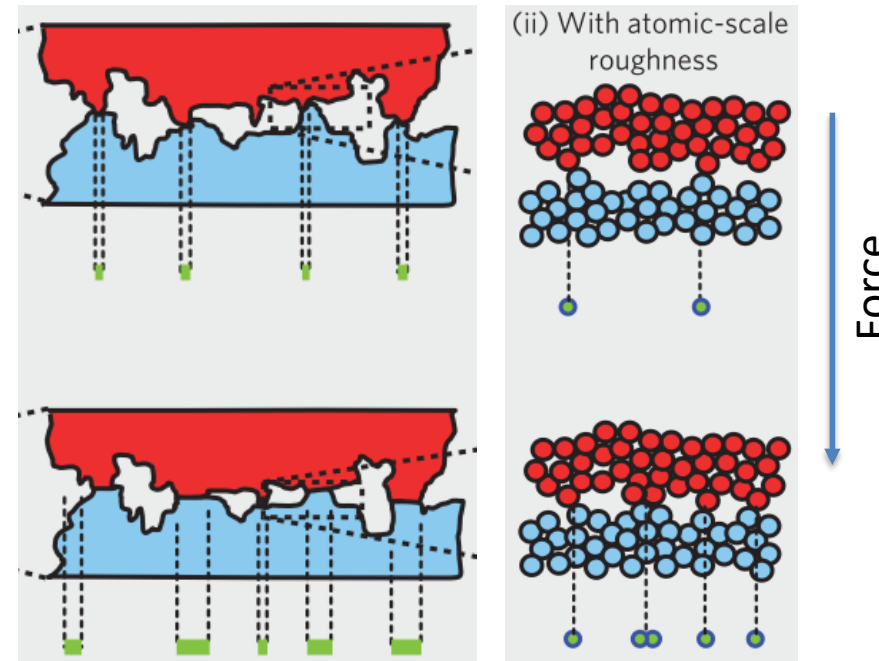
Howell et al. Microsystems & Nanoengineering (2020) 6:21

$$C = \frac{T_{cont}}{T_{heat}} = \frac{R_{subs}}{R_{tip} + R_{cont} + R_{subs}}$$

Quantum thermal transport across individual contact points.
The number of contact points increases with the applied force
+ Thermal conduction through meniscus.

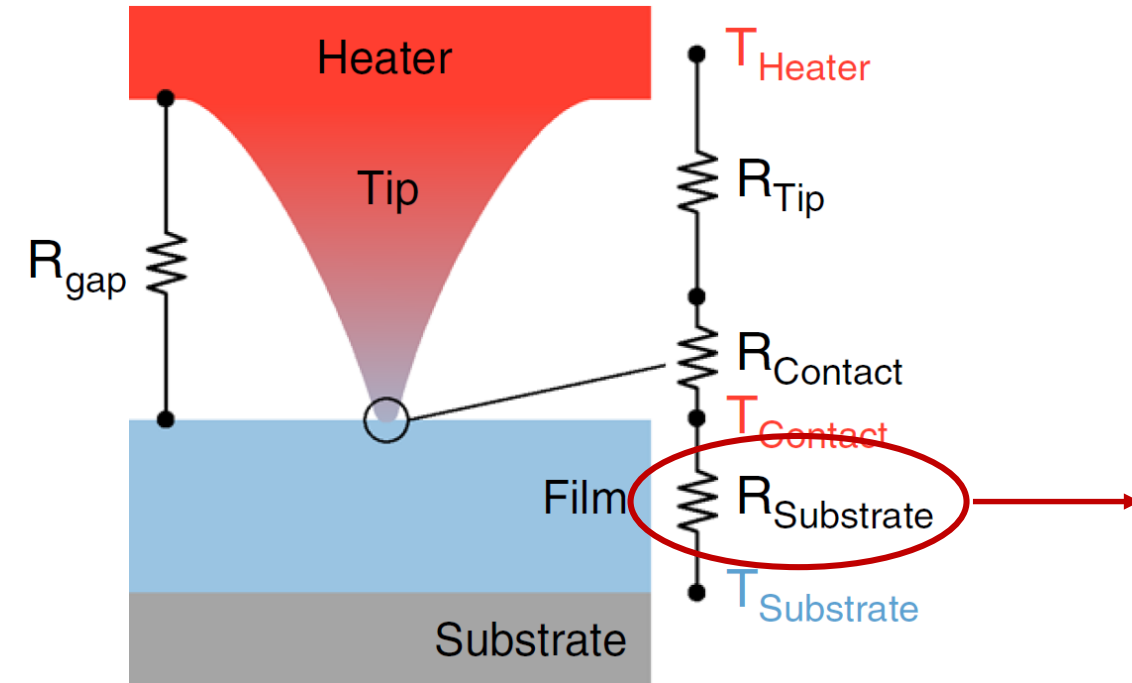
Extremely complex to predict!

Approx: a single-asperity contact characterized by a contact diameter d_0 .



Thermal transport from tip to sample

Tip/Sample Thermal resistance model



Howell et al. Microsystems & Nanoengineering (2020) 6:21

Well understood and depends on the thermal conductance of the film, film thickness, contact point diameter, substrate thermal conductance.

$$R_{\text{sp}} = \frac{1}{2\kappa_s d_0} - \frac{1}{2\pi\kappa_s t} \log\left(\frac{2}{1 + \kappa_s/\kappa_{\text{sub}}}\right)$$

κ_s thermal cond film

d_0 contact diameter

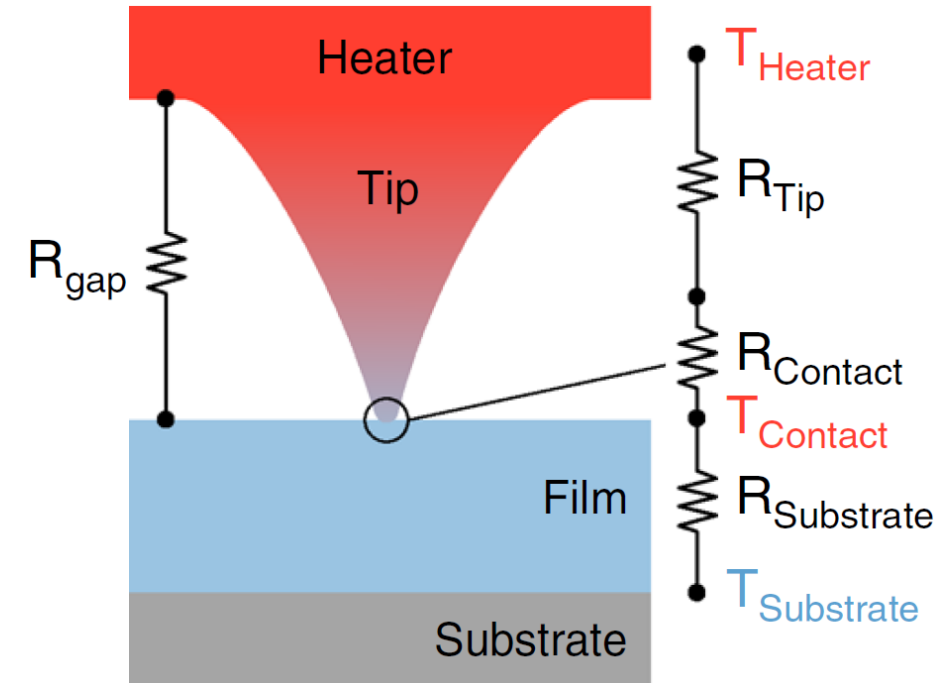
t film thickness

κ_{sub} thermal cond substrate

$$C = \frac{T_{\text{cont}}}{T_{\text{heat}}} = \frac{R_{\text{subs}}}{R_{\text{tip}} + R_{\text{cont}} + R_{\text{subs}}}$$

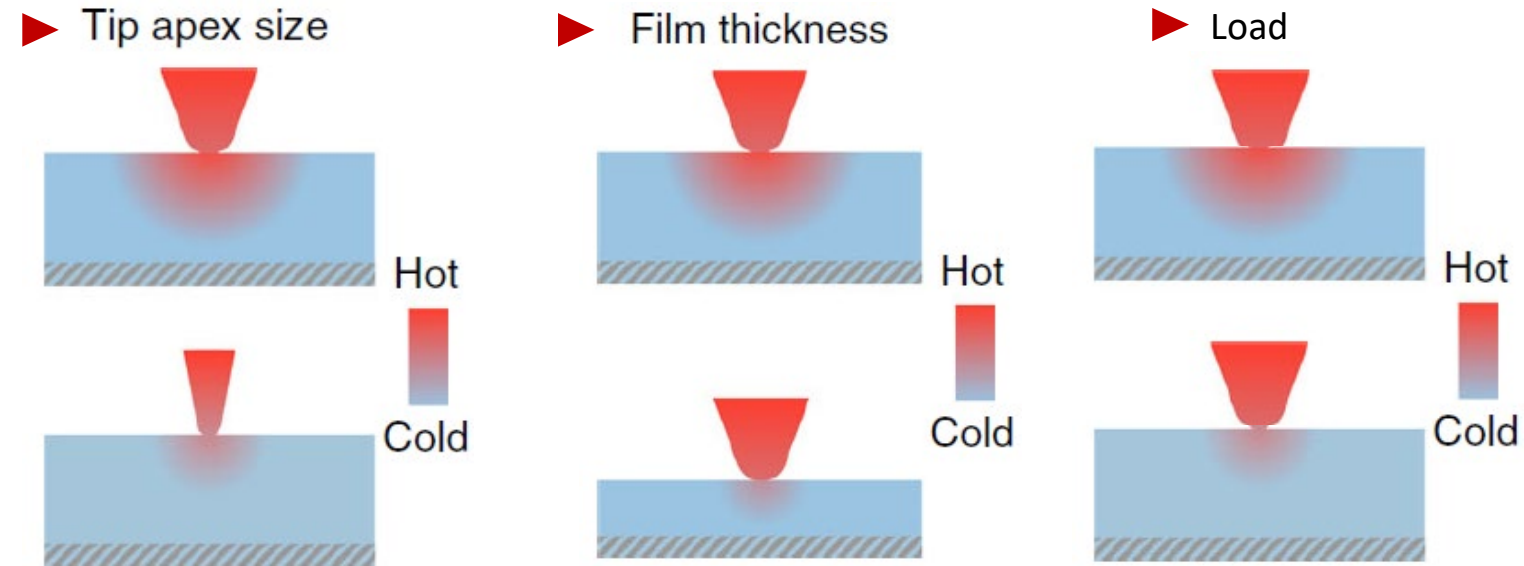
Thermal transport from tip to sample

Tip/Sample Thermal resistance model



Howell et al. Microsystems & Nanoengineering (2020) 6:21

Parameters influencing T_{contact}



Howell et al. Microsystems & Nanoengineering (2020) 6:21

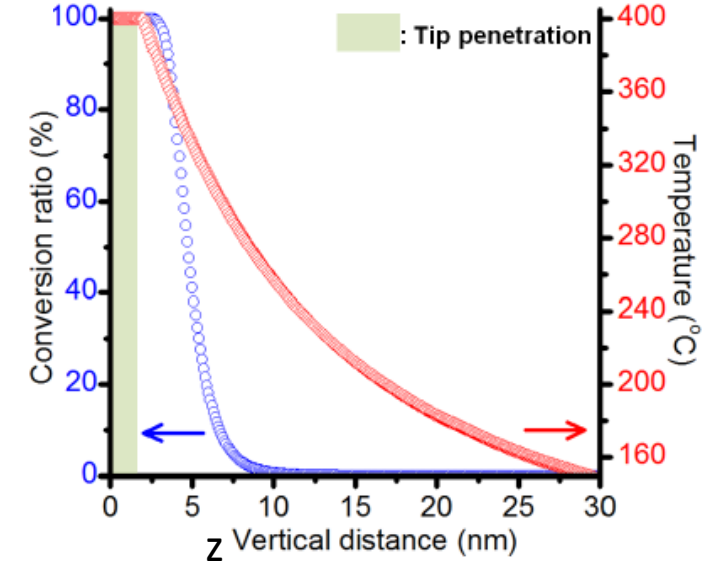
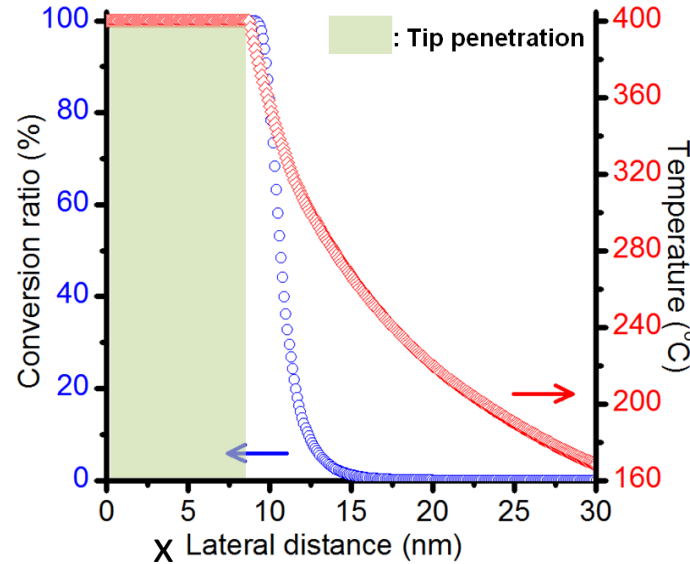
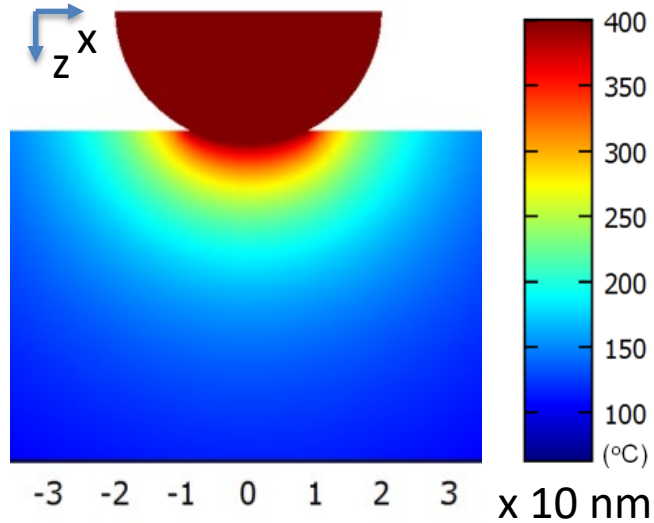
- Film thermal conductivity (Higher K : lower T , higher resolution)

$$C = \frac{T_{\text{cont}}}{T_{\text{heat}}} = \frac{R_{\text{subs}}}{R_{\text{tip}} + R_{\text{cont}} + R_{\text{subs}}}$$

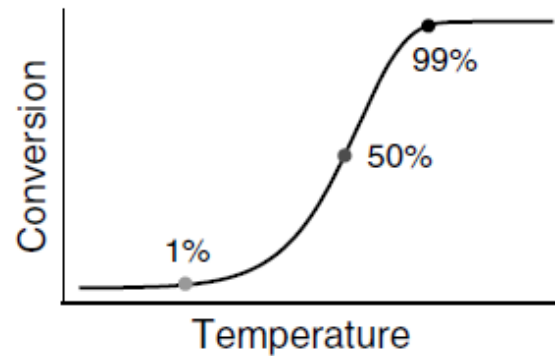
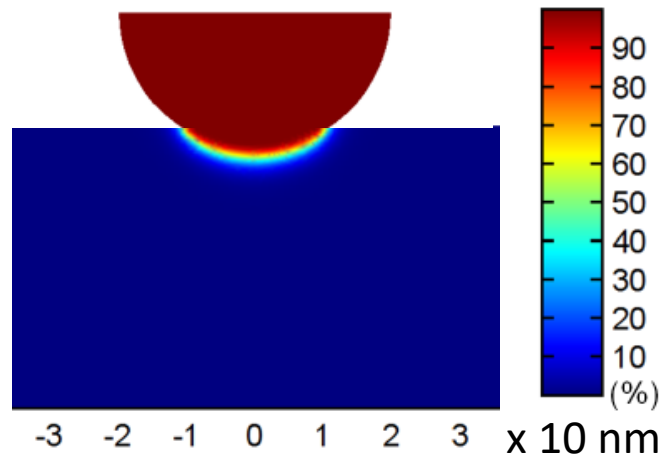
Influence of the temperature on the conversion efficiency

Finite element modelling (FEM) of the temperature and amine conversion profile inside a carbamate copolymer.

Temperature vs distance



Conversion ratio vs distance



The effective conversion profile depends on the COMBINATION of the thermal profile and the temperature dependence of the reaction

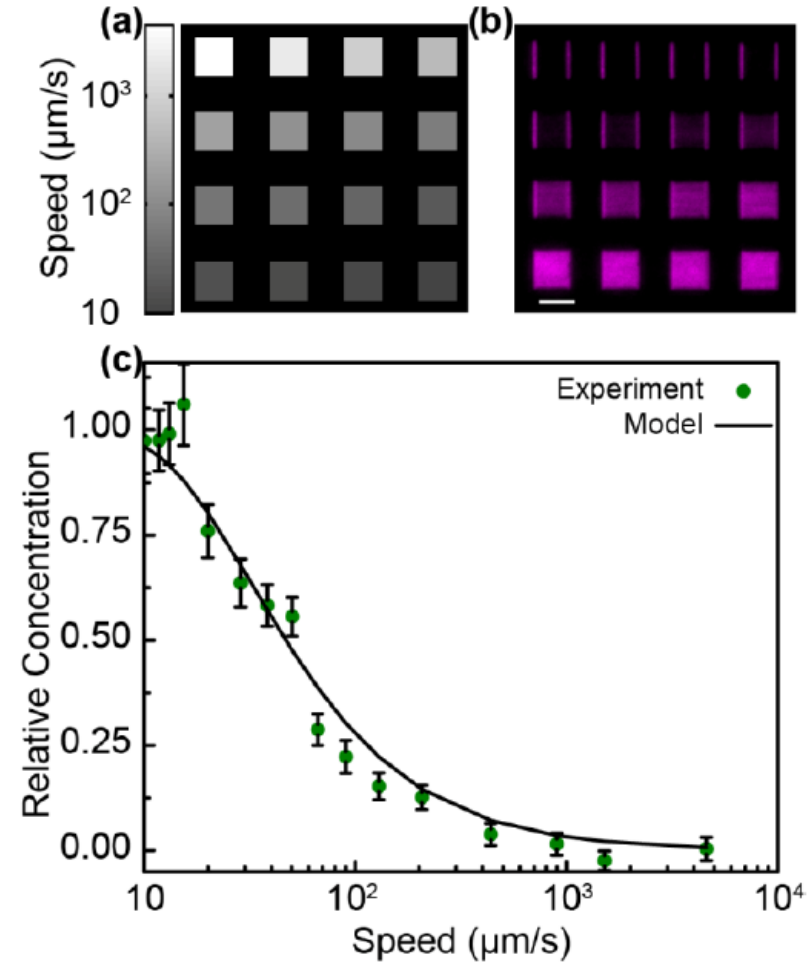
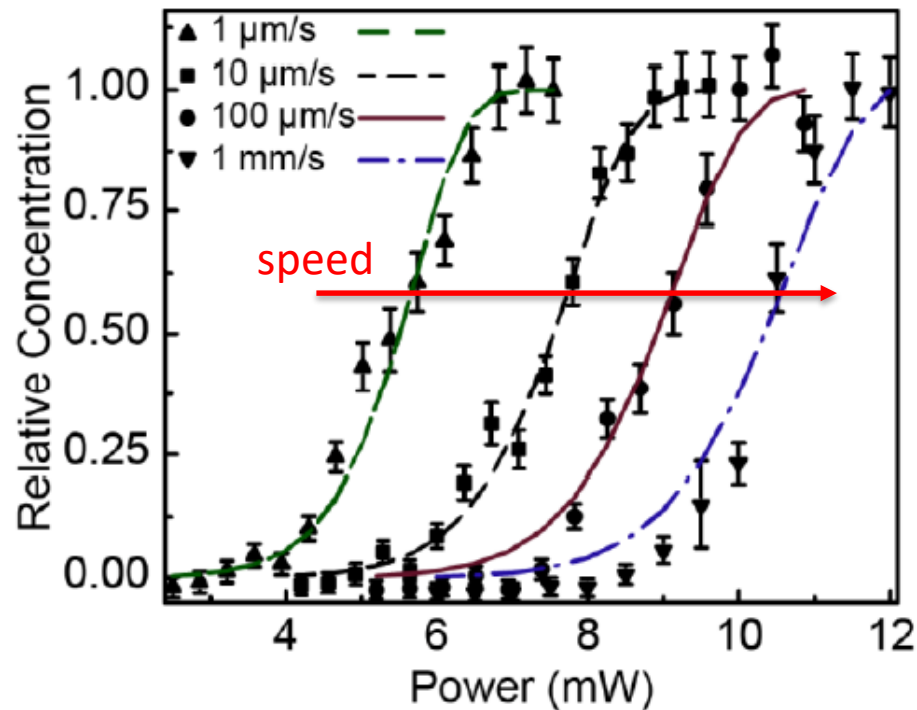
Debin Wang, Ph.D. Thesis GeorgiaTech 2010

Influence of the patterning speed on the conversion efficiency

Controlled thermally-induced deprotection of amine groups from a polymeric film

Fixed temperature, varying speed

Conversion efficiency at different speed



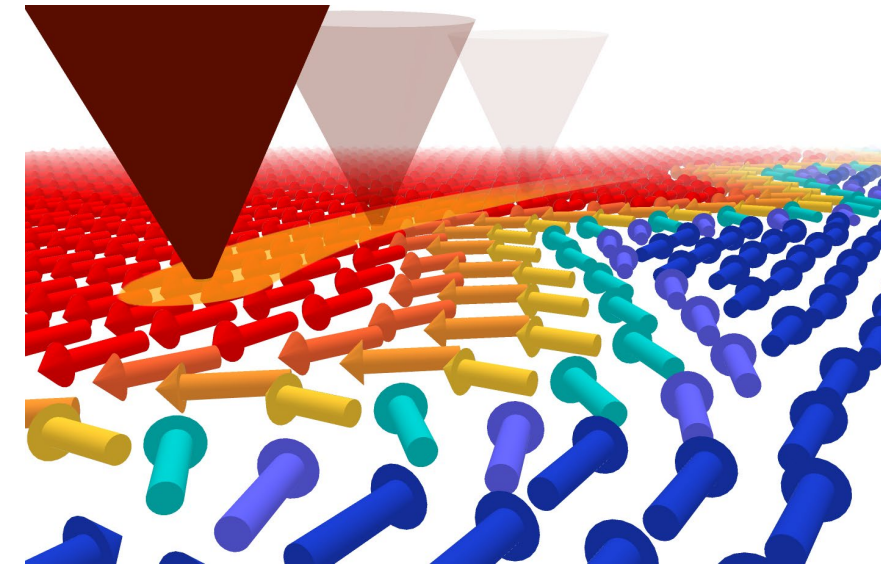
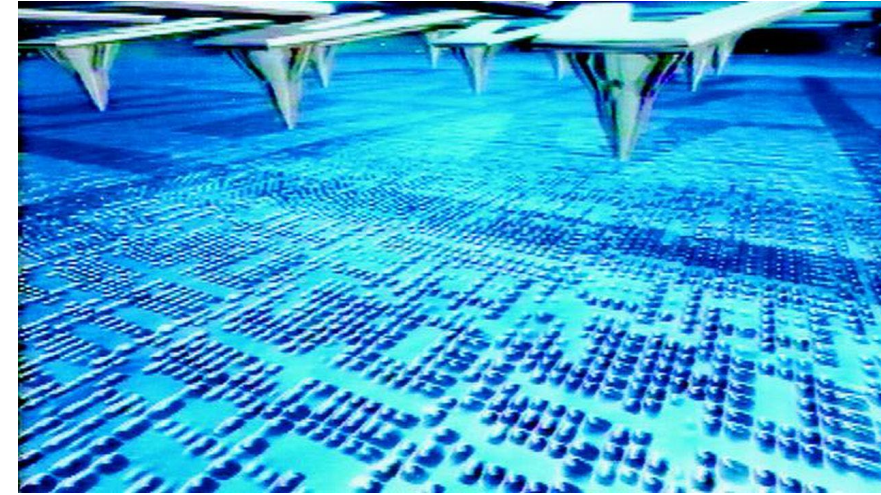
Higher speed exposes the system to the temperature profile for less time, resulting in a decreased rate of reaction.

Keith Carroll, Ph.D. Thesis GeorgiaTech 2013

Outlook

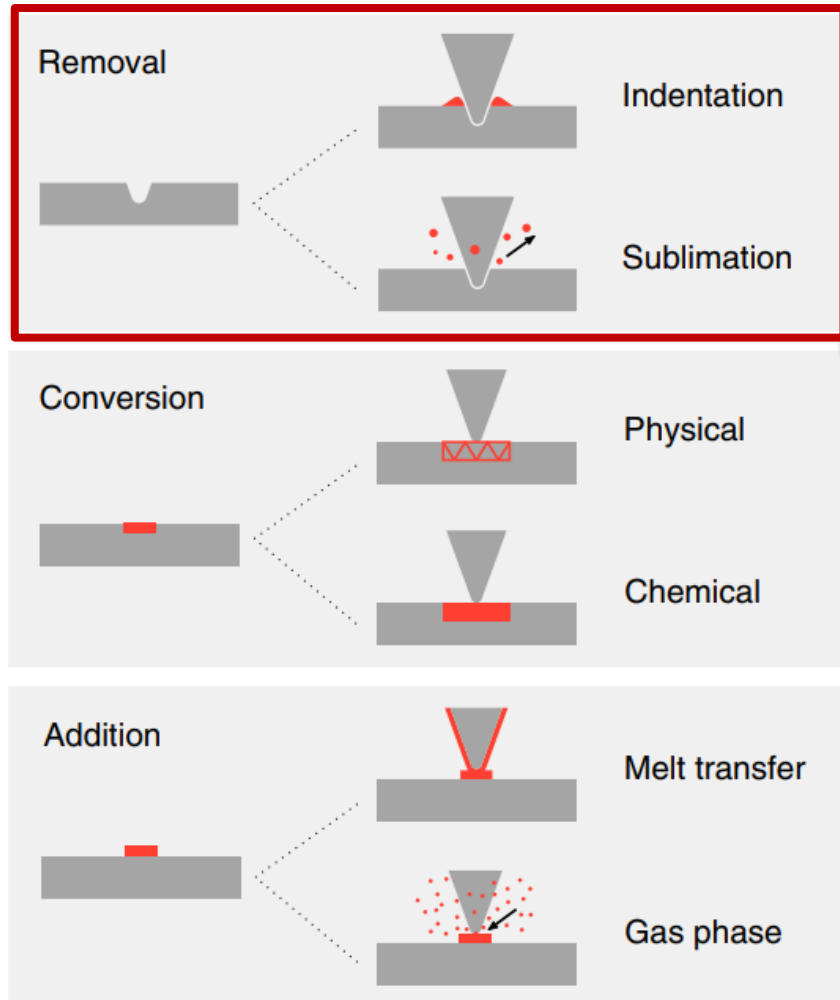
- ▶ *Scanning Probe Microscopy / Lithography*
- ▶ *Brief history of t-SPL: from milli-pedes to nano-structures*
- ▶ *Experimental: features and limitations of t-SPL*

- ▶ ***Applications:***
 - 1) ***REMOVAL*** Direct sublimation of organic resists / lithography
 - 2) «**CHEMICAL** conversion» at the nanoscale
 - 3) «**PHYSICAL** conversion»: t-SPL for magnetism



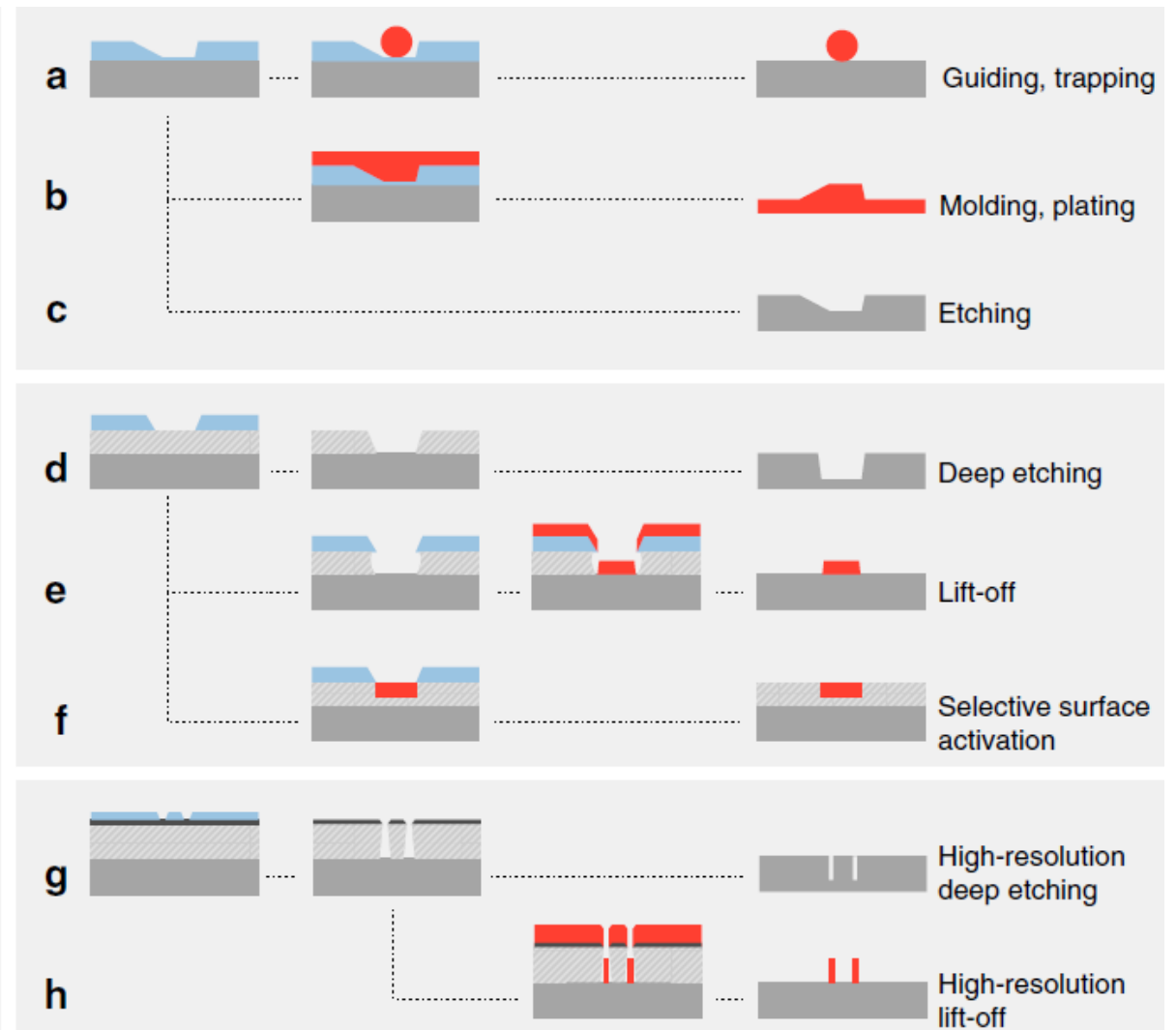
Applications of *t*-SPL: material removal

Heat as a universal stimulus



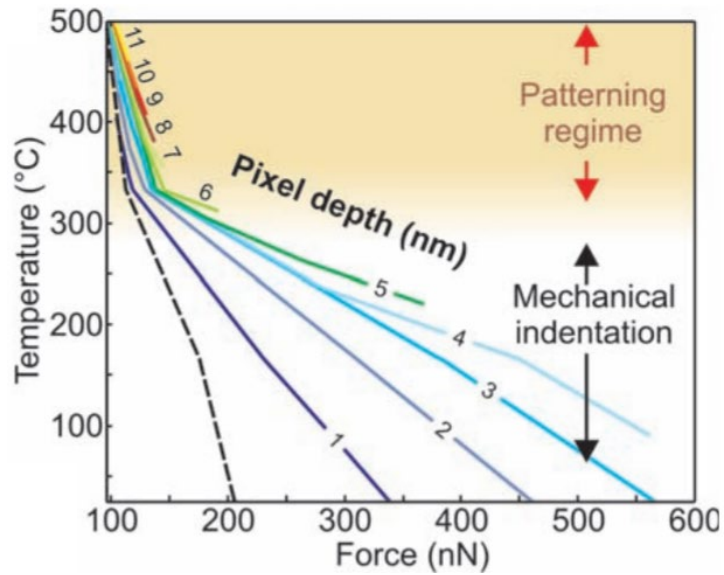
Howell et al. Microsystems & Nanoengineering (2020) 6:21

Processes involving material removal



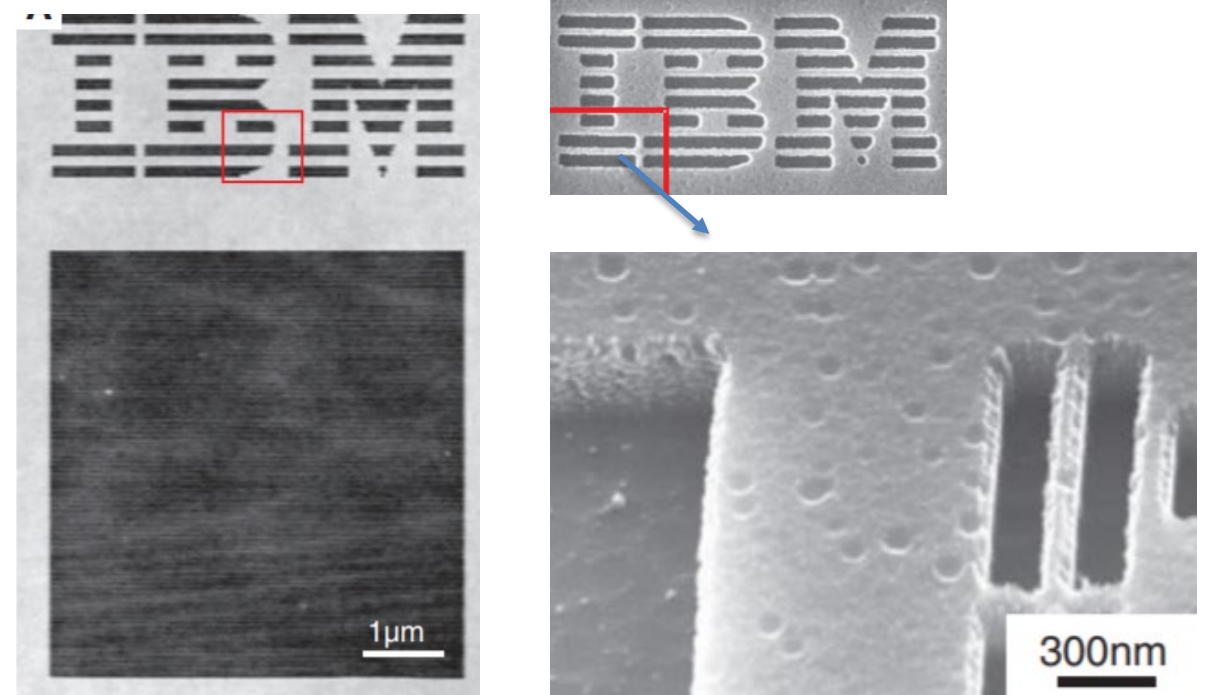
3D nanostructures in resist and transfer in Si

Equi-depth lines in resist

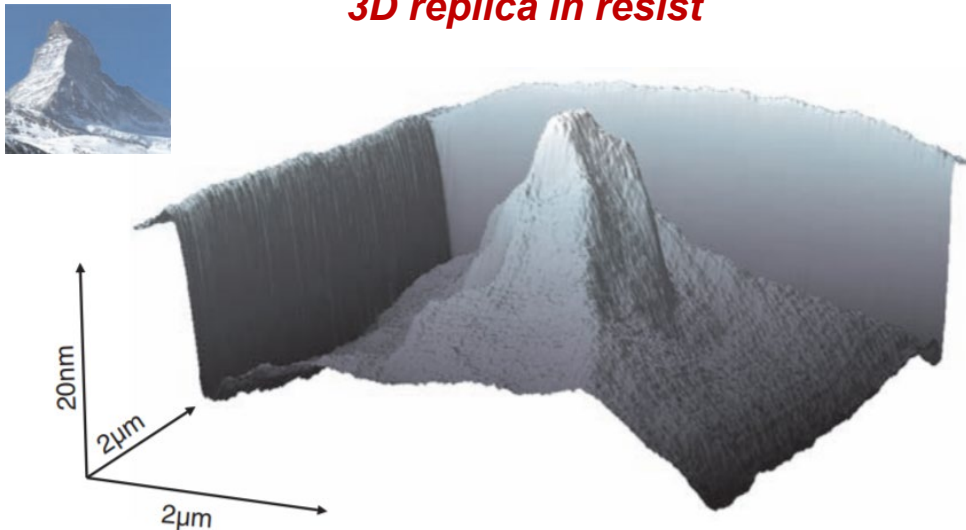


Local desorption of a glassy organic resist. Smallest width in Si 30 nm, by first transferring the pattern into a SiO₂ etch mask, and then performing a second etching step.

Pattern transfer in Si



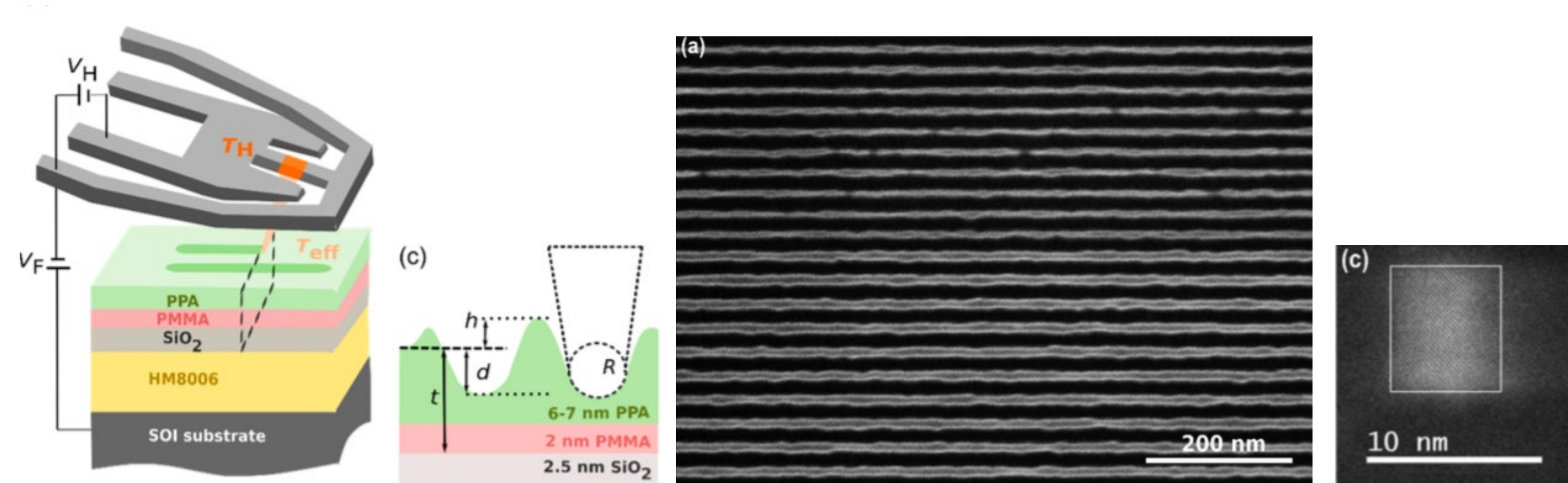
3D replica in resist



Science 328, 732–735 (2010).

Sub-10 nm features in Si via pattern transfer

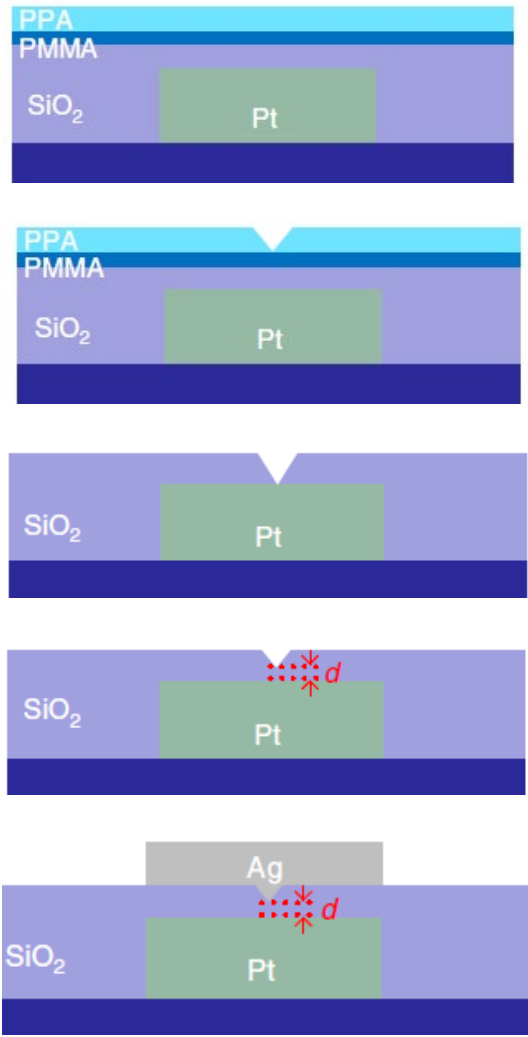
Thin lines in polyphthalaldehyde (PPA) layer, then transferred into Si. The best pattern geometry is obtained at a heater temperature of $\sim 600^\circ\text{C}$, which is below or close to the transition from mechanical indentation to thermal evaporation. For the 14 nm half-pitch lines in silicon, a line edge roughness of 2.6 nm (3σ), and a feature size of the patterned walls of 7 nm (12 nm thick Si).



ACS Nano 2017, 11, 11890–11897

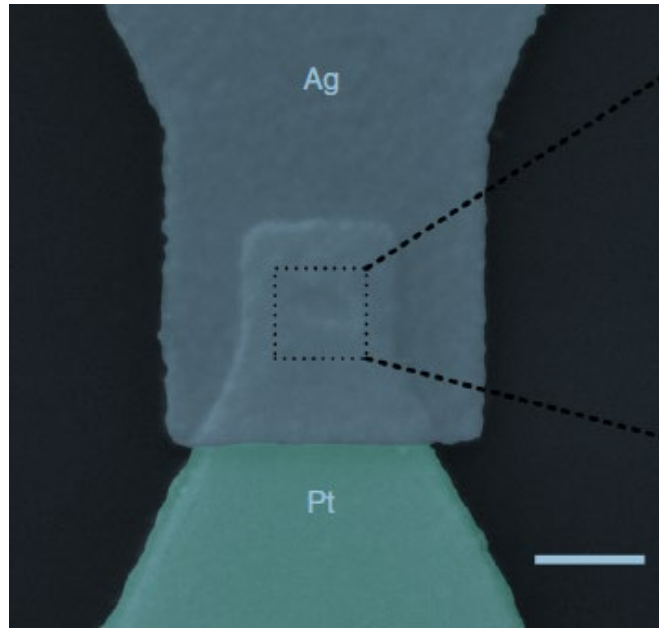
Atomic scale memristor fabrication

Fabrication process

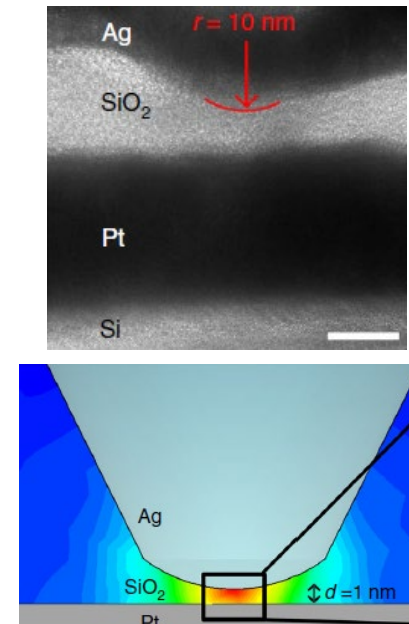


Tip-shaped structure patterned via t-SPL. Highly confined electric field at nanometer size and feature low switching voltage around 100 mV, operation speed in the nanosecond range, extinction resistance ratio as high as 6×10^5 , reliable operations despite its atomic scale dimensions, and the possibility to achieve multi-level behavior.

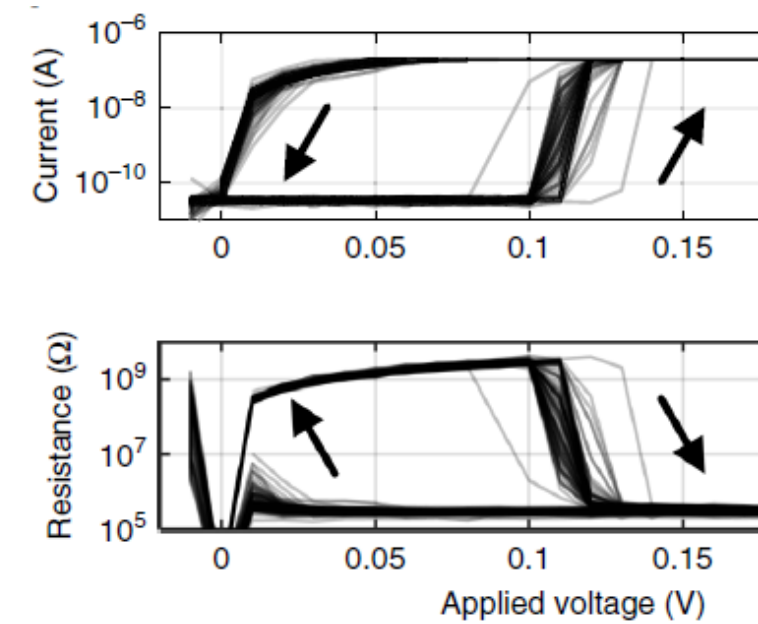
SEM top view



TEM cross section



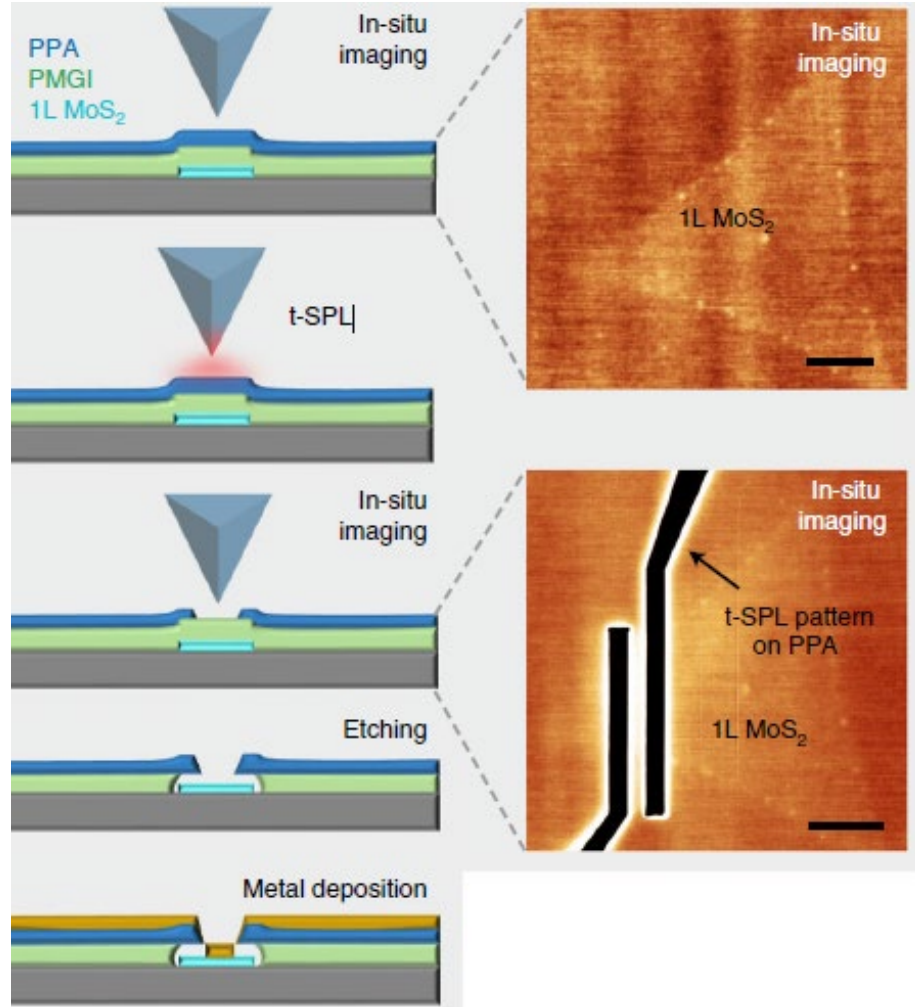
Switching characteristics



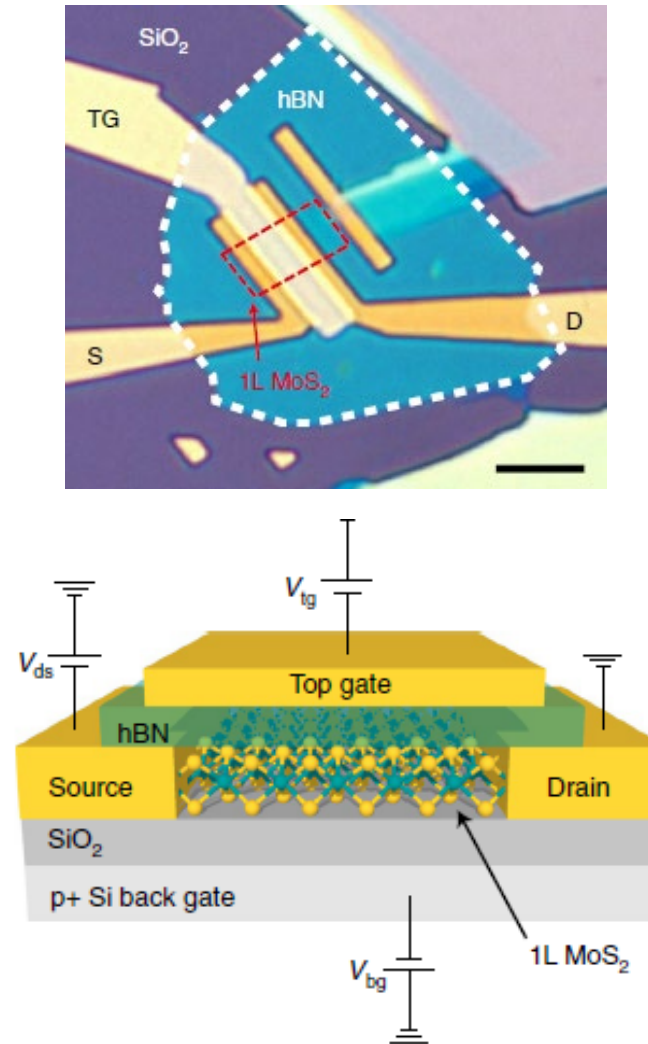
Commun. Phys. 2, 28 (2019)

Field effect transistors based on MoS_2

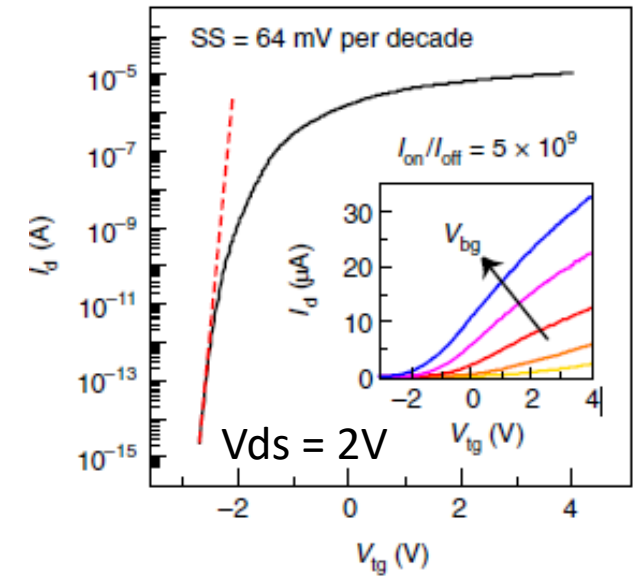
Fabrication process



Top gate FET



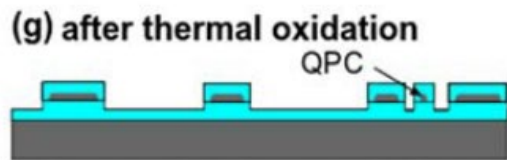
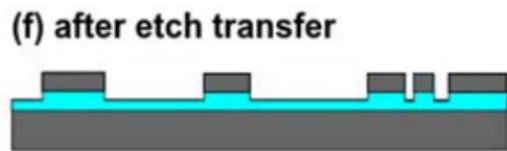
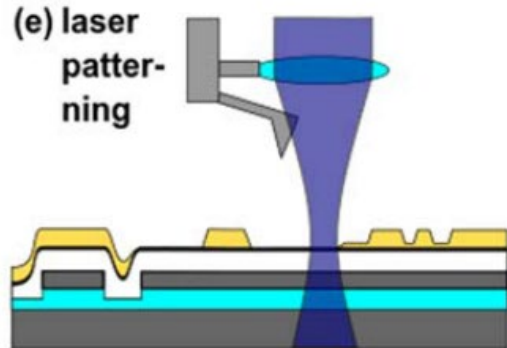
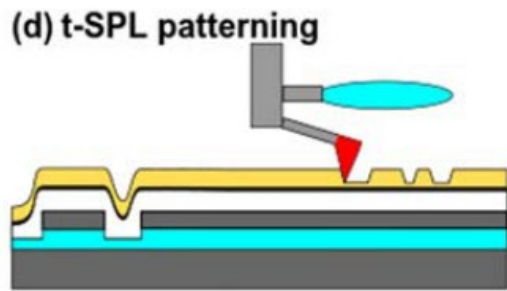
Transfer curve



X. Zheng., EA et al. Nat. Electron. 2, 17–25 (2019)

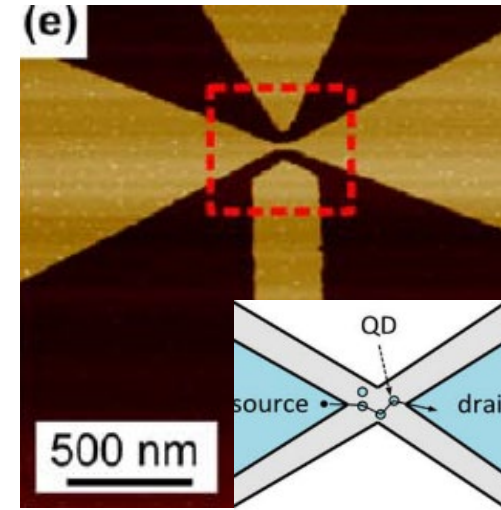
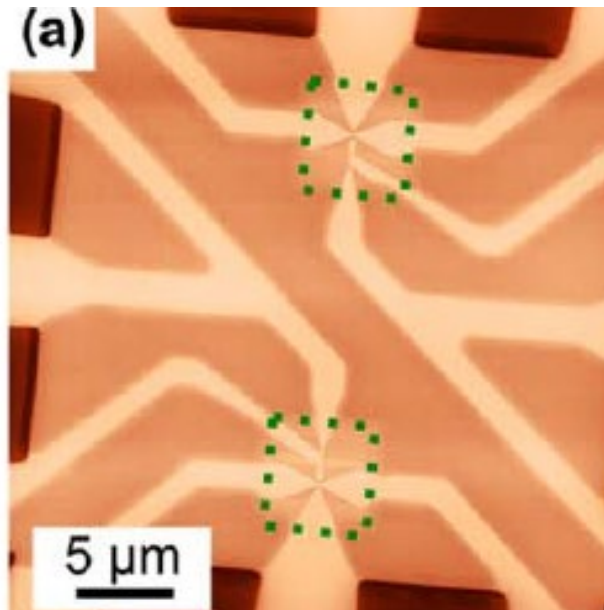
Quantum Dot Transistors via Hybrid *t*-SPL / laser writing

Fabrication process

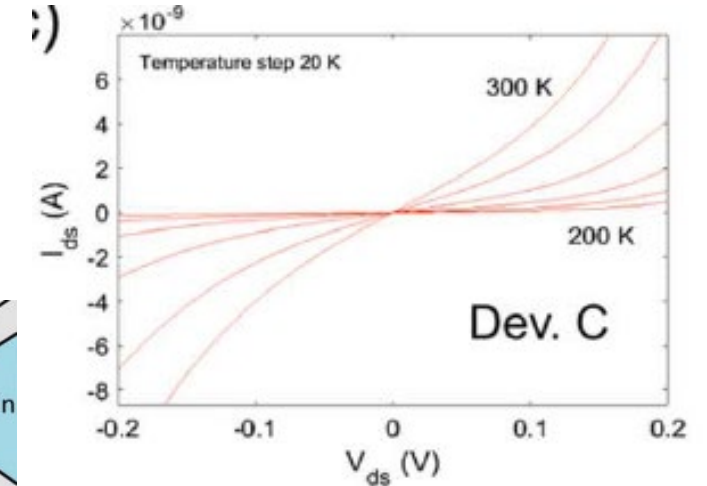


Room temperature (RT) single electron transistors (SETs) based on point-contact tunnel junctions. Electron localization within nanocrystals or phosphorous atoms embedded within the SiO2 allowed to reach tunneling behavior at RT.

Hybrid Laser + *t*-SPL patterns



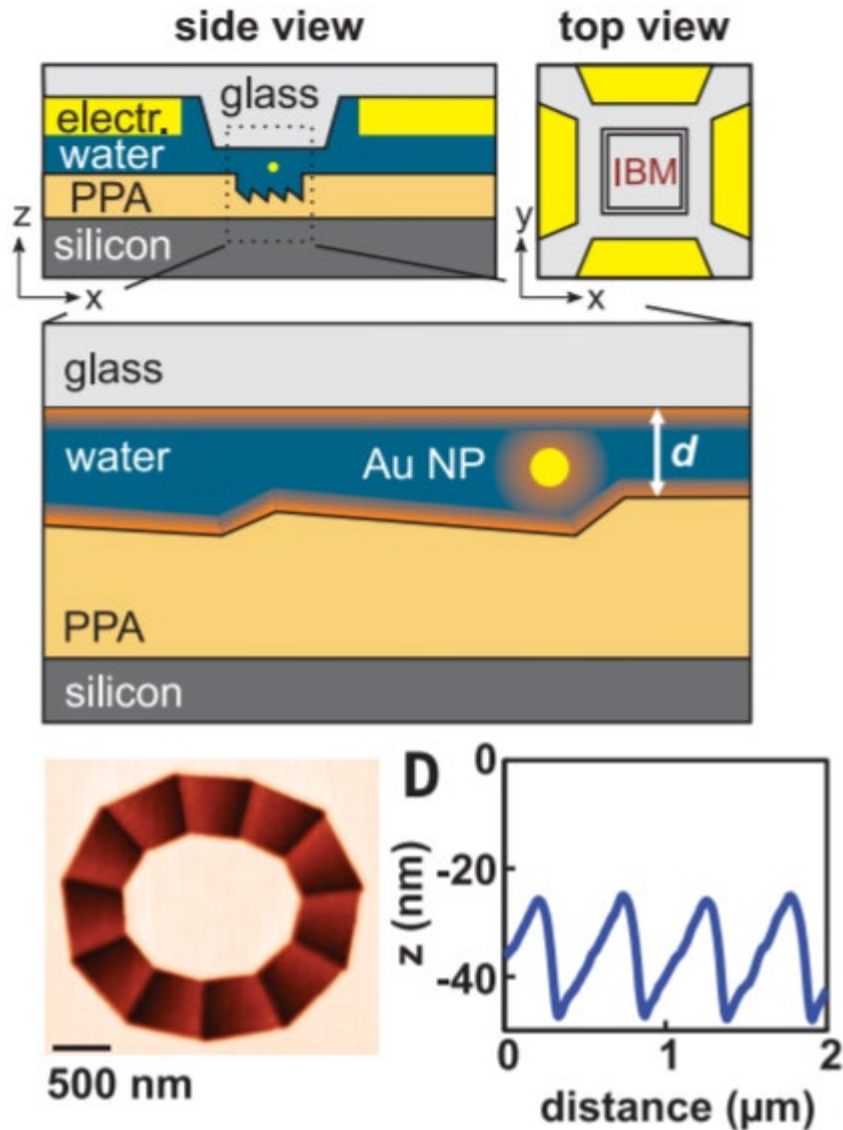
Tunnel dominated conduction at RT



Nanotechnology 29, 505302 (2018).

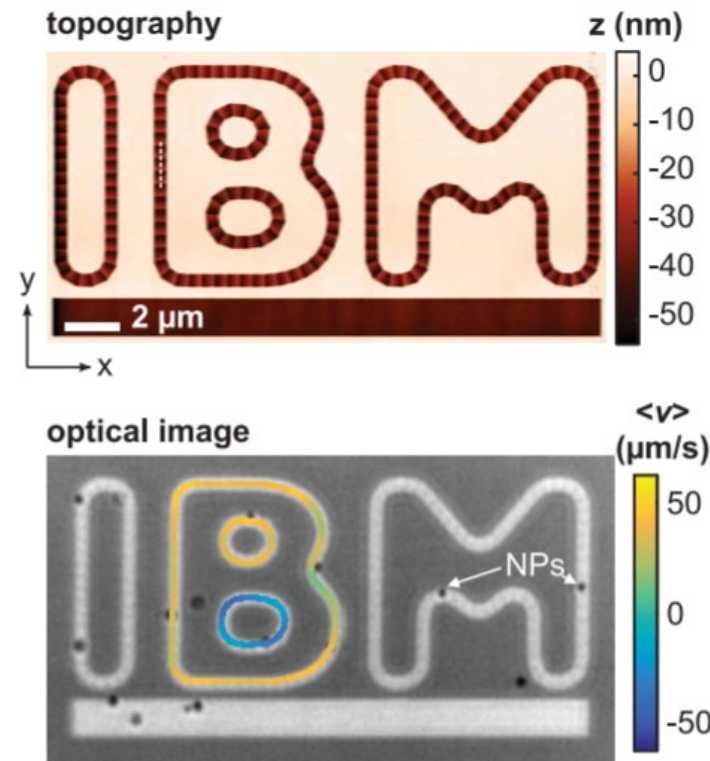
Nanofluidic Rocking Brownian motors for nanoparticle manipulation

Concept / fabrication

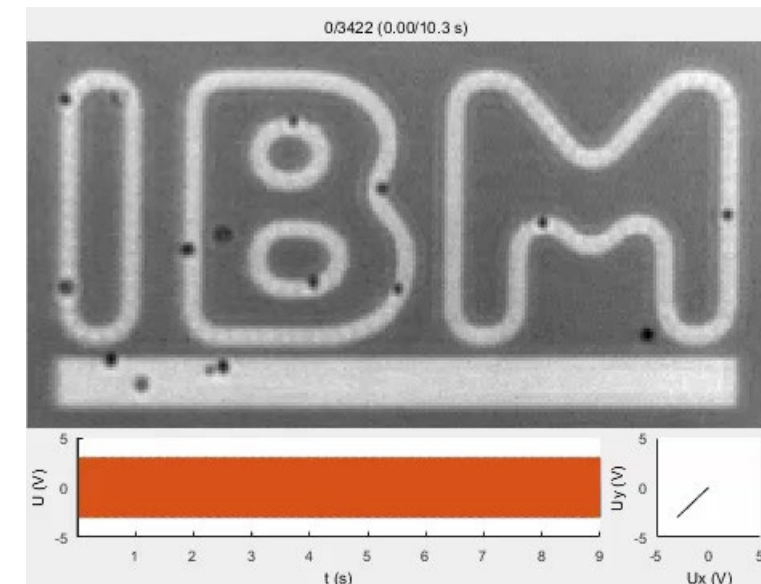


Energy landscapes for nanoparticles by accurately shaping the geometry of a nanofluidic slit and exploiting the electrostatic interaction between like-charged particles and walls. Directed transport was performed by combining asymmetric potentials with an oscillating electric field to achieve a rocking Brownian motor.

Nanoparticle Path



Directed transport via rotating E field

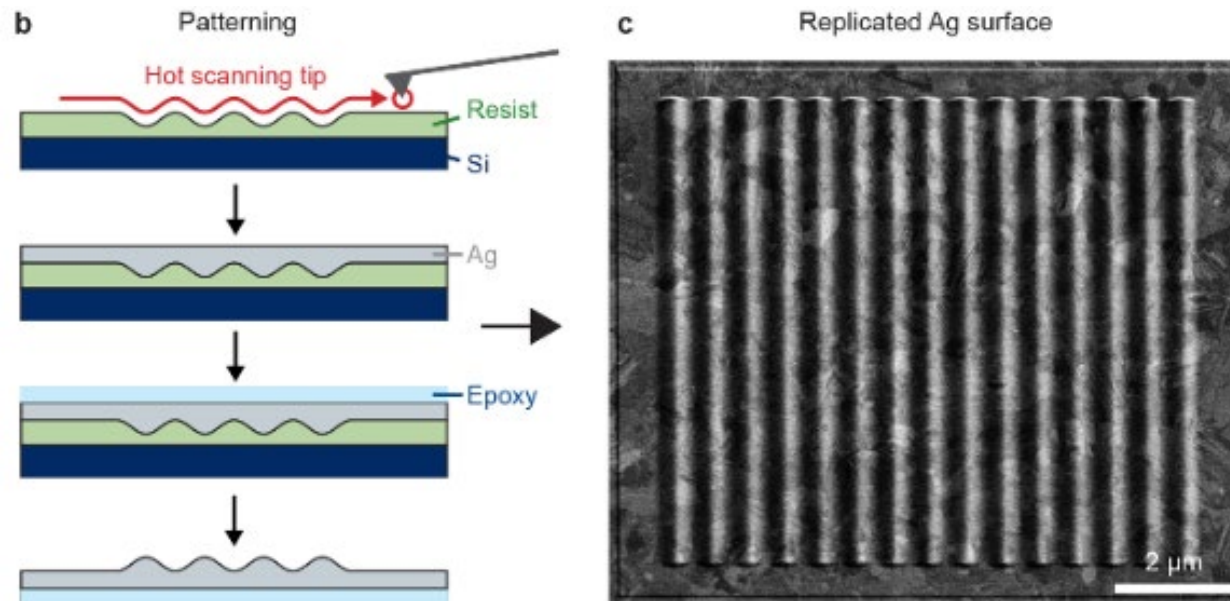


Science 359, 1505–1508 (2018).

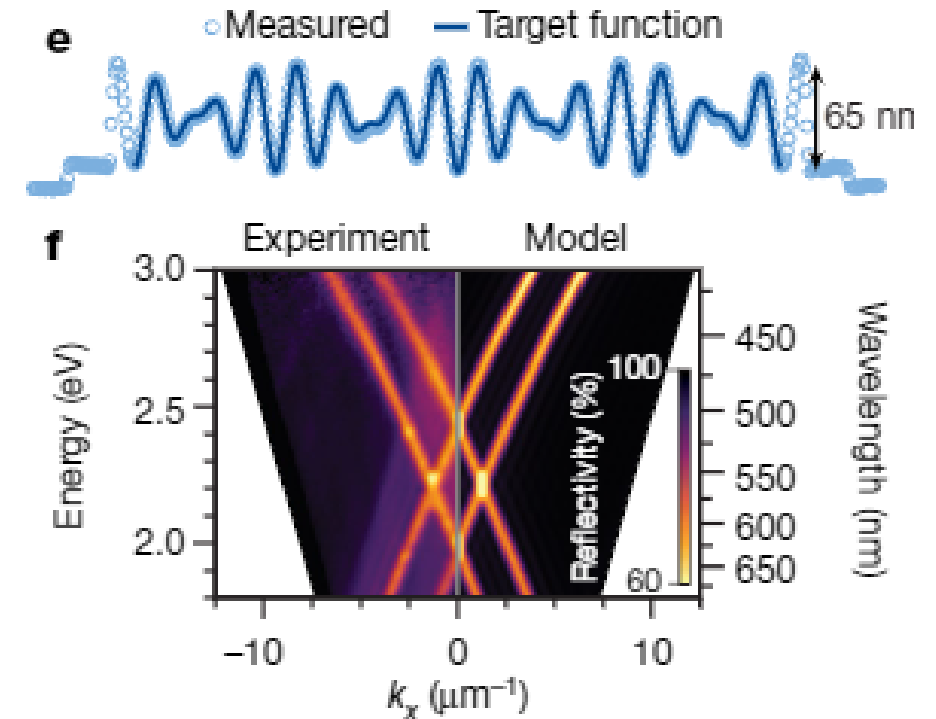
Optical Fourier Surfaces: 3D optical metasurfaces

The surface pattern generates a desired diffracted output through its Fourier transform. To shape the optical wavefront, **the ideal surface profile should contain a precise sum of sinusoidal waves**, each with a well defined amplitude, spatial frequency and phase.

Fabrication



Fourier Surface Model VS Experiment

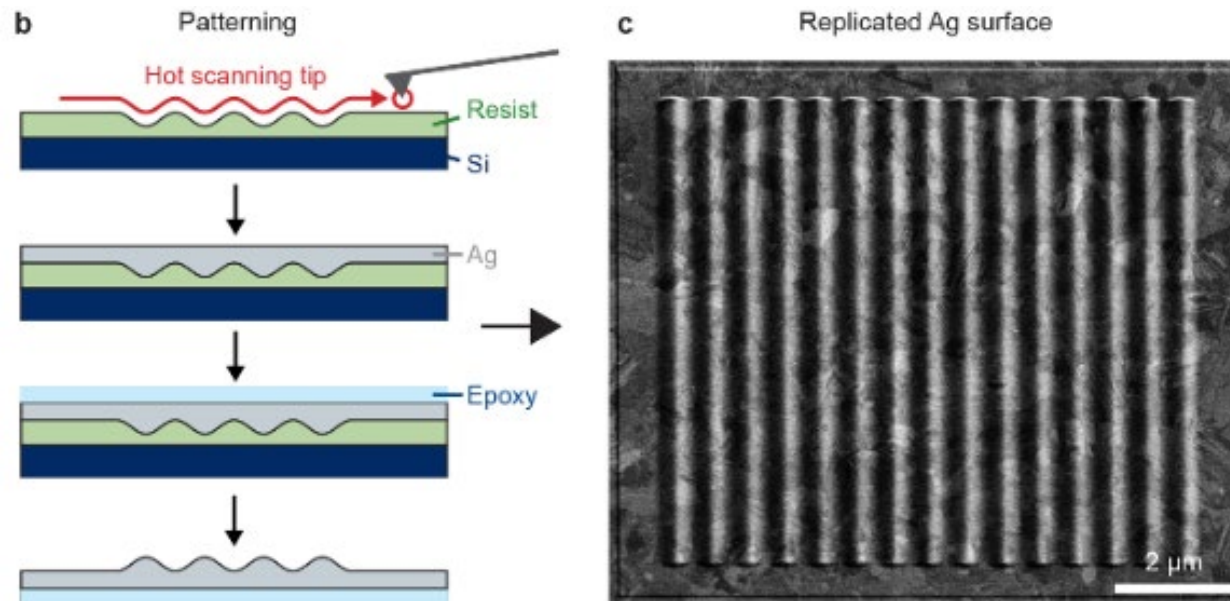


Nature 582, 506–510 (2020)

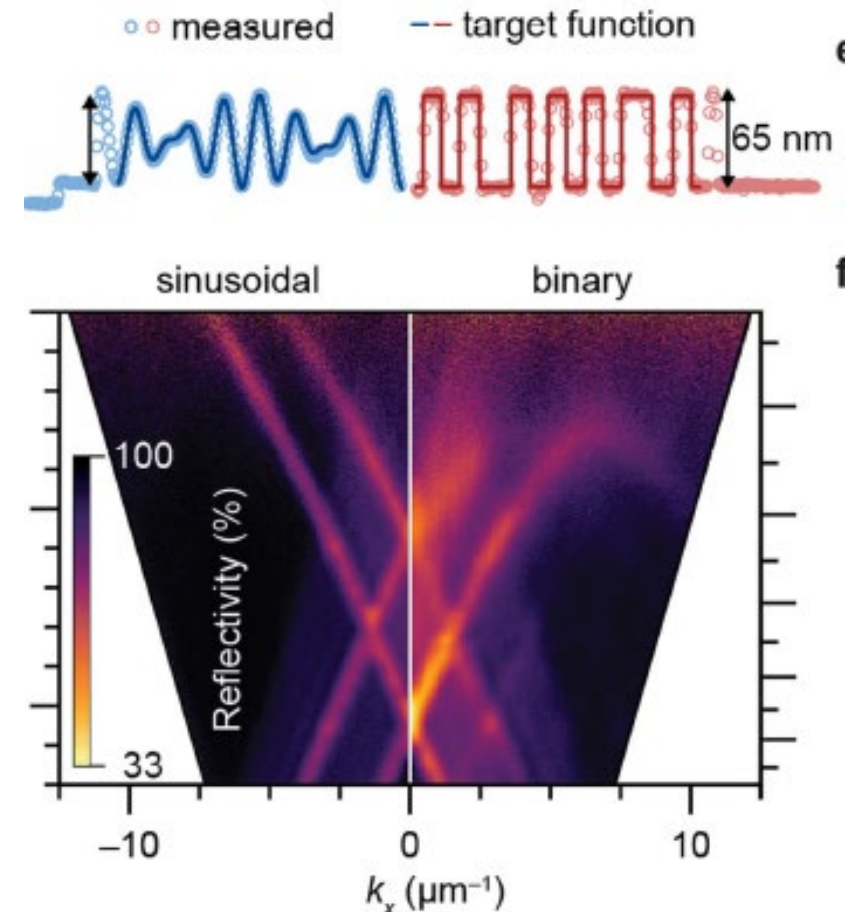
Optical Fourier Surfaces: 3D optical metasurfaces

The surface pattern generates a desired diffracted output through its Fourier transform. To shape the optical wavefront, **the ideal surface profile should contain a precise sum of sinusoidal waves**, each with a well defined amplitude, spatial frequency and phase.

Fabrication



Sinusoidal VS binary

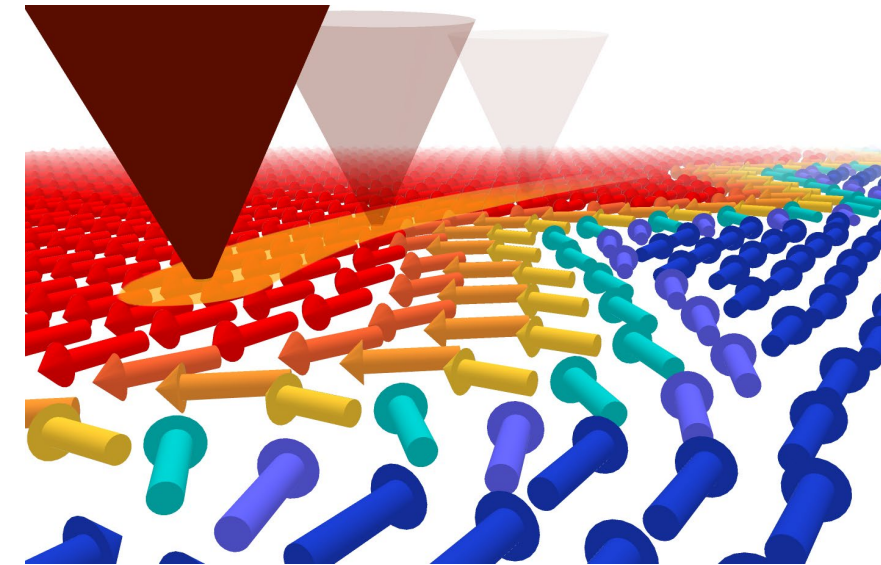
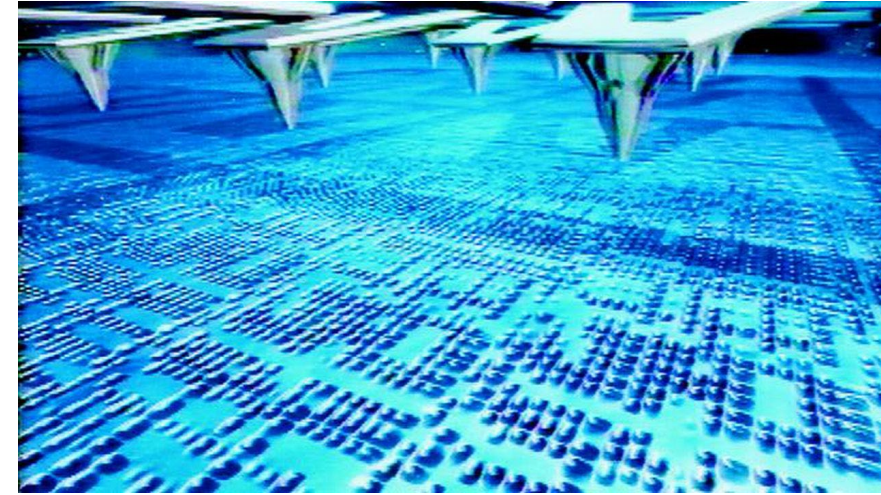


Nature 582, 506–510 (2020)

Outlook

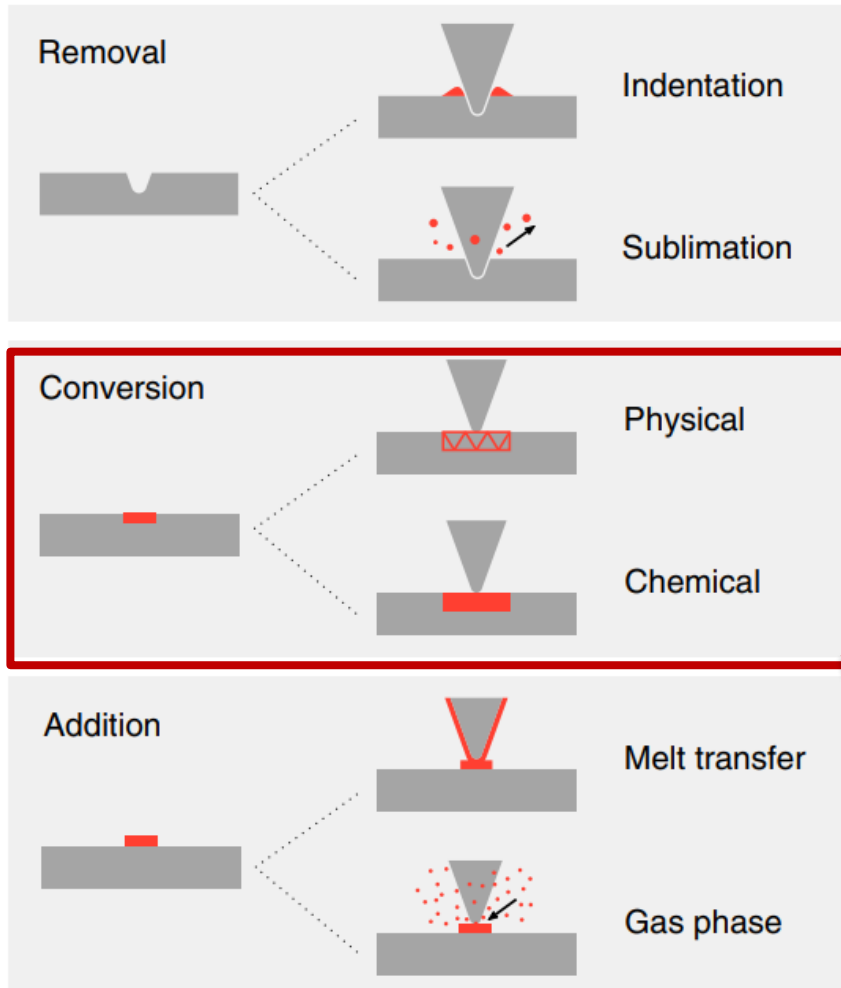
- ▶ *Scanning Probe Microscopy / Lithography*
- ▶ *Brief history of t-SPL: from milli-pedes to nano-structures*
- ▶ *Experimental: features and limitations of t-SPL*

- ▶ ***Applications:***
 - 1) *REMOVAL Direct sublimation of organic resists / lithography*
 - 2) *«CHEMICAL conversion» at the nanoscale*
 - 3) *«PHYSICAL conversion»: t-SPL for magnetism*



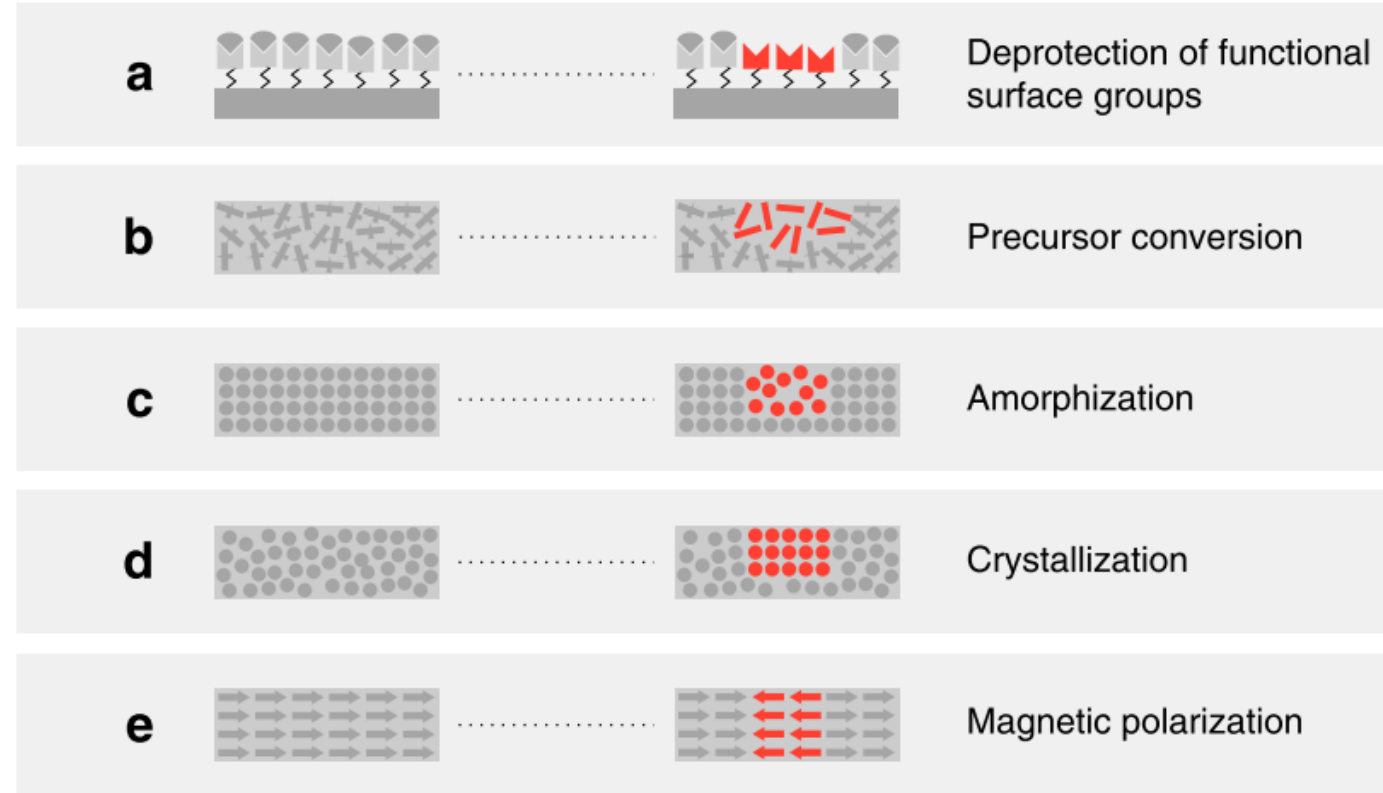
Direct material conversion

Heat as a universal stimulus



Conversion

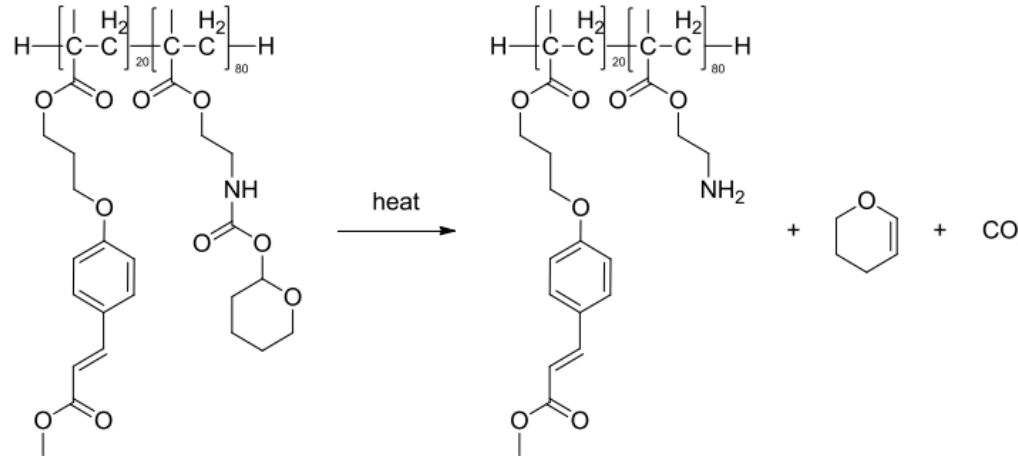
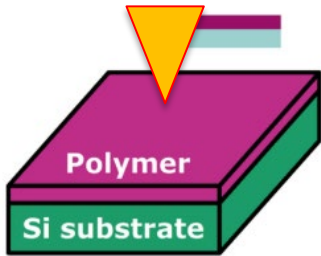
Conversion processes (not exhaustive)



Howell et al. Microsystems & Nanoengineering (2020) 6:21

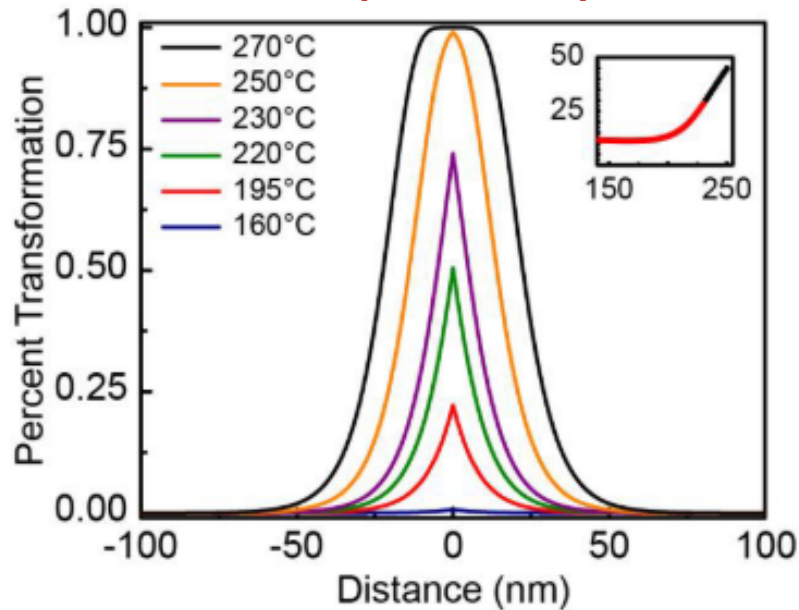
Controlled deprotection of functional groups

Thermally-induced deprotection of reactive amines

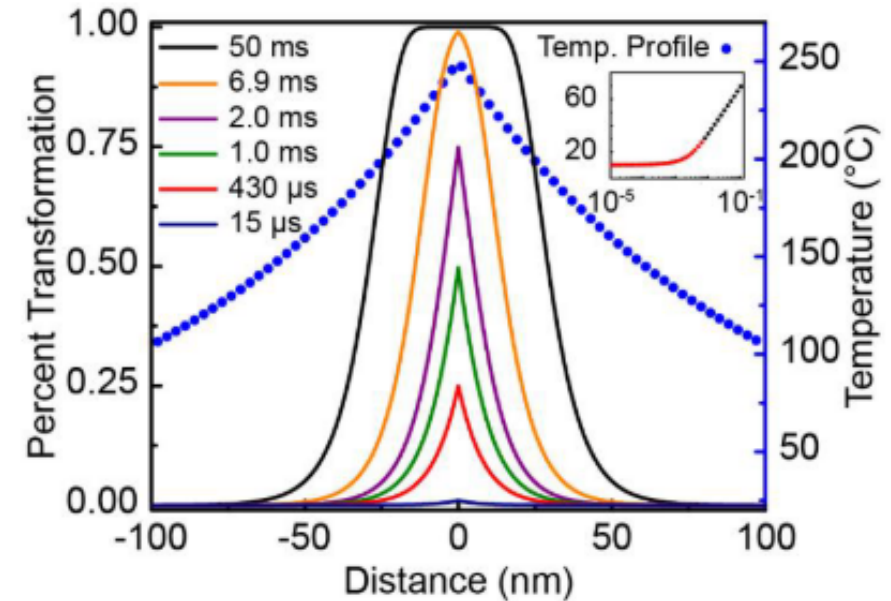


$$\frac{[P]}{[P_{tot}]} = 1 - e^{-kt} = 1 - e^{-A \cdot t \cdot e^{\frac{-E_a}{RT}}}$$

Model: Temperature dependence



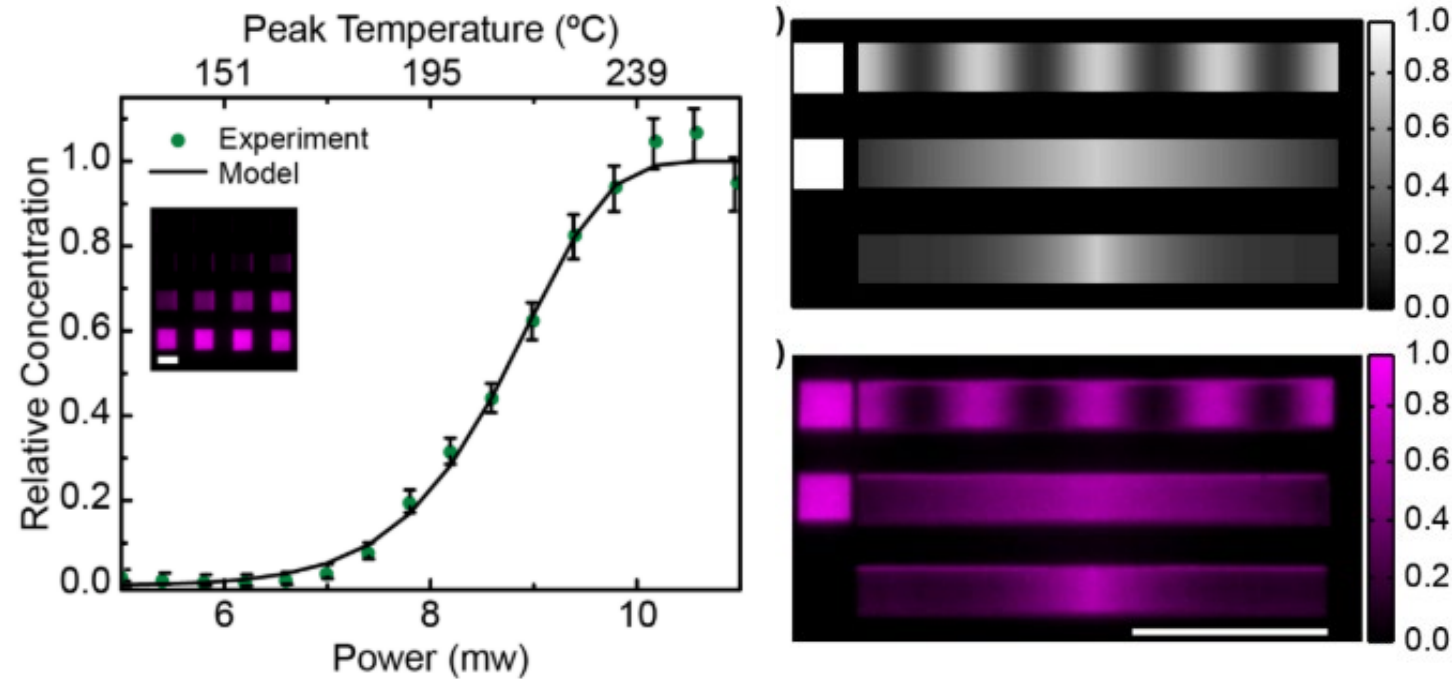
Model: Time-dependence



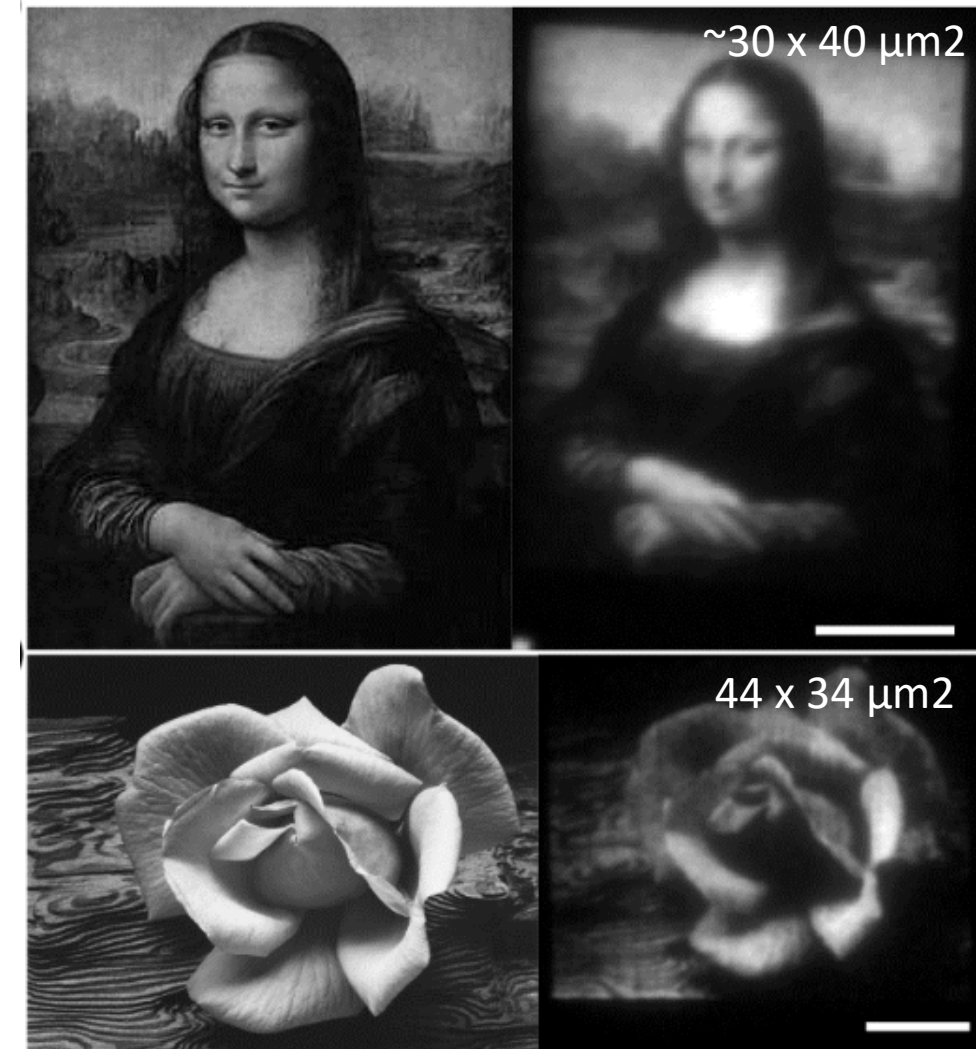
Carroll K M et al Langmuir 29 8675–82 (2013)

Controlled deprotection of functional groups

Exp: Controlled amine gradients



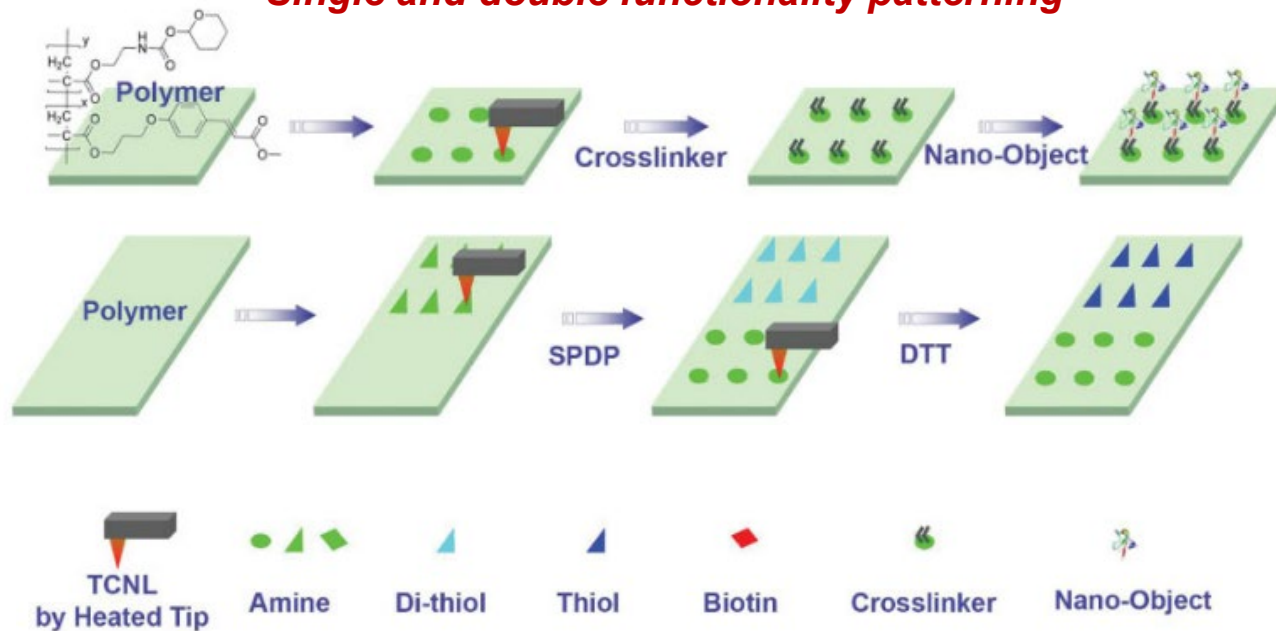
Grayscale map of amine concentration



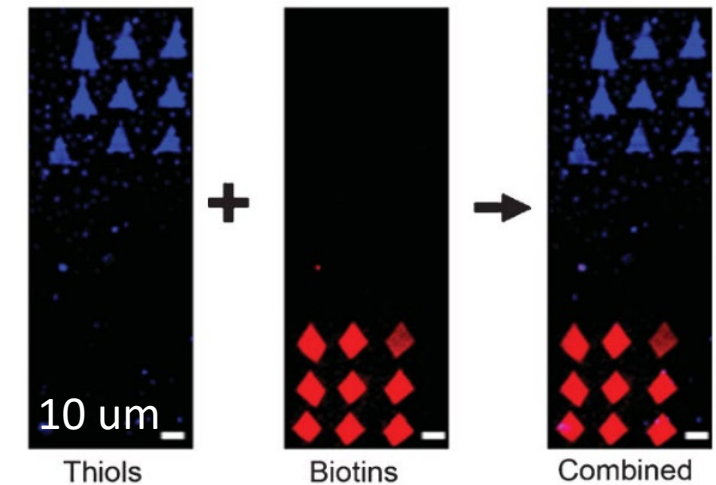
Controlled immobilization of multiple nano-objects

Nanoscale chemical patterning of different chemical species (amine, thiol, aldehyde, and biotin) in independent nanopatterns is achieved by the iterative application of thermochemical nanolithography (TCNL) and control the surface positioning of patterns followed by their chemical conversion to other functional groups.

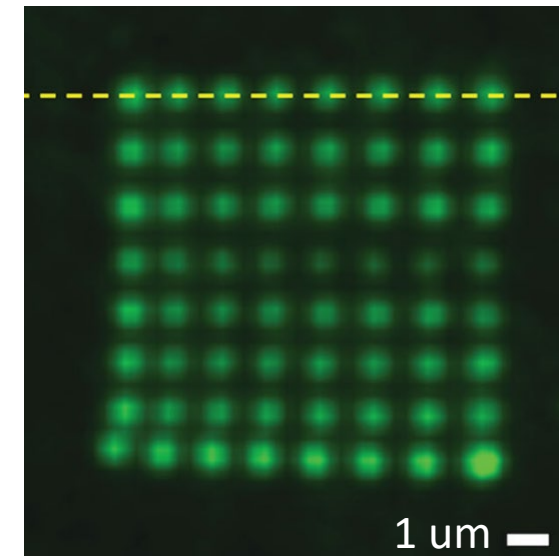
Single and double functionality patterning



Fluorescence image

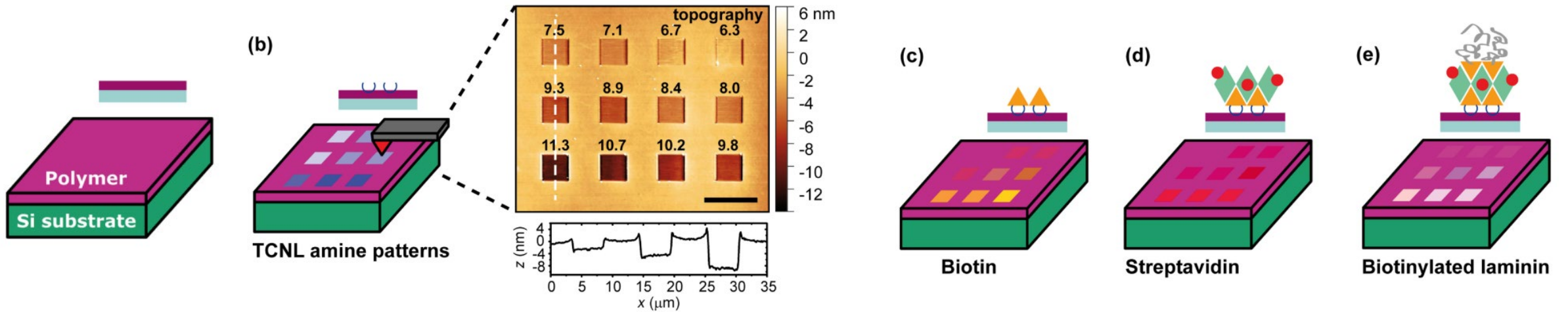


Nanopatterning fibronectin arrays

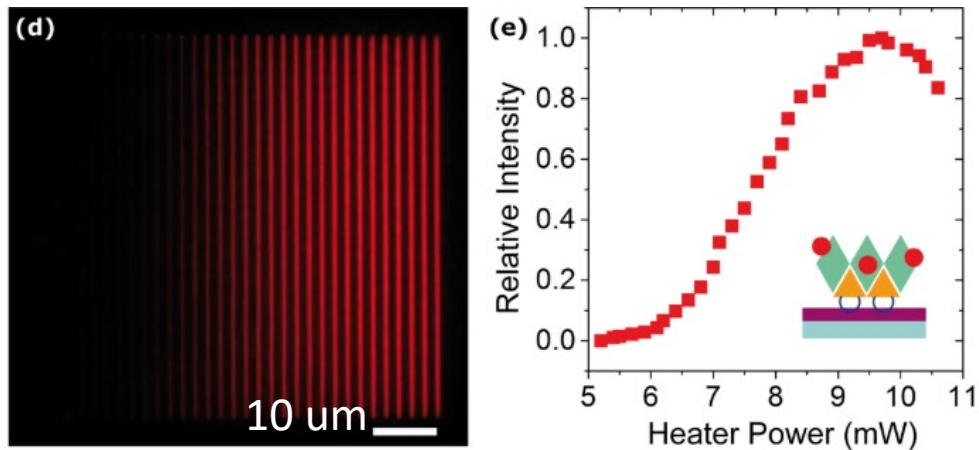


Immobilizing protein gradients with nanoscale resolution

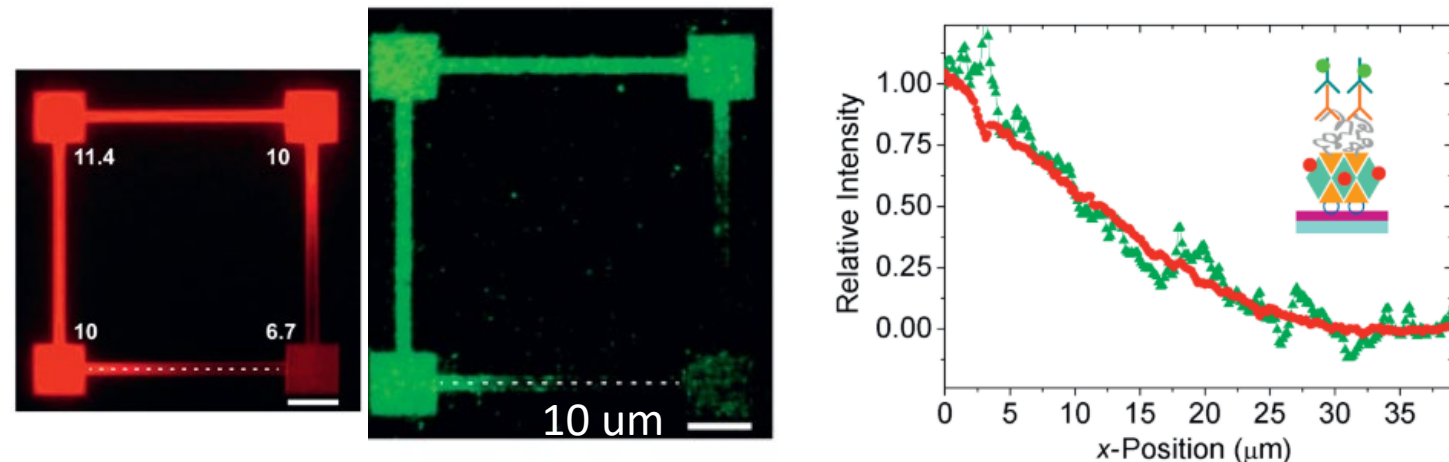
Protein immobilization process



Fluo Streptavidin gradients



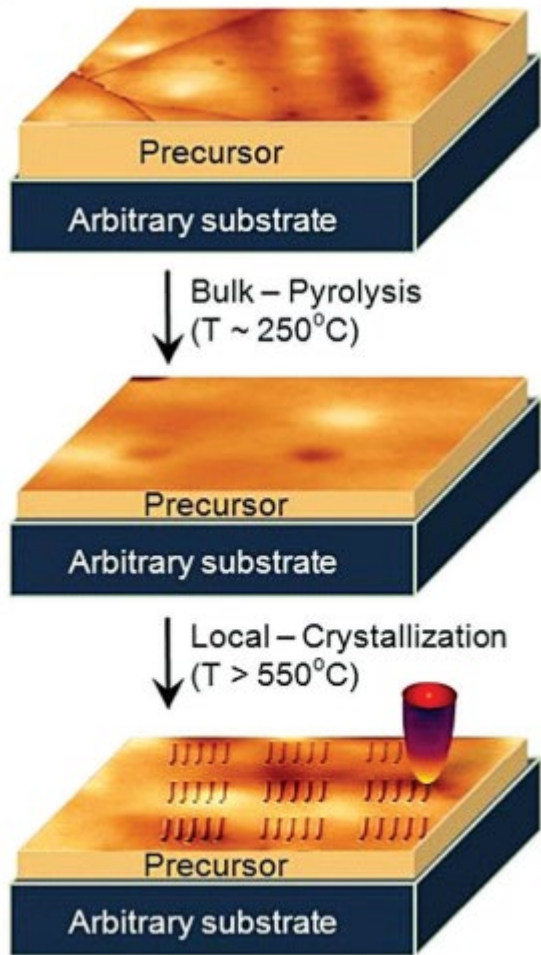
Fluo Streptavidin + Laminin gradients



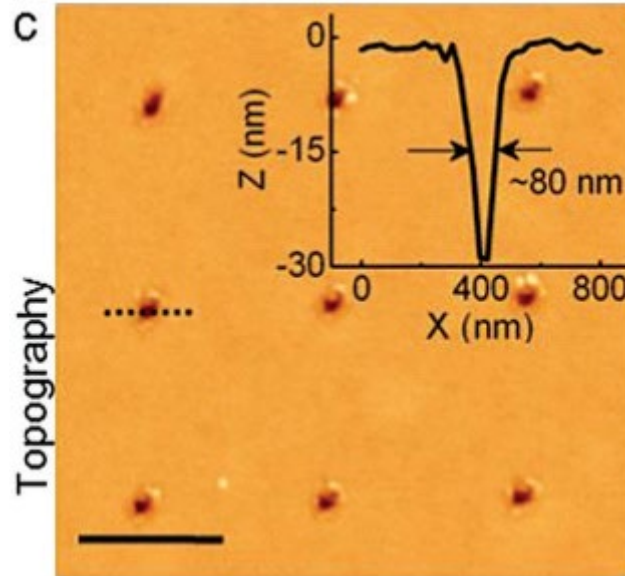
Direct nanofabrication of ferroelectric nanostructures

Fabrication process in PTO and PZT

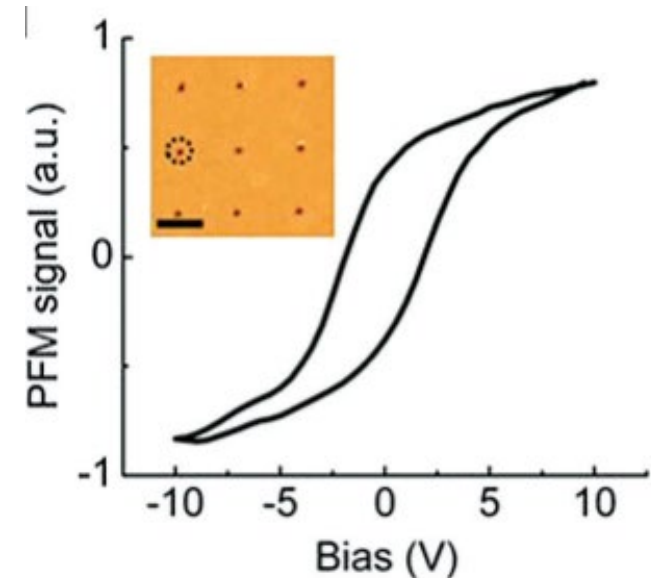
After deposition of a sol-gel precursor film of PZT and PTO and baking for removing the solvent, t-SPL is performed in order to locally crystallize the film into PZT or PTO. $T_{\text{cryst}} > 550^{\circ}\text{C}$. The piezoelectric properties of the directly written nanostructures are measured via PFM.



Topography of FE patterns



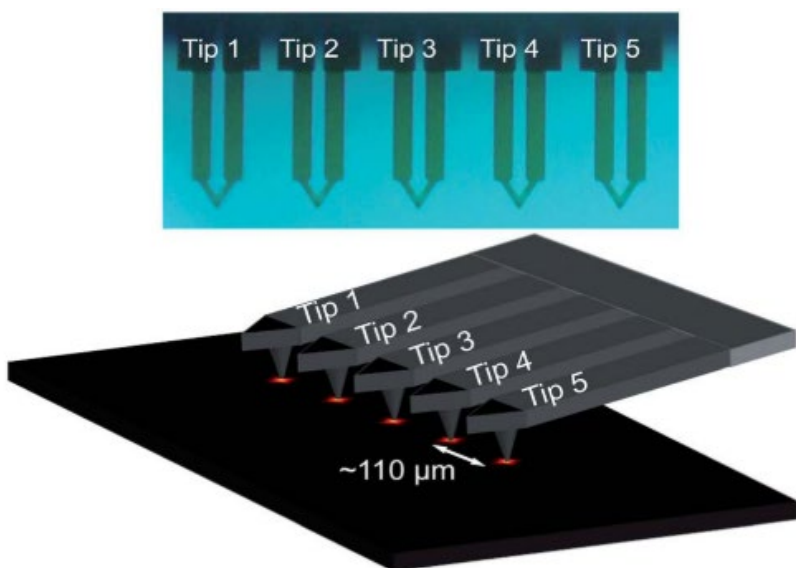
PFM hysteresis loop



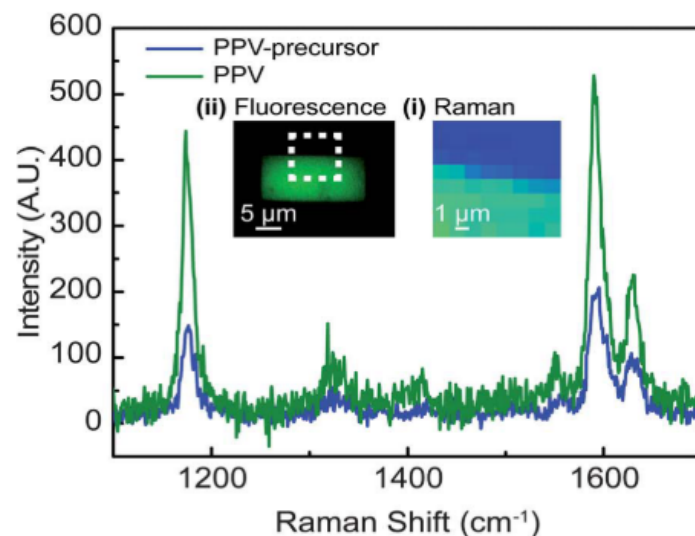
Parallelization via tip array: direct patterning of PPV nanostructures

An array of 5 tips independently addressable was used for the fabrication of conjugated polymer nanostructures. A precursor film is locally heated and converted in PPV, which is a photo-luminescent semi-conducting organic polymer. The photoluminescence is controlled by the degree of conversion, related to temperature.

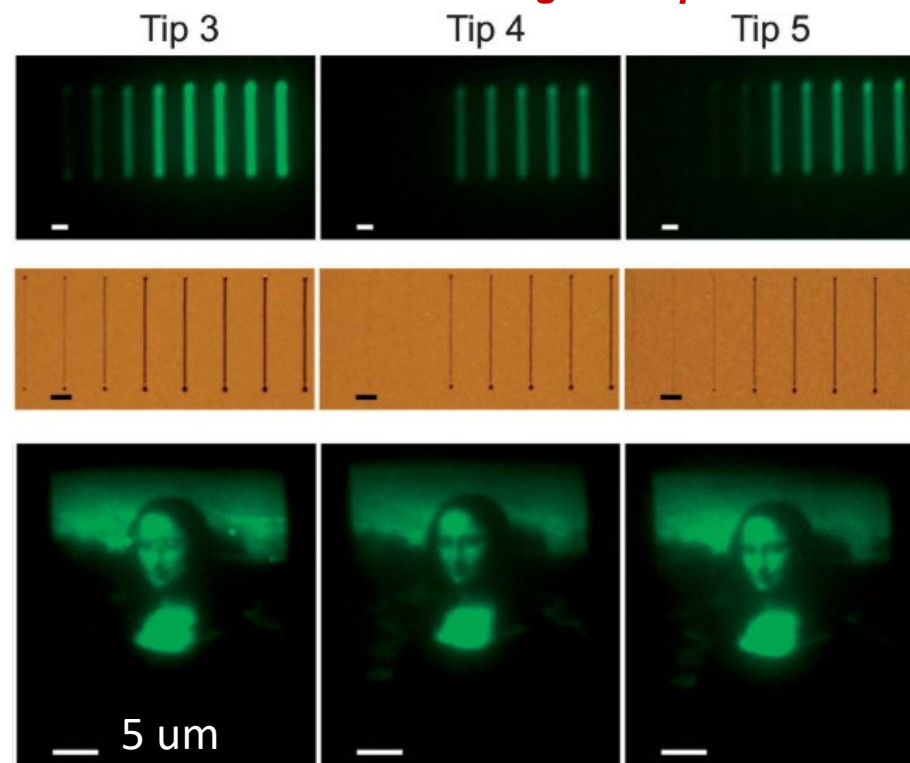
Leveled tip array



Micro Raman PPV fingerprints

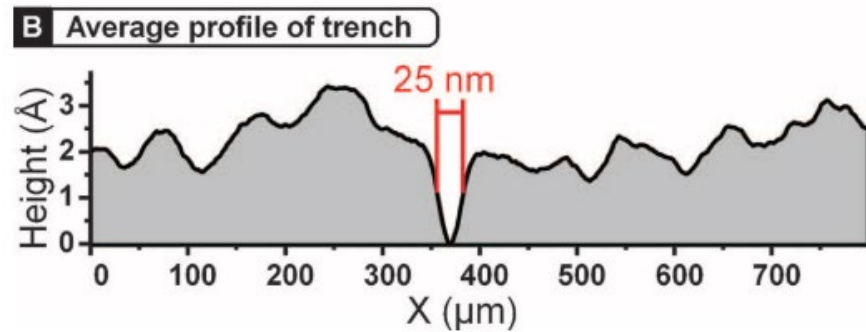
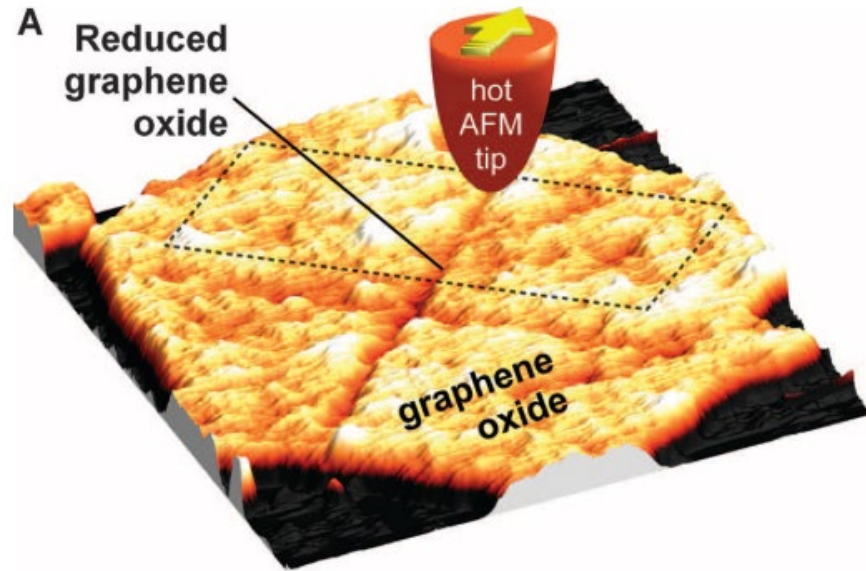


Photoluminescent graded patterns

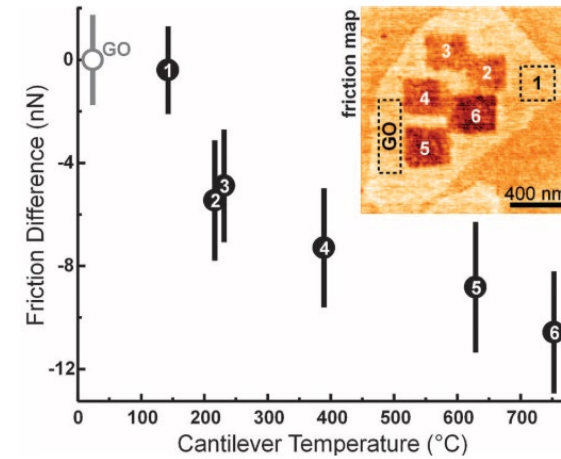


Tunable reduction of Graphene Oxide

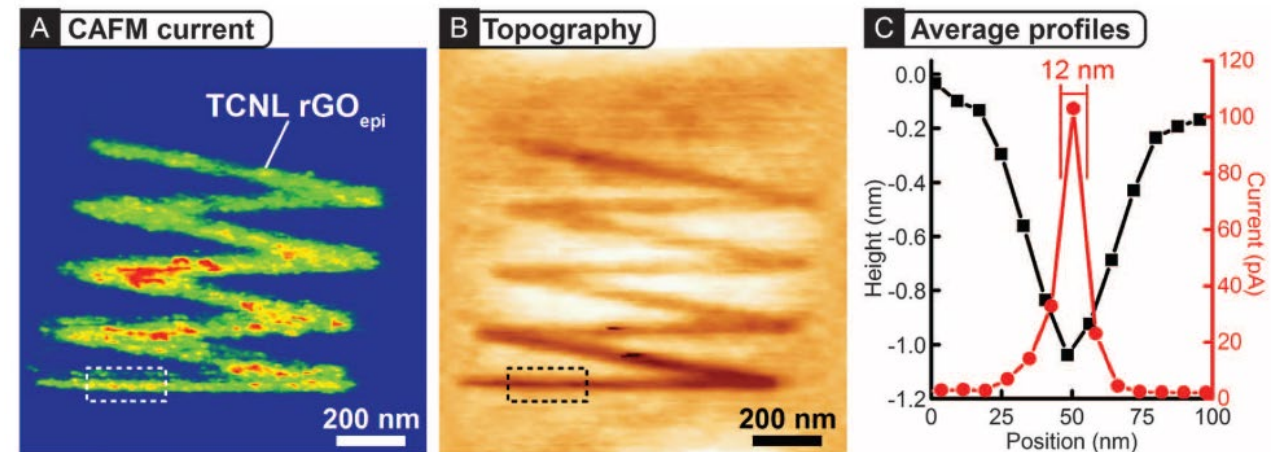
Topography of reduced grOX



Tunable friction with temperature

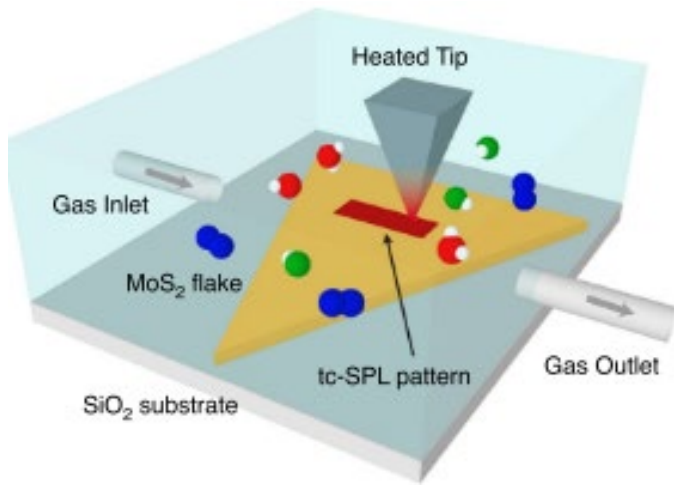


Nanoscale conductivity via C-AFM

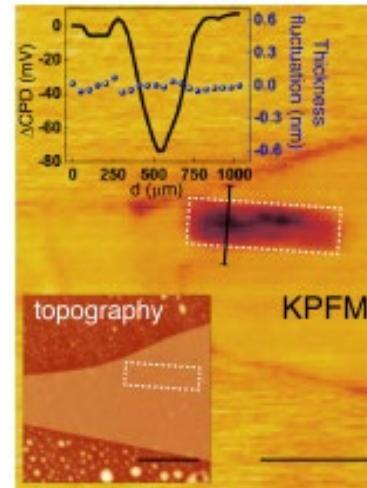


Spatial defect nanoengineering in MoS₂

t-SPL in a controlled atmosphere

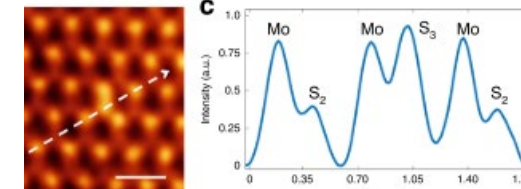
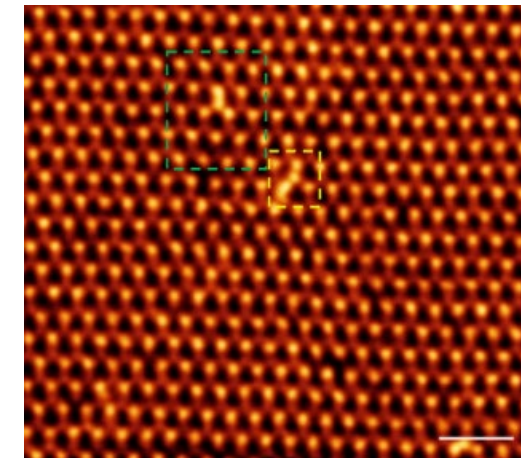


KPFM

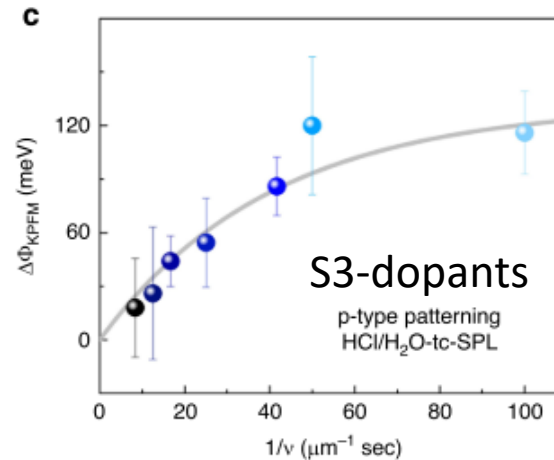
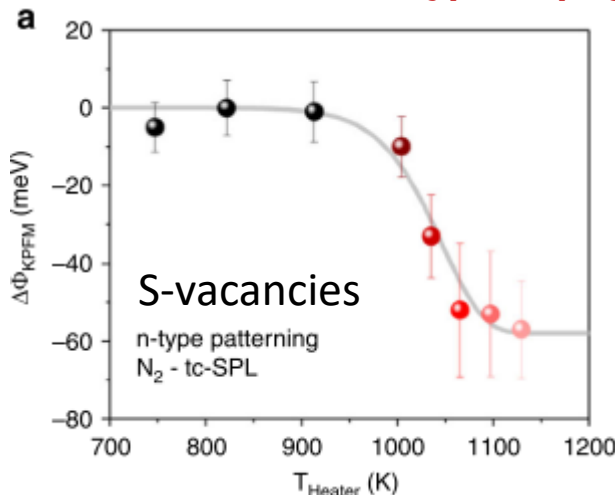


t-SPL in combination with a gas cell is used for generating defects in MoS₂. Nanoscale control of defects in monolayer MoS₂. The defects can present either p- or n-type doping on demand, depending on the gas used, allowing to realize p-n junctions.

*S*3 dopants in HRTEM



n-type or *p*-type patterning

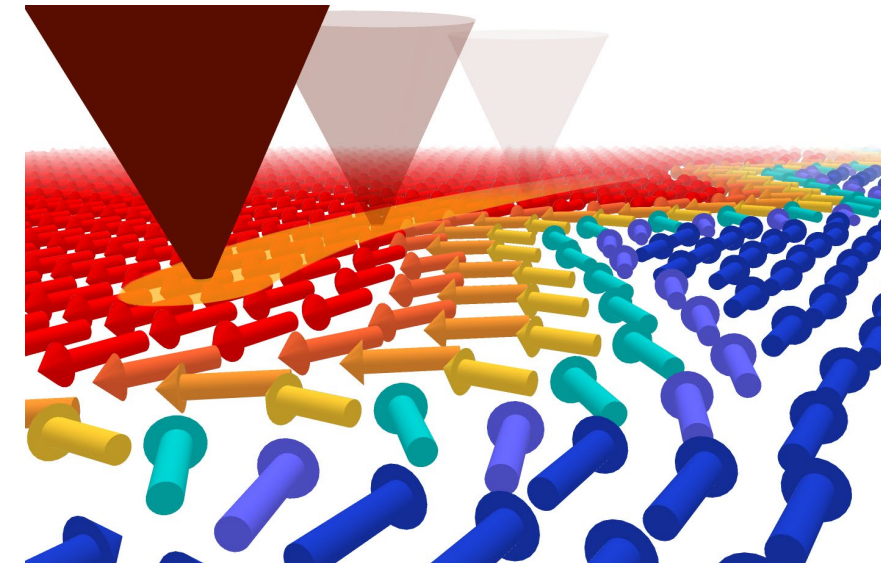
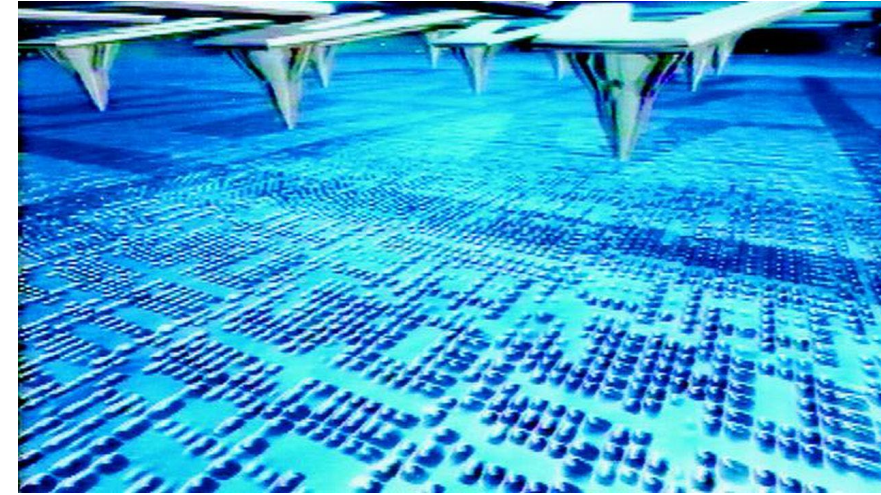


Zheng X, EA, et al Nat. Commun. 11 1–12 (2020)

Outlook

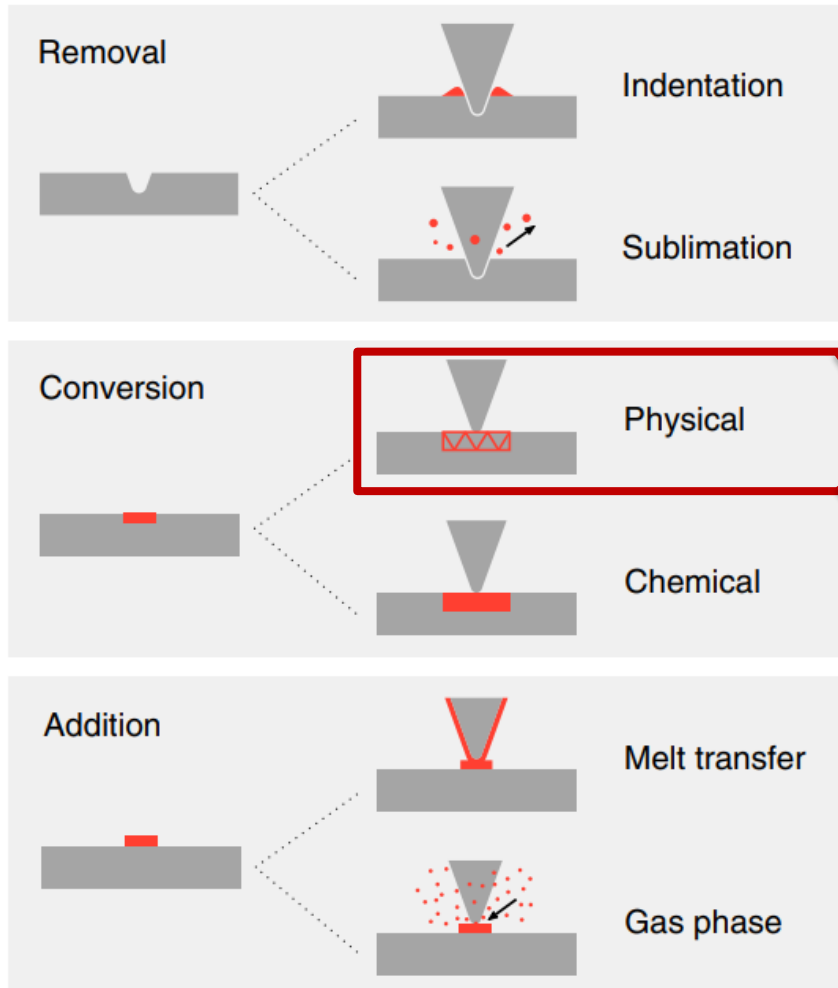
- ▶ *Scanning Probe Microscopy / Lithography*
- ▶ *Brief history of t-SPL: from milli-pedes to nano-structures*
- ▶ *Experimental: features and limitations of t-SPL*

- ▶ ***Applications:***
 - 1) *REMOVAL Direct sublimation of organic resists / lithography*
 - 2) *«CHEMICAL conversion» at the nanoscale*
 - 3) *«PHYSICAL conversion»: t-SPL for magnetism*

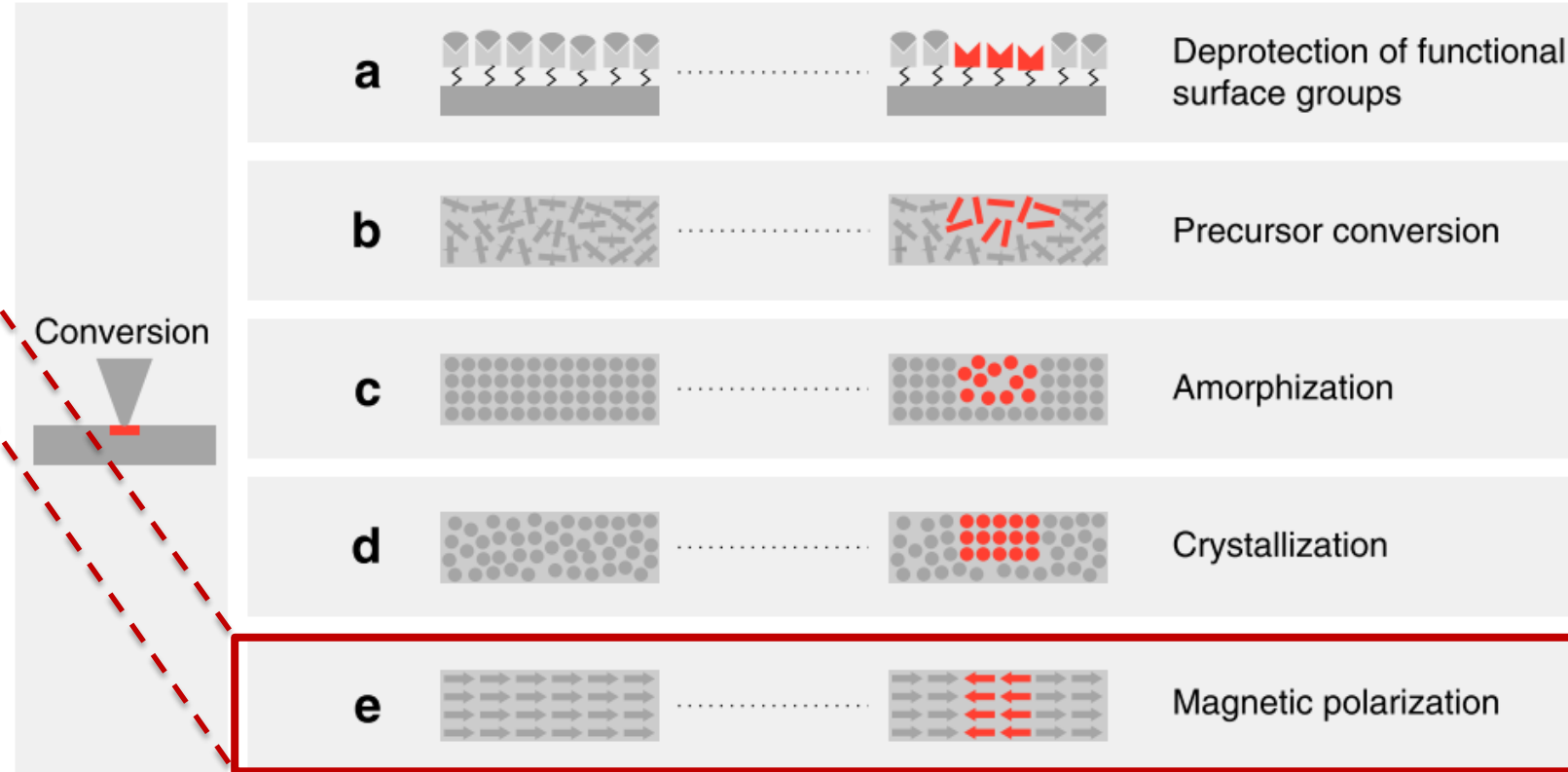


«Physical» material conversion: Nanopatterning Magnetism

Heat as a universal stimulus



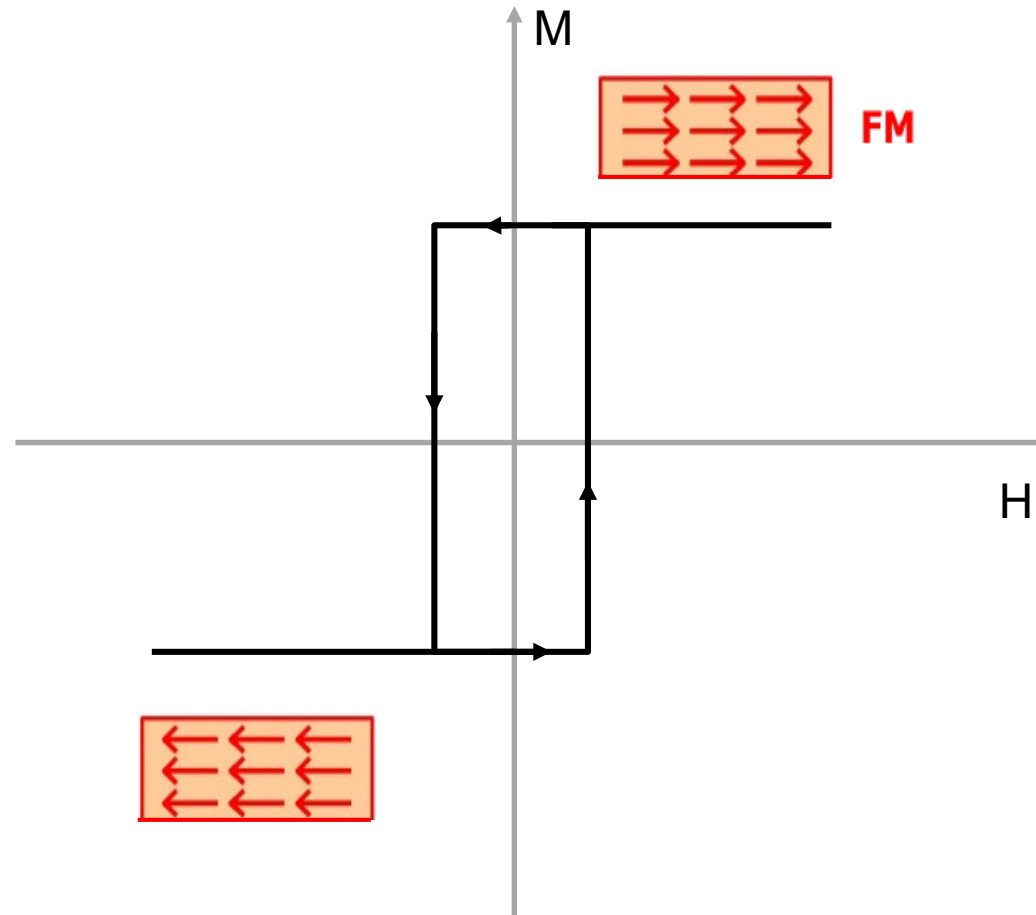
Conversion processes (not exhaustive)



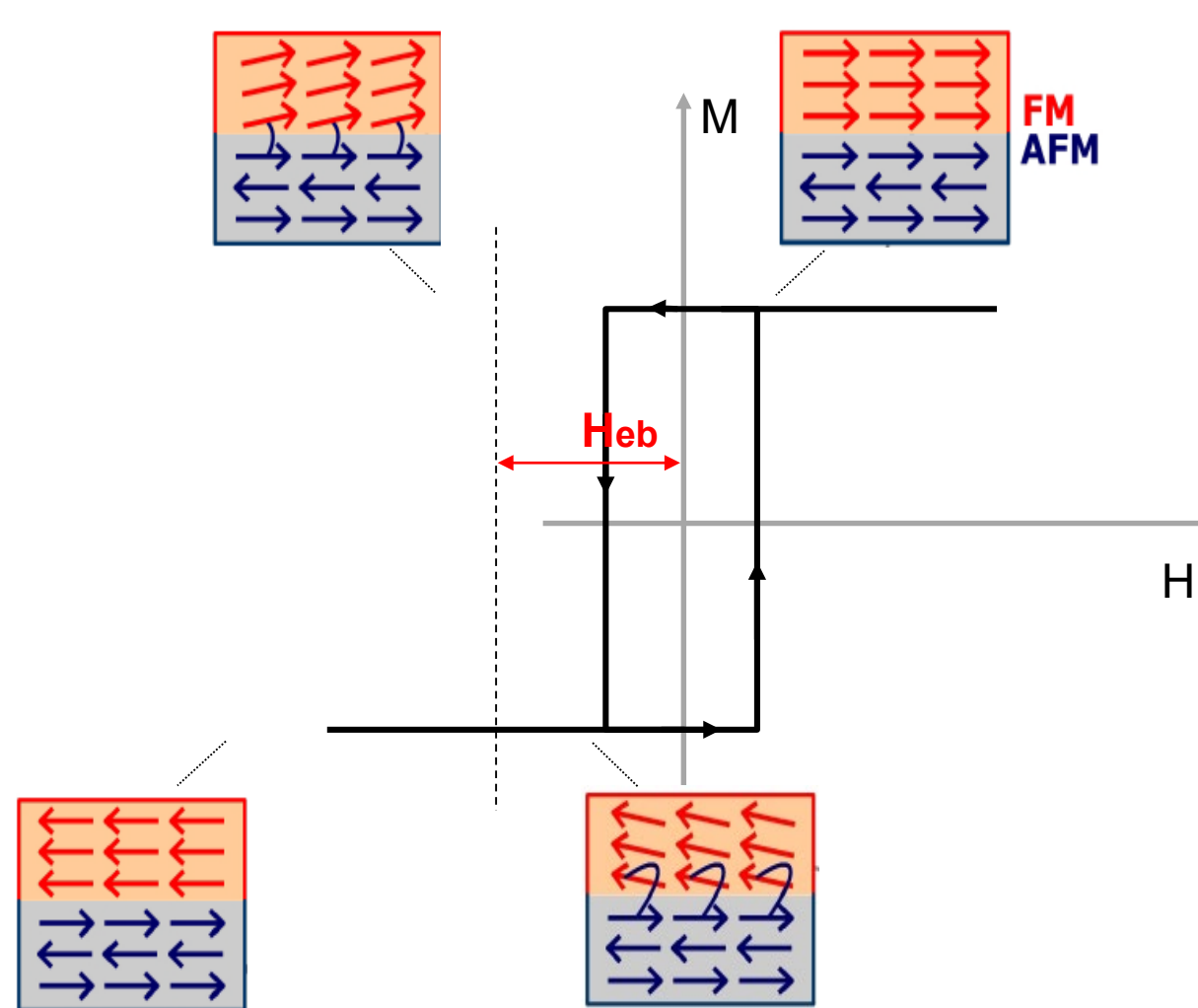
► *t-SPL for magnetism*

Howell et al. Microsystems & Nanoengineering (2020) 6:21

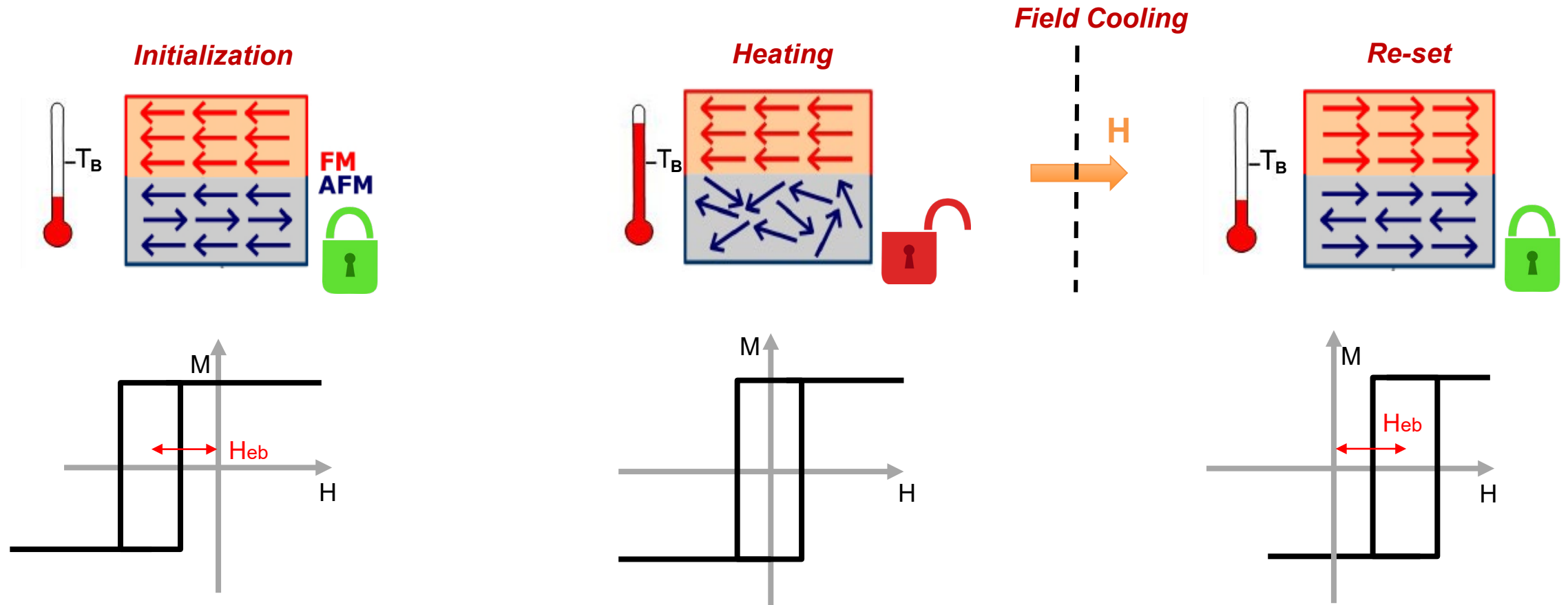
Exchange bias at the FM / AF interface



Exchange bias at the *FM / AFM* interface

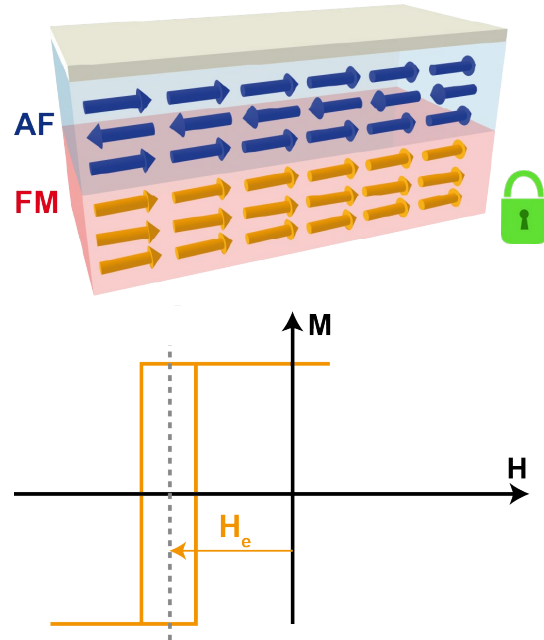


Setting the exchange bias with temperature

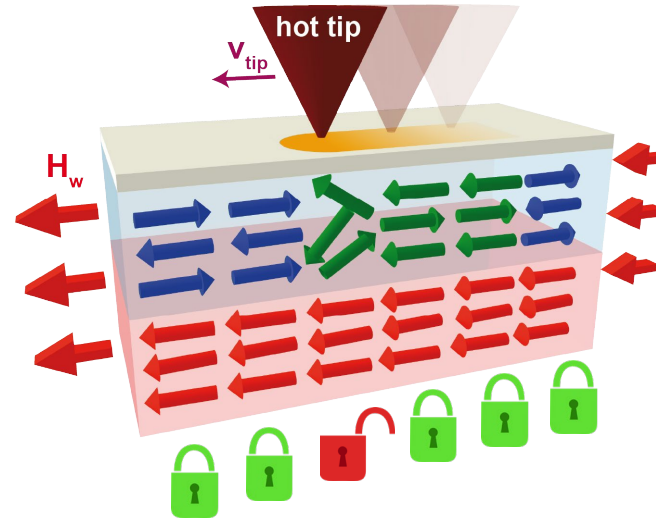


Thermally assisted magnetic Scanning Probe Lithography (tam-SPL)

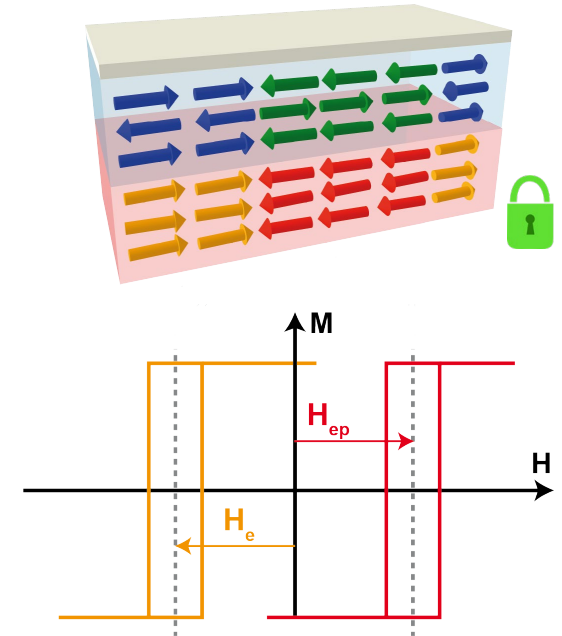
Initialization



Patterning



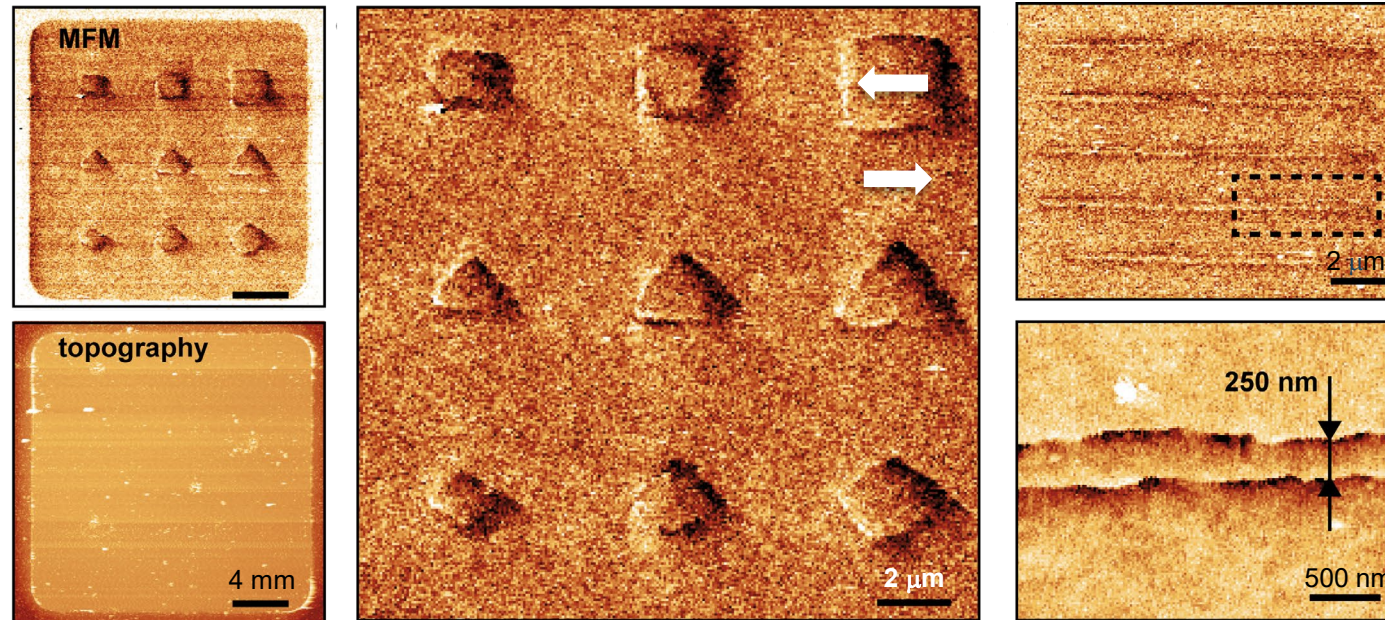
Magnetic pattern



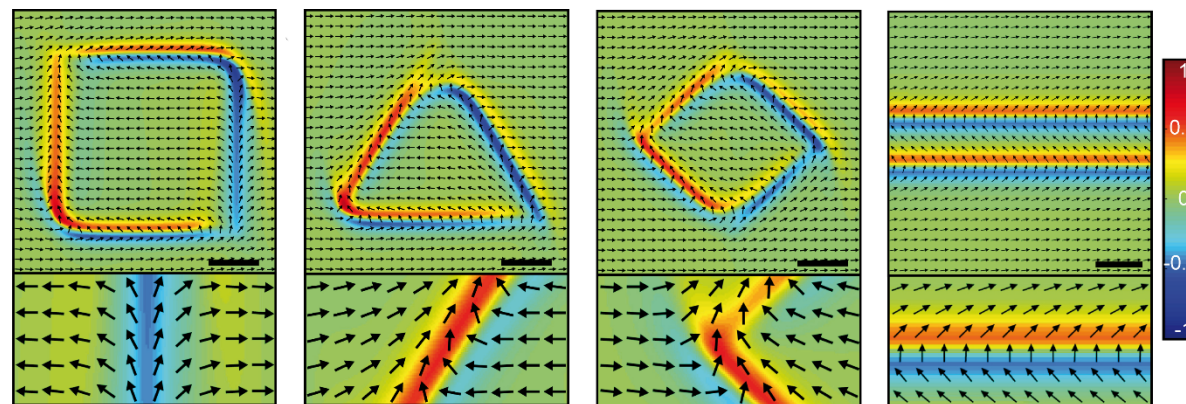
- ▶ *Single step, non-destructive, ambient conditions*
- ▶ *Reconfigurable patterns (erase – rewrite)*
- ▶ *Robust vs external fields*
- ▶ *Finely tunable*

Patterning magnetic domains / domain walls

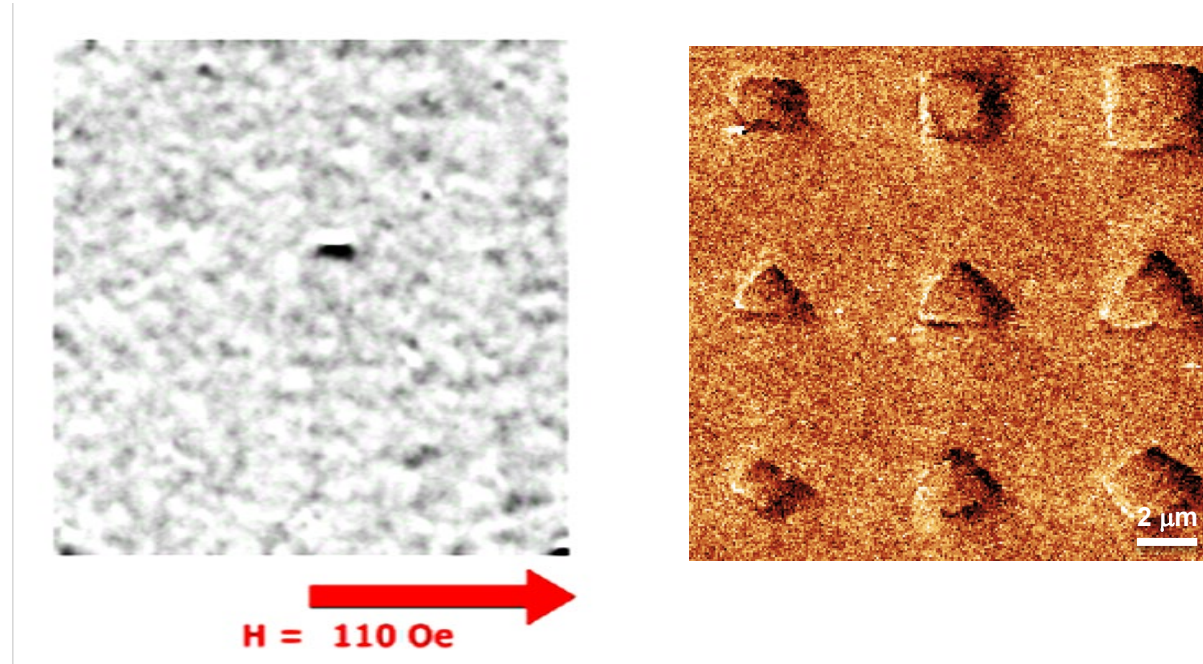
Experiments



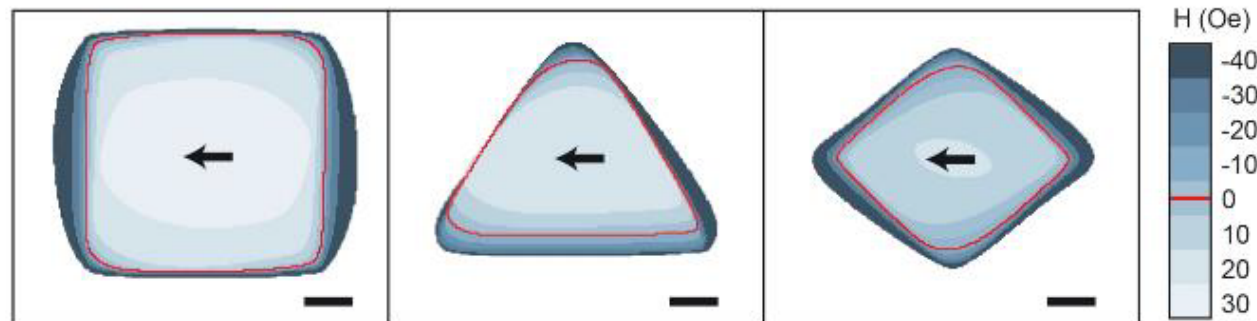
Micromagnetic Simulations



Spin-texture evolution with external field



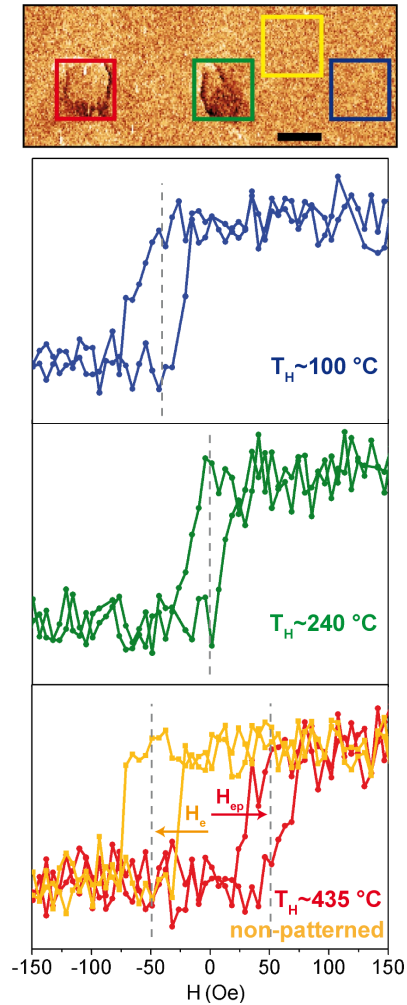
Displacing domain walls with H , before switching



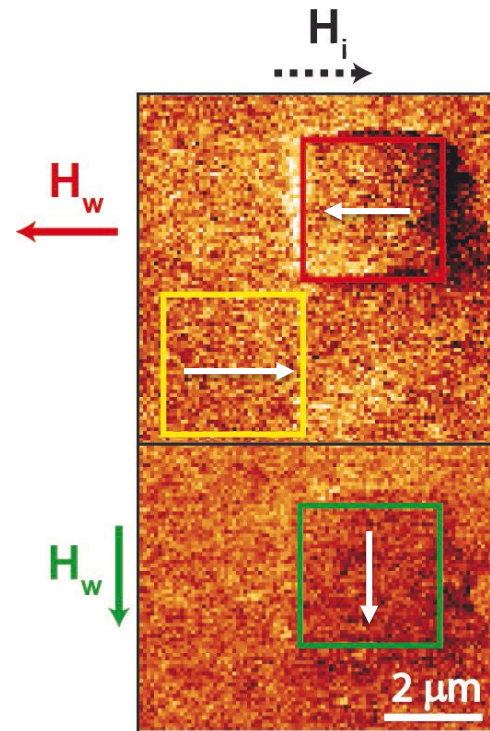
Writing / rewriting on a magnetic blackboard



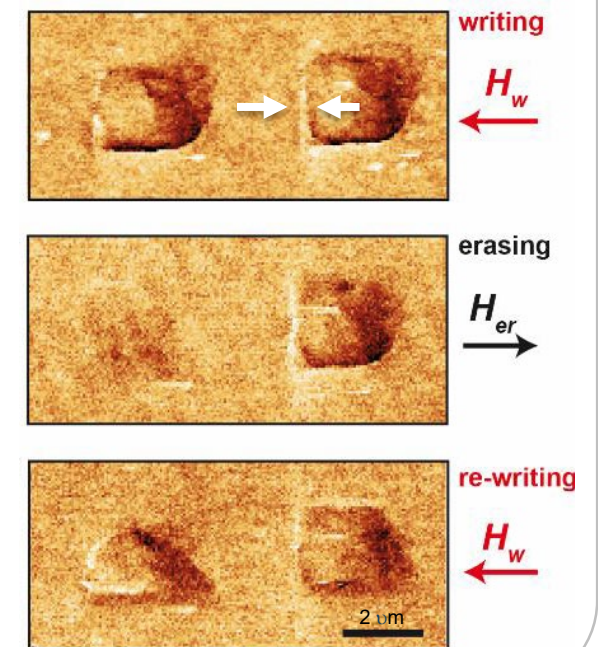
Tuning EB strength



Tuning magnetization direction



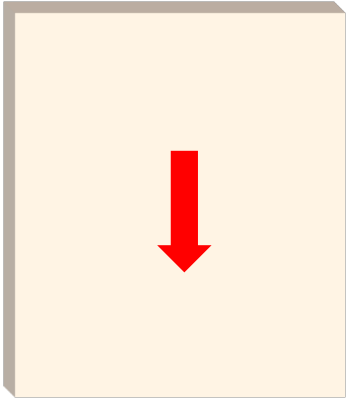
Writing, erasing, rewriting



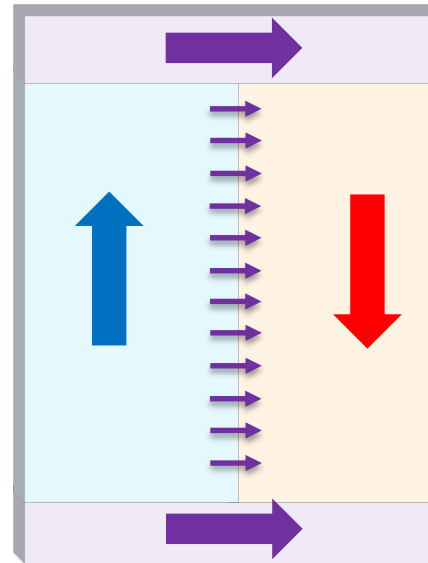
From 2D domains to 1D domain walls, to 0D topological solitons



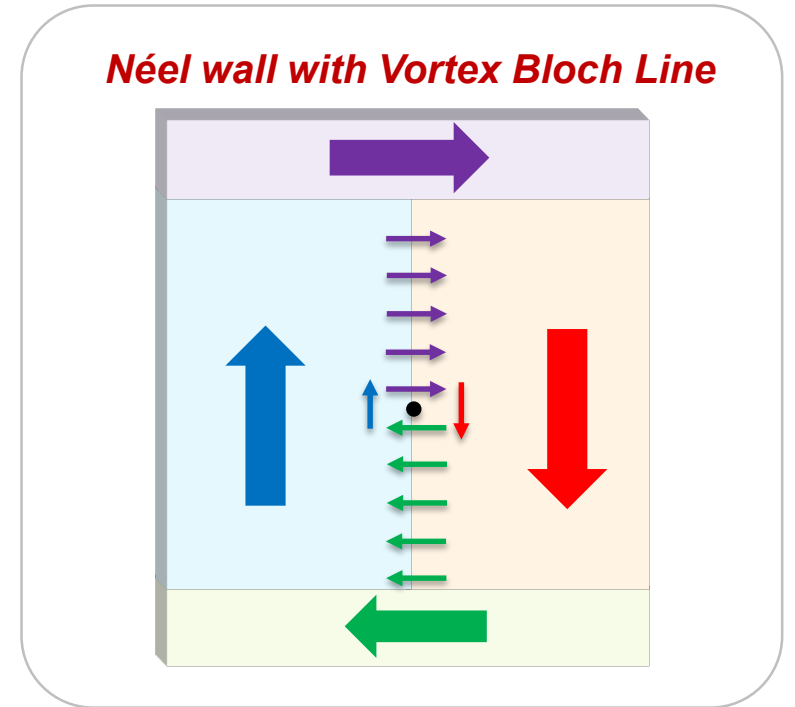
Uniform domain



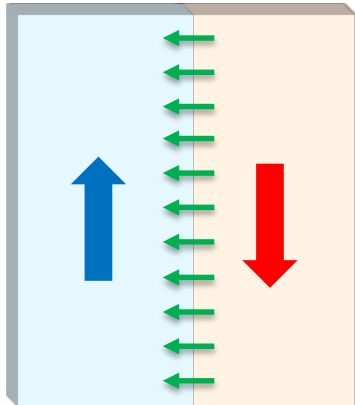
Néel wall with fixed chirality



Néel wall with Vortex Bloch Line

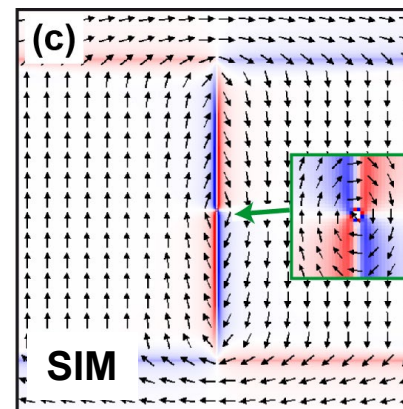
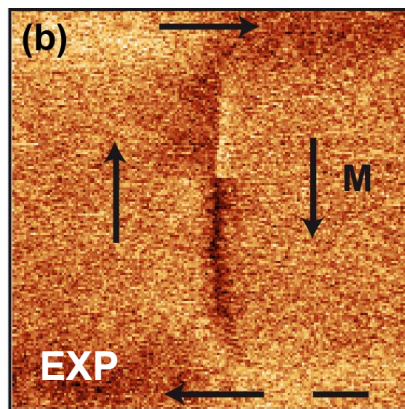
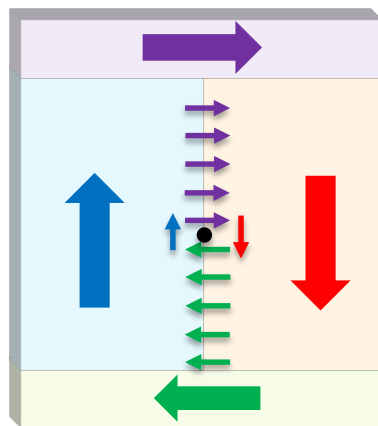


Néel wall

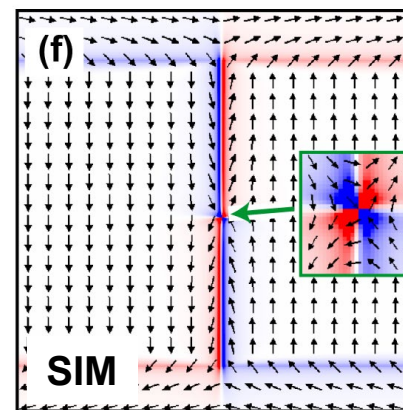
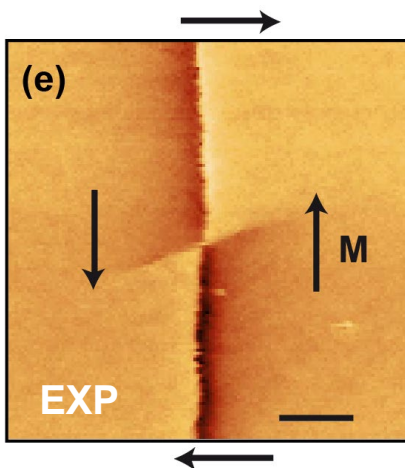
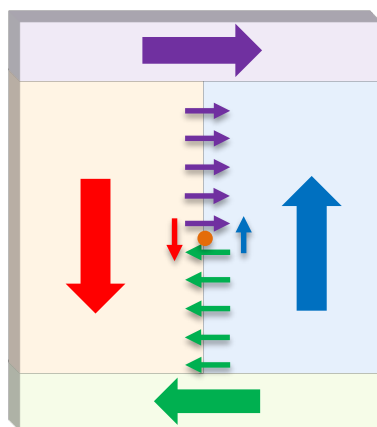


Deterministic control on position, vorticity and circularity

Vortex Bloch Line within Néel wall (CW)



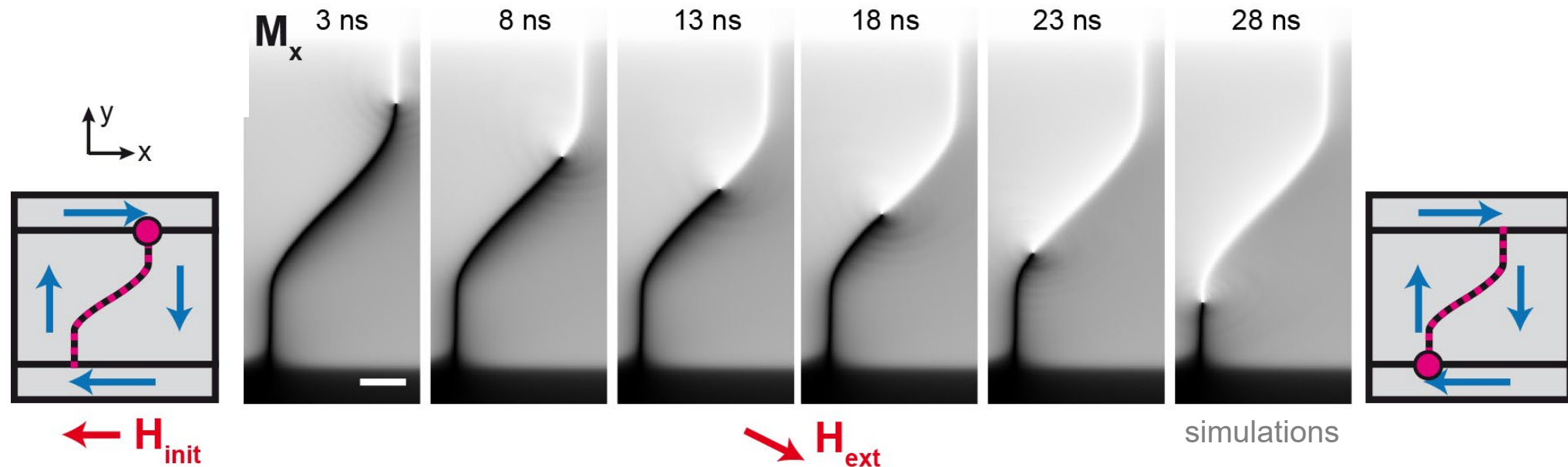
Anti-Vortex Bloch Line within Néel wall



Manipulation of magnetic solitons within tam-SPL DWs



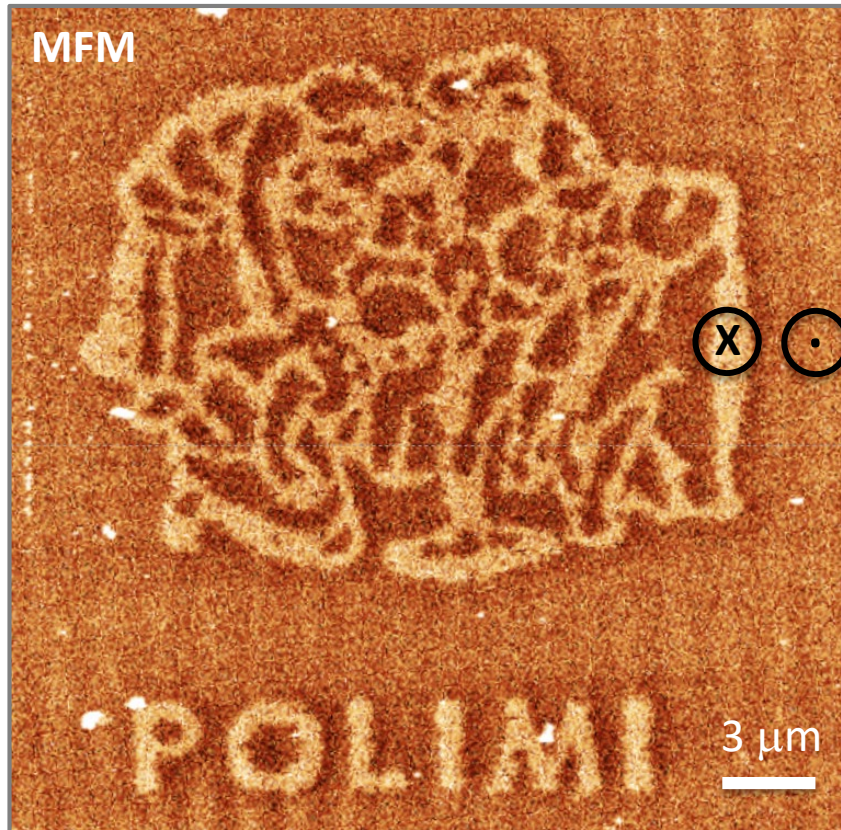
Vortex displacement along arbitrarily-shaped Néel wall



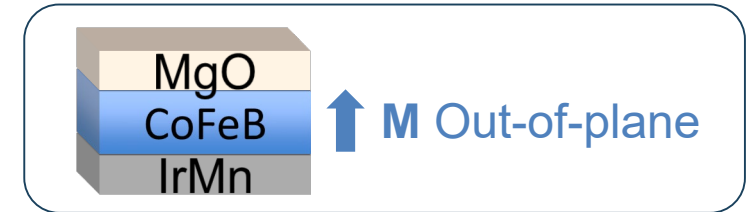
► DWs as reconfigurable racetracks

Patterning out-of-plane EB, magnetization (..and skyrmion phase)

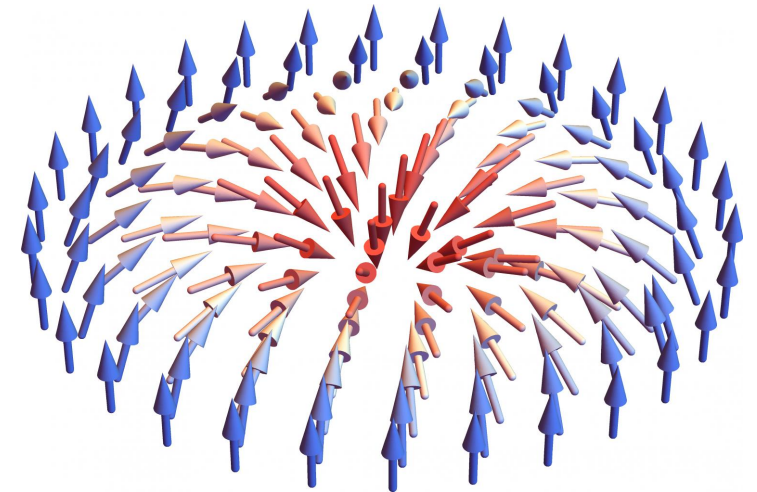
OOP complex domains



EA et al., *unpublished*

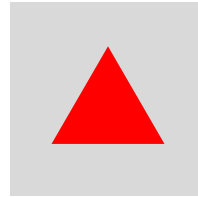
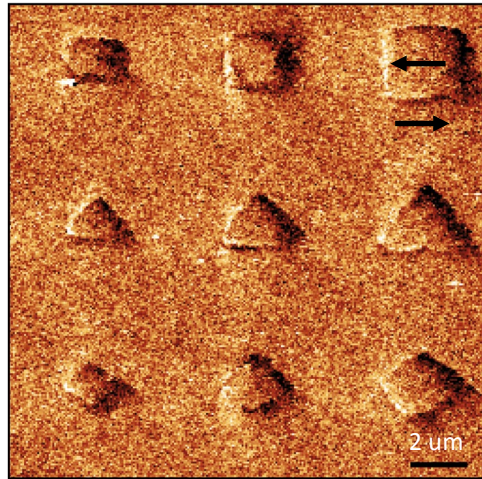


Topological textures e.g. Néel Skyrmions

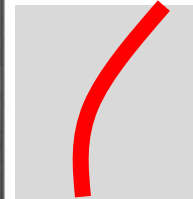
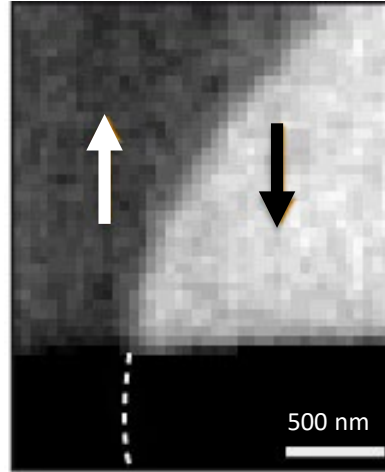


Summary: nanopatterning rewritable multidimensional spin-textures

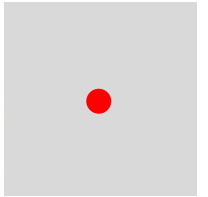
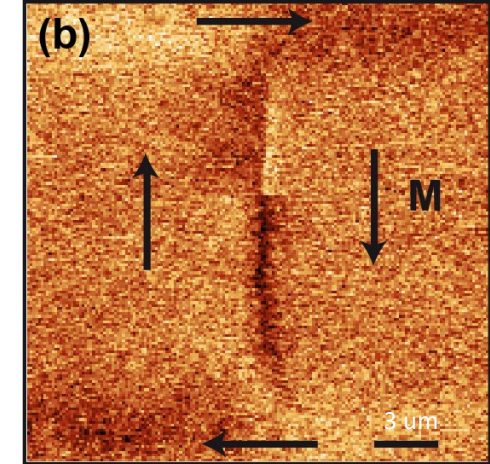
2D Magnetic domains



1D Domain walls



0D Topological solitons



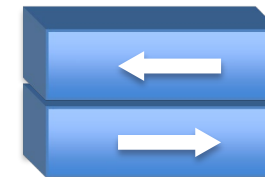
In plane



Out-of-plane

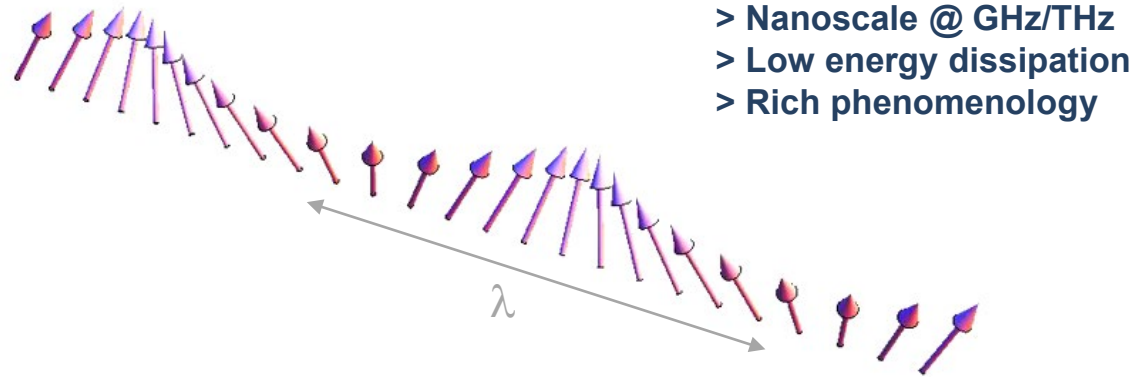


Synthetic AFs



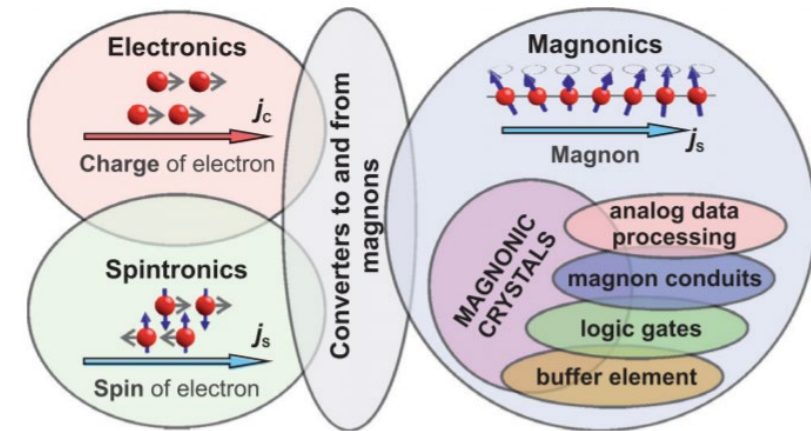
Applications of tam-SPL: manipulating spin-waves

Spin-waves



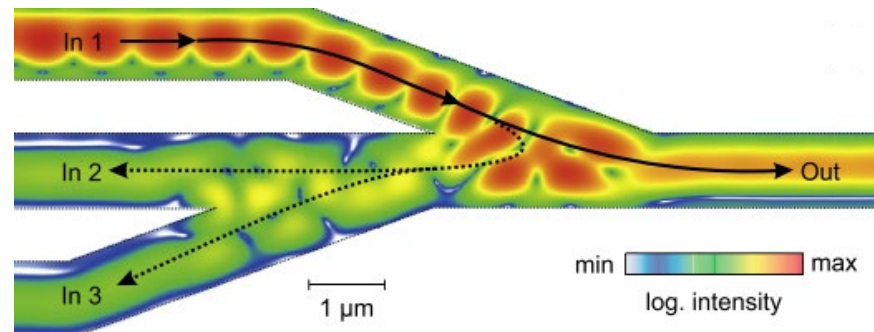
<https://www.youtube.com/watch?v=pWQ3r-2Xjeo>

Magnonics

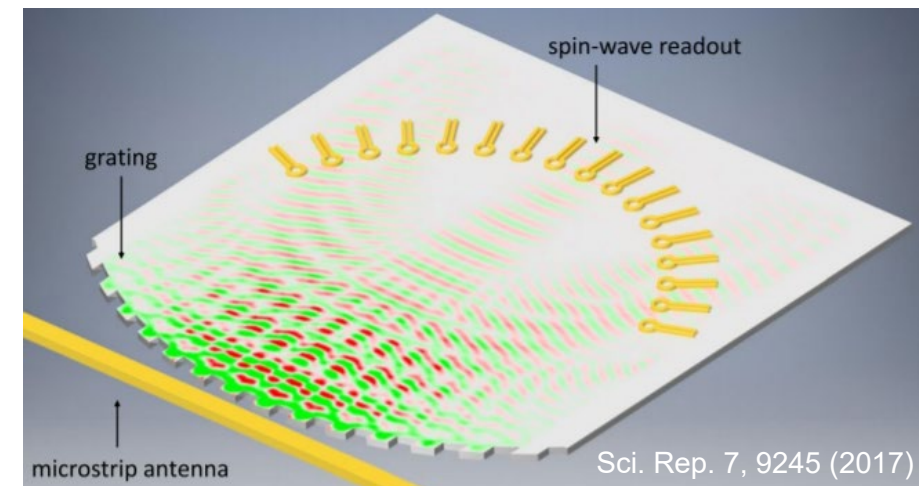


J. Phys. D: Appl. Phys. 50 (2017) 244001

Computing with spin-waves (digital / analog)



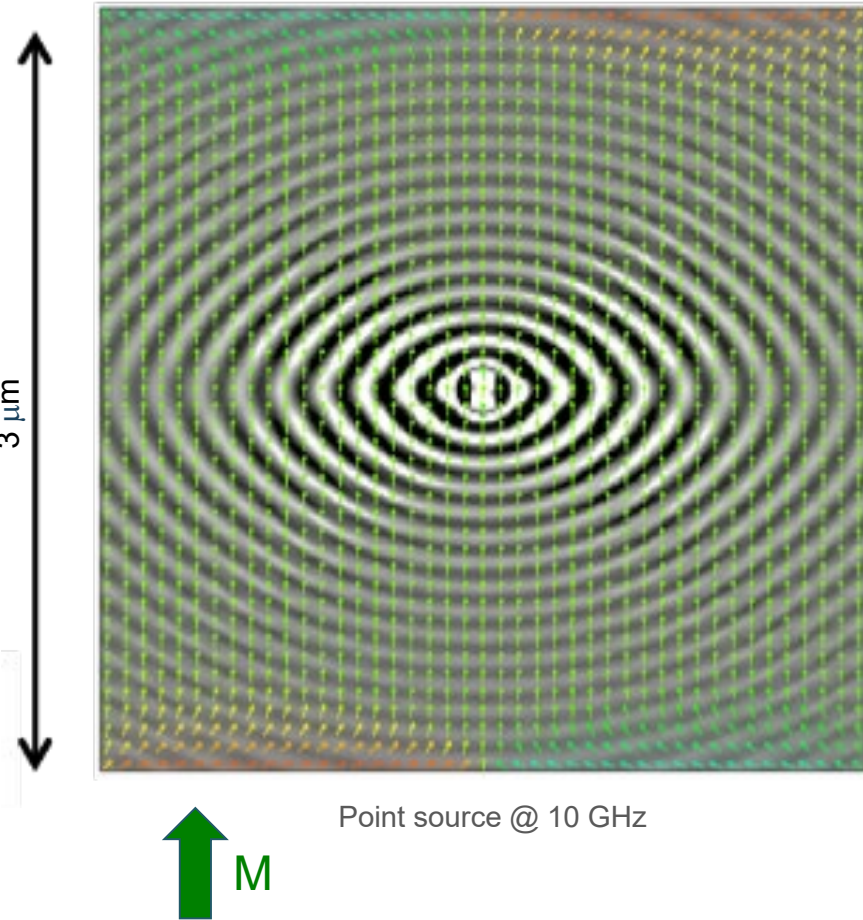
Physics Letters A 381 (2017) 1471–1476



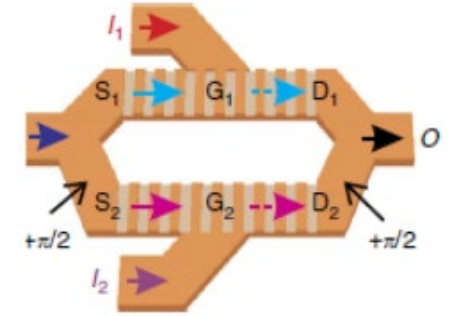
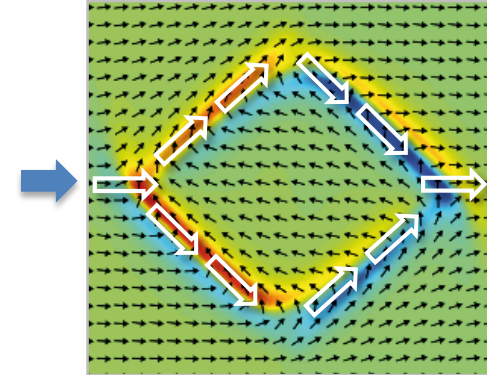
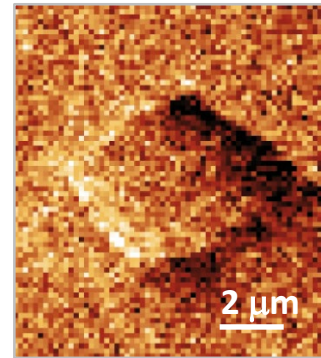
Sci. Rep. 7, 9245 (2017)

Manipulating spin-waves with tam-SPL spin-textures

Anisotropic excitation / propagation

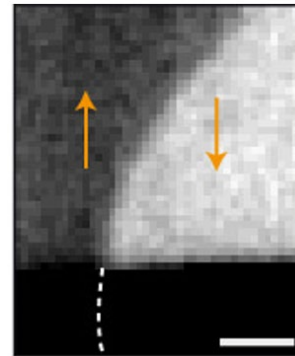


«Magnonics in-a-domain»



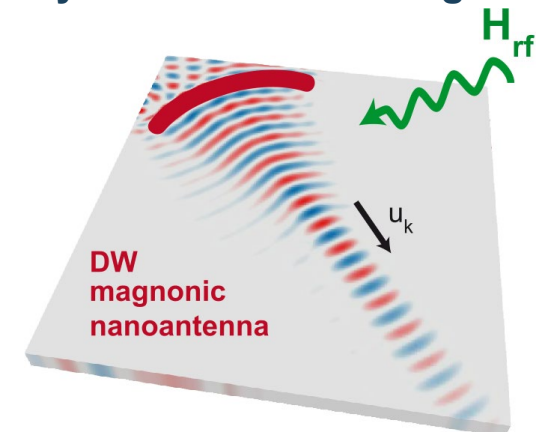
Chumak et al., Nat. Comm. 5, 4700 (2014)

Waveguides for SWs domain walls



EA et al., Comms. Phys., 1, 56 (2018)

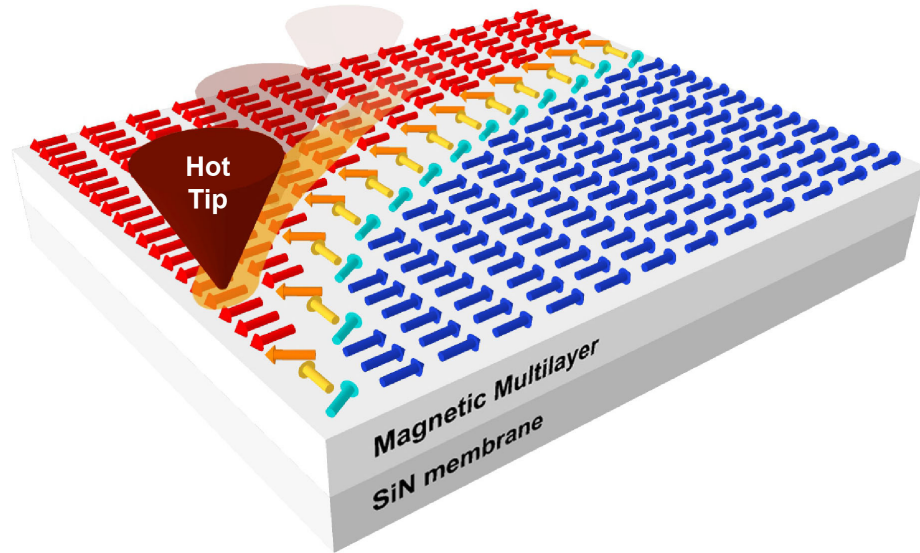
Nanoantennas for SWs synthetic antiferromagnets



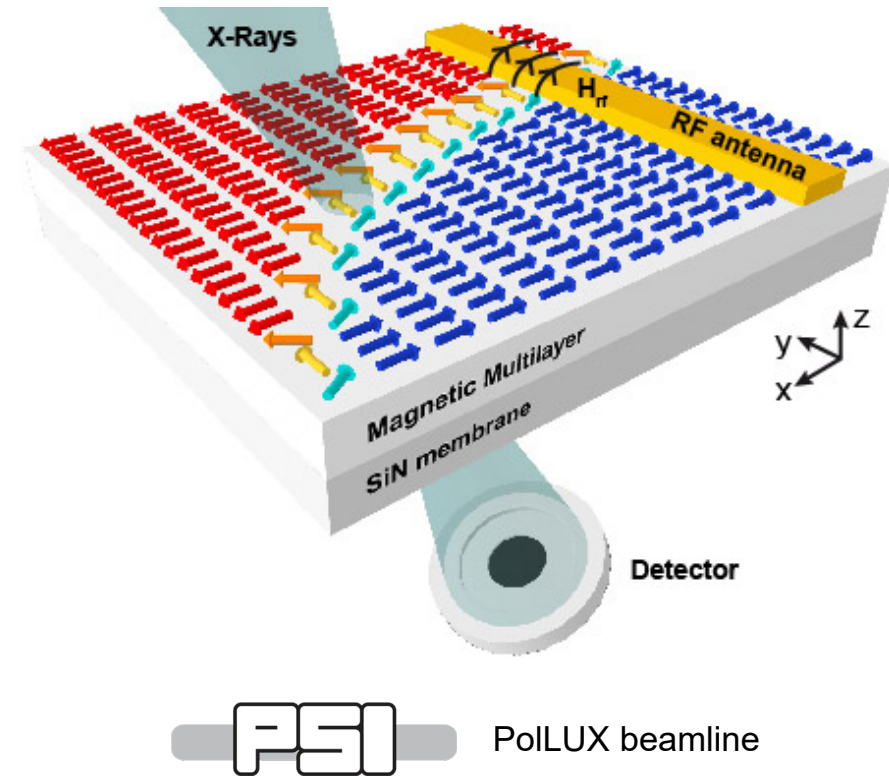
EA et al., Adv. Mater. 32, 1906439 (2020)

Nanoscale circuits for SWs based on domain walls

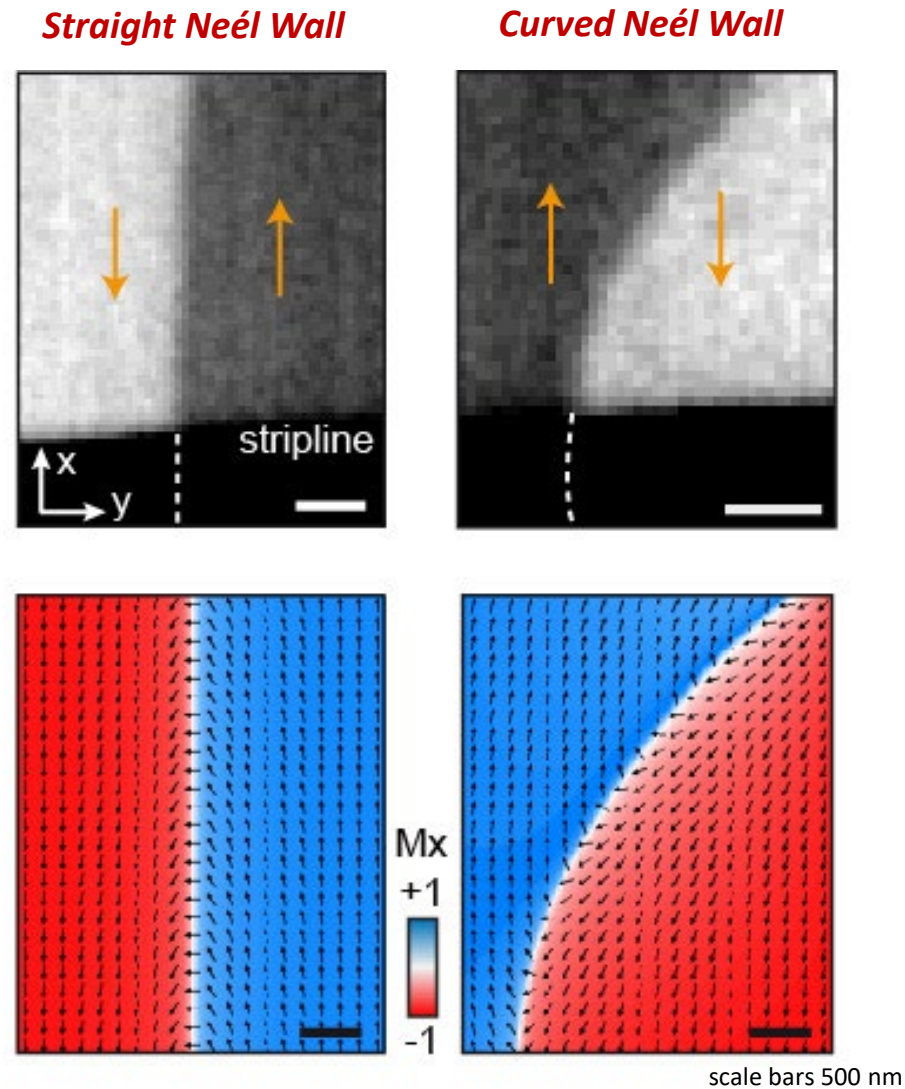
Patterning tailored domain walls



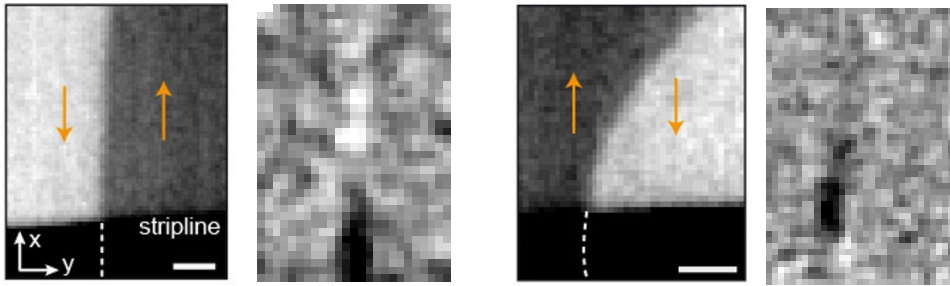
XMCD-STXM for SW visualization



Patterned spin-textures: static STXM

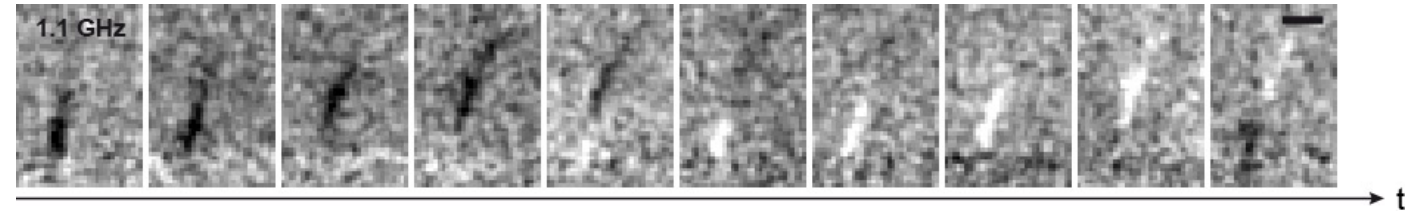


Guiding spin-waves with shaped walls

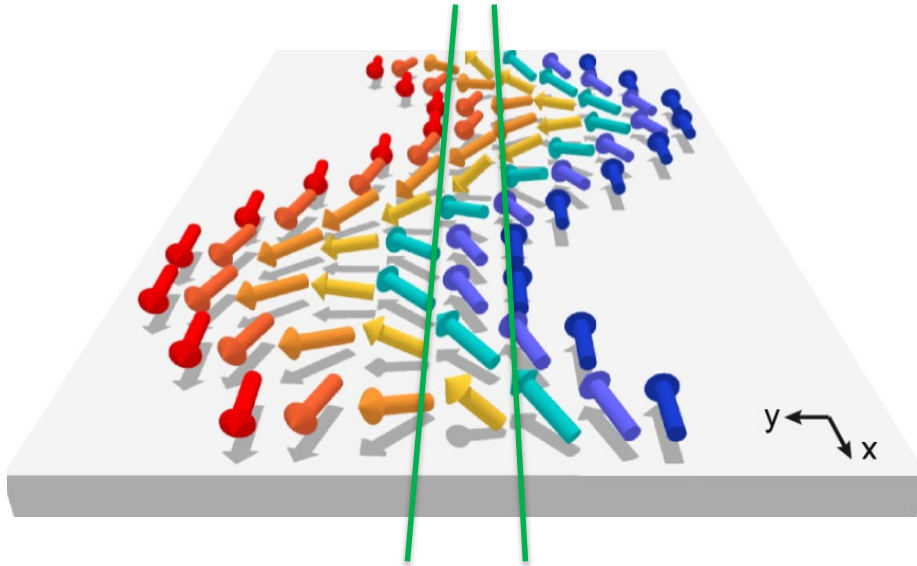


In-plane sensitivity

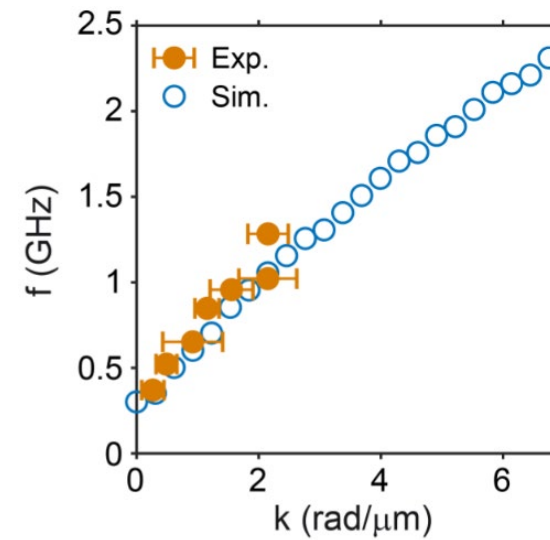
scale bars 500 nm



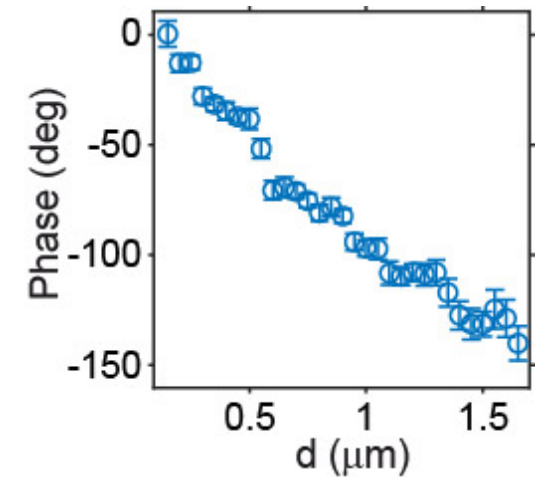
Winter modes



Dispersion



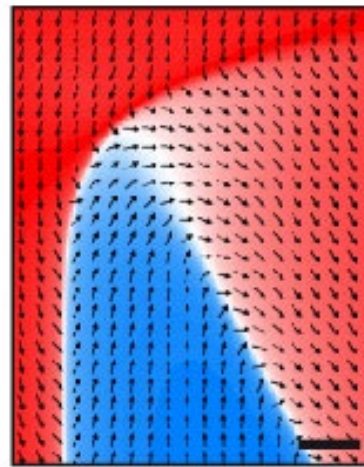
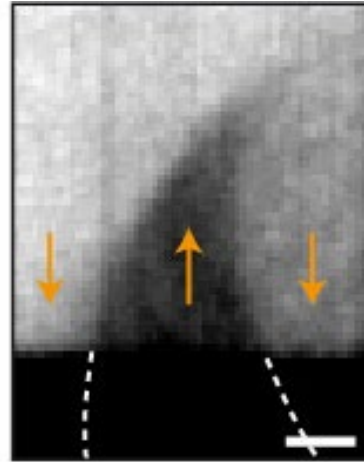
Propagating



Domain wall-based spin wave circuit



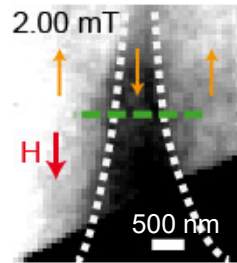
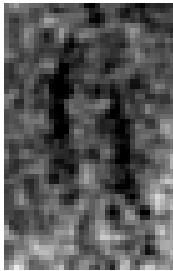
2 Neel walls



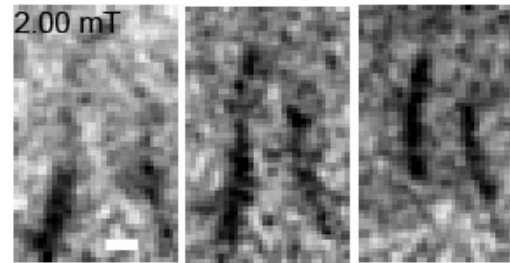
500 nm

Tunable spatial superposition of guided modes

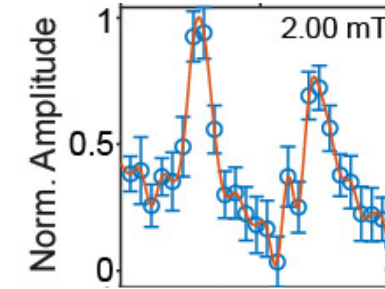
STXM videos



STXM frames

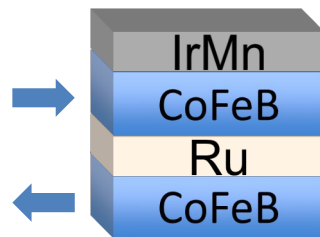
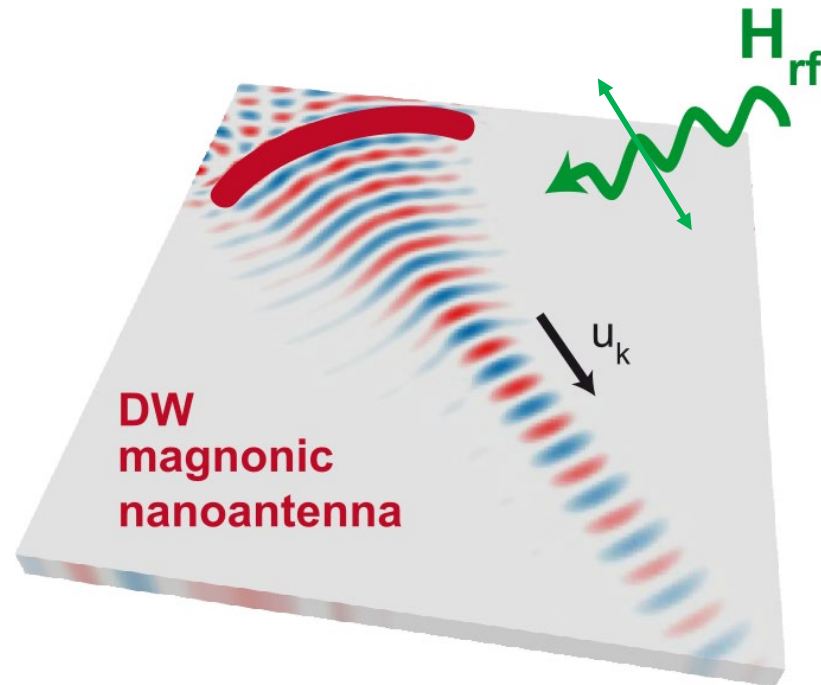


Amplitude profile (green line)



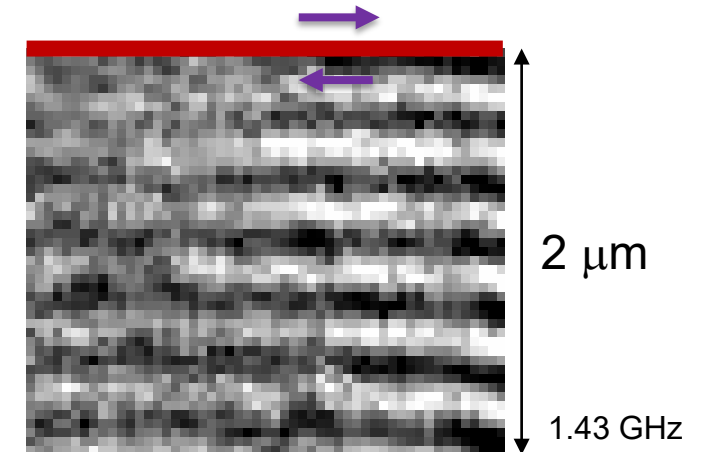
Spin-textures as nanoantennas for spin-waves

Launching magnons with nanoantennas

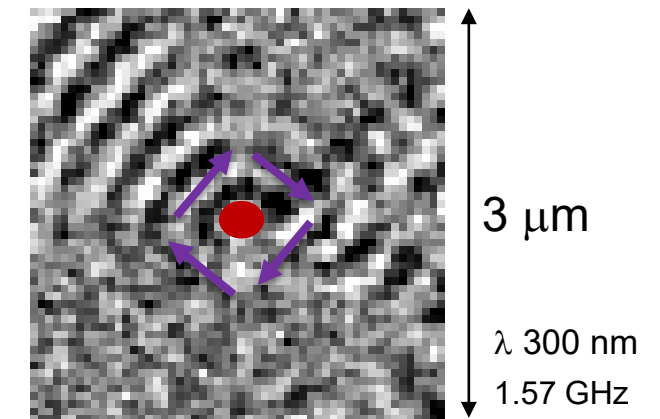


Synthetic
Antiferromagnet

Straight wall: planar wavefront

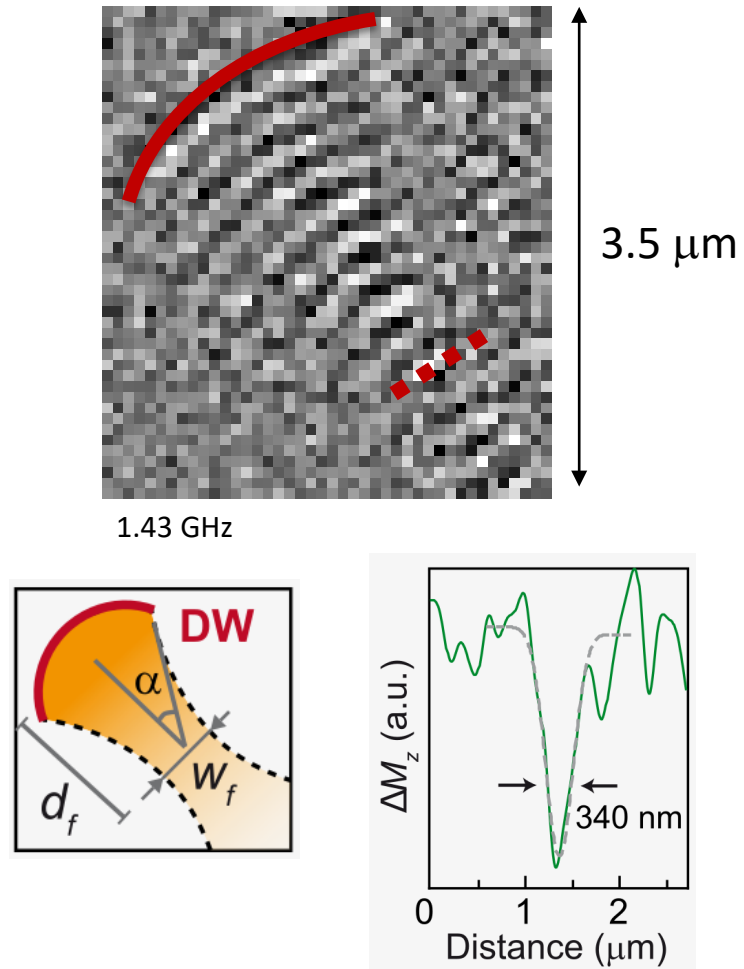


Vortex: radial wavefront

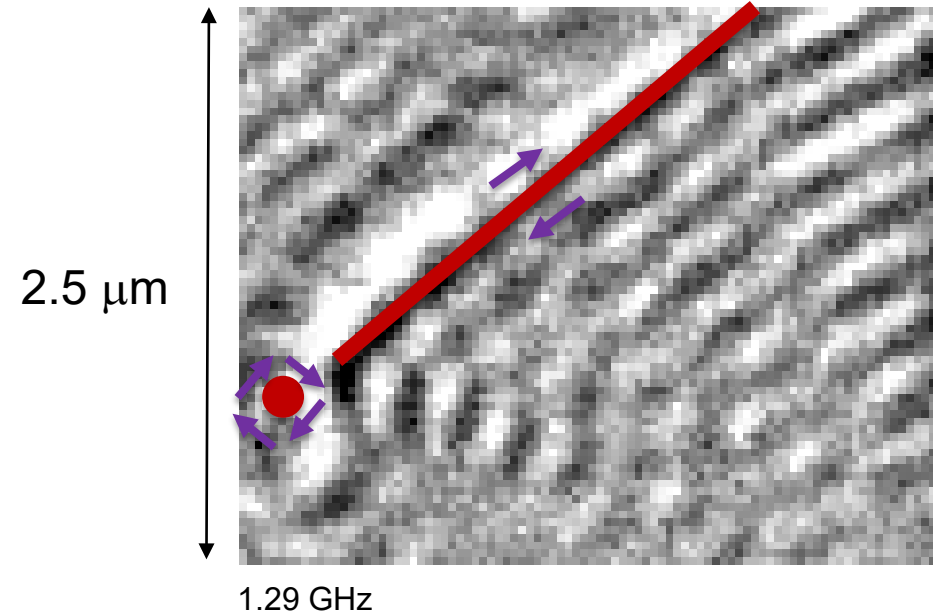


Spin-wave wavefront shaping with spin-texture emitters

Focusing SWs



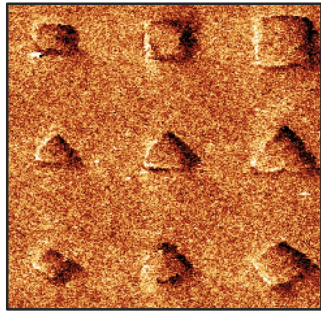
Interference pattern generation via multiple sources



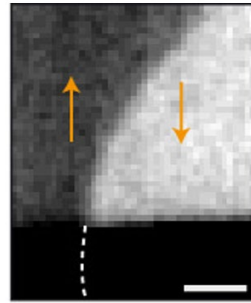
...Towards integrated analog processing using SW

Summary: tam-SPL and applications

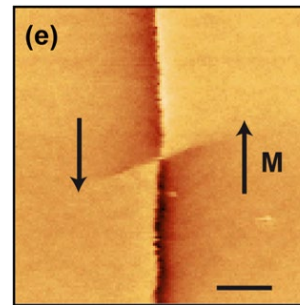
Tailored, deterministic 2D-1D-0D spin-textures



2D domains

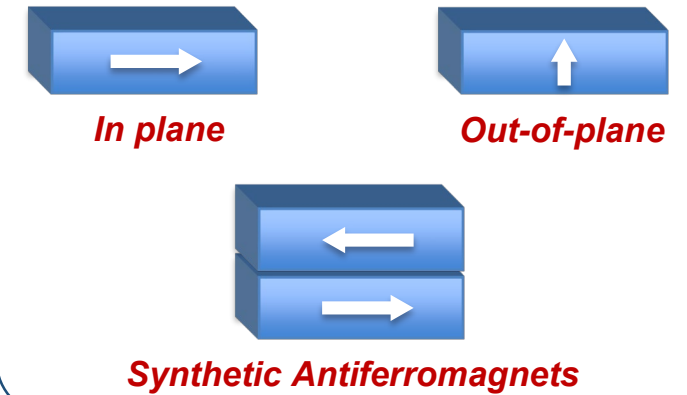


1D domain walls



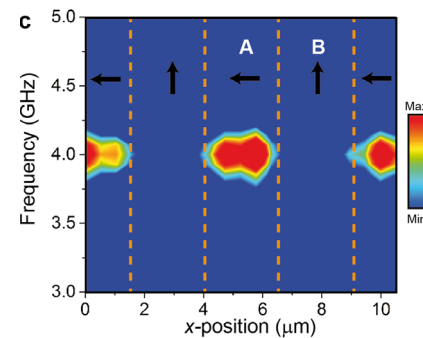
0D topological solitons

EB systems

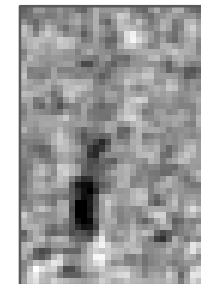


Nat. Nanotech. **11**, 545–551 (2016)
J. Magn. Magn. Mater. **400** 230–235 (2016)
AIP Advances **7**, 055601 (2017)
Comms. Phys., **1**, 56 (2018)
Appl. Phys. Lett. **113**, 162401 (2018)
Adv. Mater. **32**, 1906439 (2020)

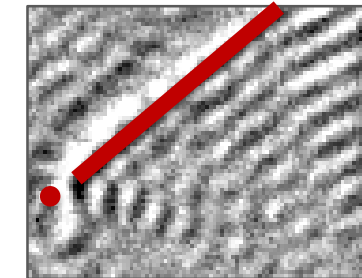
Manipulating spin-waves with patterned spin-textures



Spatial control in domains



Domain wall SW circuits



Optically-inspired magnonics

Thanks!

D. Petti
R. Bertacco



P. Vavassori
M. Pancaldi



A. Calò
X. Zheng



E. Riedo



S. Finizio
S. Wintz
J. Raabe



M. Spiezer



M. Madami
S. Tacchi
R. Silvani
G. Carlotti



A. Papp
G. Csaba
W. Porod



A. Knoll



We are hiring!
Openings for PhD / PostDocs.



Beyond Nanofabrication via
Nanoscale phase-engineering of matter

The research leading to these results was funded by the European Union's Horizon 2020 research and innovation programme under grant agreements 705326 (SWING), 730872 (CALIPSOplus), 948225 (B3YOND).



**Thanks for
your attention**



Multiphoton Lithography: Techniques, Materials,
and Applications, Wiley